

**BIOLOGICAL APPLICATIONS OF
ATMOSPHERIC PRESSURE PLASMA LIQUID DEPOSITION**

by

Sara Lynne Wargo

Bachelor of Chemical Engineering, University of Dayton, 2002

Submitted to the Graduate Faculty of
Swanson School of Engineering in partial fulfillment
of the requirements for the degree of
Doctor of Philosophy

University of Pittsburgh

2009

UNIVERSITY OF PITTSBURGH
SWANSON SCHOOL OF ENGINEERING

This dissertation was presented

by

Sara Lynne Wargo

It was defended on

February 25, 2009

and approved by

Steven R. Little, Ph.D., Assistant Professor, Department of Chemical Engineering

Kacey G. Marra, Ph.D., Assistant Professor, Department of Surgery

William R. Wagner, Ph.D., Professor, Department of Surgery

Masayuki Yamato, Ph.D., Professor, Tokyo Women's Medical University

Dissertation Director: Alan J. Russell, Ph.D. University Professor, Department of Surgery

BIOLOGICAL APPLICATIONS OF ATMOSPHERIC PRESSURE PLASMA LIQUID DEPOSITION

Sara L. Wargo, PhD

University of Pittsburgh, 2009

Surface modification is a common methodology employed to make biomaterials more compatible with the biologic environment in which they will be used or to achieve some desired biologic effect. Many methods exist for modifying materials, each with their own set of advantages and disadvantages. Plasma technology is one way researchers choose to modify materials as it typically forms coatings that are uniform and exhibit good surface adhesion. Nonthermal plasma is most frequently used in the modification of biomaterials because it operates at ambient temperature, but it also operates at vacuum pressures. Dow Corning Plasma Solutions has developed a new technology termed atmospheric pressure plasma liquid deposition (APPLD) that generates a stable glow discharge plasma at ambient temperature and pressure. To this point, the applications of this new technology have been limited to the field of chemistry. The objective of this study was to explore biological applications of the APPLD technology as it pertains to the modification of biomaterials. The aims of this study primarily focused on the deposition of monomers and polymers to make cell releasing surfaces and biocidal surfaces. In general, it was found that the APPLD technology could be used more successfully for the deposition of polymers than monomers. This is most notably demonstrated by the extensive studies of N-isopropylacrylamide (NIPAAm) deposition. Contrary to what was expected, the polymerization of the NIPAAm monomer was very limited in the APPLD system. When the focus of the experiments shifted to deposition of poly(N-isopropylacrylamide) pNIPAAm,

covalent modification of a high molecular polymer was observed. Only after this was cellular release, the desired biologic effect, observed. Similar observations were made for the deposition of biocidal monomers and polymers as the APPLD system again proved to be more effective when biocidal polymers were used as the liquid precursors. These findings have demonstrated that there is utility of APPLD for biological applications and has provided a base for future experimentation.

TABLE OF CONTENTS

LIST OF TABLES	x
LIST OF FIGURES	xi
NOMENCLATURE.....	xvi
PREFACE.....	xviii
1.0 INTRODUCTION.....	1
1.1 TISSUE ENGINEERING	1
1.2 CELL SHEET ENGINEERING	2
1.2.1 Temperature responsive cultureware	3
1.2.2 Applications of cell sheet constructs.....	7
<i>1.2.2.1 Corneal constructs</i>	<i>7</i>
<i>1.2.2.2 Cardiac constructs</i>	<i>8</i>
<i>1.2.2.3 Esophageal constructs</i>	<i>8</i>
<i>1.2.2.4 Future cell sheet engineered constructs</i>	<i>9</i>
1.2.3 Emerging technologies.....	10
<i>1.2.3.1 Electron beam irradiation.....</i>	<i>10</i>
<i>1.2.3.2 Plasma polymerization by radio frequency glow discharge.....</i>	<i>11</i>
<i>1.2.3.3 UV crosslinking.....</i>	<i>12</i>
<i>1.2.3.4 Atmospheric pressure plasma liquid deposition</i>	<i>12</i>
1.3 PLASMA TECHNOLOGY	13

1.3.1	Thermal plasma	14
1.3.2	Nonthermal plasma.....	15
1.4	ATMOSPHERIC PRESSURE PLASMA LIQUID DEPOSITION.....	18
1.4.1	APPLD pre-production model.....	21
1.4.2	APPLD SE-2100 PlasmaStream workstation.....	24
1.5	CNC PROGRAMMING	27
1.5.1	3-Pass program for TCPS or glass slides.....	27
1.5.2	3-Pass program for 6-well plates	28
1.5.3	CNC spot program for 12-well plates	28
1.6	SPECIFIC AIMS	29
2.0	APPLD POLYMERIZATION OF N-ISOPROPYLACRYLAMIDE: PRE-PRODUCTION MODEL.....	32
2.1	INTRODUCTION.....	32
2.2	MATERIALS AND METHODS	34
2.2.1	Selecting APPLD parameters	34
2.2.2	Surface characterization	35
2.2.3	Functionalizing surfaces.....	36
2.2.4	Sterility analysis	37
2.2.5	NIH-3T3 cell culture.....	37
2.2.6	Cell release studies	38
2.2.7	Statistical analysis	38
2.3	RESULTS	39
2.3.1	Selecting APPLD parameters	39
2.3.2	Permanency of APPLD ppNIPAAm coatings	44

2.3.3	CellSeed analysis	47
2.3.4	Cellular release studies	49
2.4	DISCUSSION	50
2.5	CONCLUSIONS	52
3.0	APPLD POLYMERIZATION OF N-ISOPROPYLACRYLAMIDE:	54
3.1	INTRODUCTION.....	54
3.2	MATERIALS AND METHODS	55
3.2.1	Optimization of APPLD parameters for effective deposition	55
3.2.2	Chemical characterization	56
3.2.3	Surface characterization	56
3.2.4	Cell release studies	57
3.2.5	Statistical analysis	58
3.3	RESULTS	58
3.3.1	Optimization of APPLD parameters for effective deposition.....	58
3.3.2	Surface characterization and cellular release on 6-well plates	64
3.3.3	Development of the CNC spot program.....	65
3.3.4	Chemical analysis of ppNIPAAm by the CNC spot program.....	68
3.3.5	Cellular release studies on 12-well plates.....	70
3.4	DISCUSSION	71
3.5	CONCLUSIONS	73
4.0	APPLD DEPOSITION OF POLY(N-ISOPROPYLACRYLAMIDE): SE-2100 PLASMASTREAM	75
4.1	INTRODUCTION.....	75
4.2	MATERIALS AND METHODS	76

4.2.1	Substrate modification.....	76
4.2.2	Chemical characterization	77
4.2.3	Surface characterization	77
4.2.4	Cell release studies	78
4.2.5	Cellular viability assay	79
4.2.6	Statistical analysis	79
4.3	RESULTS	80
4.3.1	Chemical characterization of APPLD deposited pNIPAAm	80
4.3.2	Surface behavior at temperatures above and below the LCST	81
4.3.3	Cellular viability and release studies.....	85
4.4	DISCUSSION	89
4.5	CONCLUSIONS	91
5.0	APPLD DEPOSITION OF BIOCIDAL MOLECULES.....	93
5.1	INTRODUCTION.....	93
5.2	MATERIALS AND METHODS	95
5.2.1	Materials	95
5.2.2	Synthesis of antimicrobial quaternary ammonium compounds.....	95
5.2.3	Preparation of the APPLD deposited QA substrates	98
5.2.4	Fluorescein staining	99
5.2.5	Dual polarization interferometry	99
5.2.6	Biocidal activity.....	100
5.3	RESULTS	100
5.3.1	Evaluating APPLD coatings of QA compounds.....	100

5.4	DISCUSSION	106
5.5	CONCLUSIONS	108
6.0	SUMMARY	109
6.1	PRE-PRODUCTION MODEL OF THE APPLD SYSTEM	109
6.2	APPLD AS A MEANS FOR MAKING CELL RELEASING SURFACES	110
6.3	APPLD AS A MEANS FOR MAKING BIOCIDAL SURFACES.....	112
6.4	LIMITATIONS OF THE APPLD SYSTEM	113
7.0	FUTURE DIRECTIONS.....	115
7.1	CONTINUED WORK ON THE USE OF THE APPLD SYSTEM FOR THE DEPOSITION OF BIOMOLECULES.....	115
7.2	USE OF APPLD FOR PATTERNED DEPOSITION.....	115
7.3	IMMOBILIZATION OF PNIPAAm BY APPLD ONTO SOFT CONTACT LENSES	116
	APPENDIX A	117
A.1	¹H NMR Spetrum of NIPAAm	117
A.2	¹H NMR Spetrum of pNIPAAm	118
A.3	¹H NMR Spetrum of APPLD polymerized pNIPAAm.....	119
A.4	¹H NMR Spetrum of APPLD deposited pNIPAAm.....	120
	BIBLIOGRAPGHY	121

LIST OF TABLES

Table 1-1. Contact angle measurements of pNIPAAm modified TCPS as published in Yamada et al. [57]. Contact angles are larger at temperatures above the LCST than they are at temperatures below the LCST demonstrating the switch in surface hydrophobicity	5
Table 2-1. Varying system parameters of the pre-production APPLD system. Process parameters varied were the solution flow rate and the number of times of the substrate was coated. Optimal parameters for coating were found to be 5- μ L/min and 3 times coating and are italicized in the table below.	39
Table 3-1. Varying system parameters of the production model APPLD system. Process parameters varied were the solution flow rate and carrier gas flow rate and composition. Optimal parameters for coating were found to be liquid delivery at 15- μ L/min and a carrier gas composition of strictly hydrogen at a delivery rate of 1 L/min, italicized below	62
Table 4-1. Molecular weights determined by GPC of pNIPAAm deposited by APPLD and pNIPAAm controls	80
Table 5-1. The effect of the system parameters on QA-247	101
Table 5-2. The effect of the system parameters on QA-125	101
Table 5-3. The effect of the system parameters on QA-011 with vinyl TMS.....	102
Table 5-4. The effect of the system parameters on QA-011 without vinyl TMS.....	102

LIST OF FIGURES

Figure 1-1 Chemical structure of pNIPAAm.....	3
Figure 1-2 Left, pNIPAAm chains associate with many water molecules at 10 °C causing the polymer chains to extend and swell. Right, increasing that temperature to 37 °C, an appropriate temperature for cell culture, the polymer chains shrink, sloughing off most of the previously associated water molecules. The change in the pNIPAAm solubility occurs around a lower critical solution temperature of 31 °C.....	4
Figure 1-3 Left, cells are seeded onto a modified tissue culture plate and (center) grown to a confluent monolayer. Right, by reducing the temperature, the pNIPAAm chains expand as the film swells with the additional water molecule association. Cells lift away from the edges and off of the surface of the plate with the change in hydrophobicity.	6
Figure 1-4 Voltage as a function of current as it relates to the generation of three basic types of electrical discharges. Reprinted from [52].....	14
Figure 1-5 Temperature profile of the electron and ion temperature as a function of pressure in both nonthermal and thermal plasmas. As the pressure approaches atmospheric pressure a transition occurs and thermal plasma is generated. Reprinted from [52].	16
Figure 1-6 Radio frequency glow discharge. The vacuum pump on the left is used to reduce the pressure of the reactor. A radio frequency generator, in the center, is used to supply energy to the gases that are supplied on the right. Samples inside the reactor are modified by glow discharge that is produced. Reprinted from [17].	17
Figure 1-7 Left, schematic of the nebulizer used in the SE-2100 PlasmaStream workstation. Helium is used as the nebulizing gas. It flows down the left side of the nebulizer and the liquid line flows down the right side. The liquid and gas streams meet at the tip and aerosolized droplets are formed. Right, an image of the droplets formed by the nebulizer were captured on a light microscope.	20
Figure 1-8 Pre-production model of the APPLD system. Left, (a) user control panel, (b) high voltage generator, (c) computer. Center, (d) high voltage input, (e) plasma head, (f) nebulizing gas line, (g) liquid line, (h) process gas line, (i) plasma nozzle, (j) CNC table, (k) programmable syringe pump, (l) high voltage lead, (m) nebulizing gas feed, (n) liquid line feed.....	23

- Figure 1-9** SE-2100 PlasmaStream workstation. Left, (a) electrode housing and feed lines, (b) CNC table. Right, (c) programmable syringe pump, (d) liquid feed line, (e) process gas line, (f) nebulizing gas line, (g) nebulizer, (h) high voltage generator, (i) high voltage line, (j) electrode housing and (k) plasma nozzle 26
- Figure 1-10** CNC programming for coating TCPS or glass slides (left), 6-well plates (center) or 12-well plates (right)..... 27
- Figure 2-1** Contact angle measurements as a function of NIPAAm monomer concentration. A, pre-wash measurements. B, measurements taken after a 50 °C wash cycle. C, measurements taken after a 4 °C wash cycle. Bars represent the mean \pm standard deviation. White bars represent measurements that were made at 50 °C and the black bars represent measurements made at 4 °C. Bars marked with an asterisk represent a statistically significant difference ($p < 0.05$).....41
- Figure 2-2** DPI chip modified with a 40-wt% solution of NIPAAm. The blue line represents the layer thickness, the green line is the mass per unit area and the purple line shows the surface density of ppNIPAAm. The layer thickness and mass can clearly be seen washing off of the surface with a drop in temperature..... 42
- Figure 2-3** Contact angle measurement controls. Bars represent the mean \pm standard deviation. White bars represent measurements that were made at 50 °C and the black bars represent measurements made at 4 °C. No significant difference was observed. 43
- Figure 2-4** The pre-activated TCPS slides modified with a 40-wt% solution of NIPAAm is still rendered inactive after a single cold water wash cycle. Bars represent the mean \pm standard deviation. White bars represent measurements that were made at 50 °C and the black bars represent measurements made at 4 °C. Bars marked with an asterisk represent a statistically significant difference ($p < 0.05$). 45
- Figure 2-5** Vinyl functionalized glass slides modified with a 40-wt% solution of NIPAAm do not exhibit a change in surface hydrophobicity (A) pre-wash or (B) post-wash. Bars represent the mean \pm standard deviation. White bars represent measurements that were made at 50 °C and the black bars represent measurements made at 4 °C. Bars marked with an asterisk represent a statistically significant difference ($p < 0.05$)..... 47
- Figure 2-6** Contact angle measurements of commercially available pNIPAAm modified TCPS dishes from CellSeed. Exposure to one cold water wash cycle eliminates the temperature switch in surface hydrophobicity. Bars represent the mean \pm standard deviation. White bars represent measurements that were made at 50 °C and the black bars represent measurements made at 4 °C. Bars marked with an asterisk represent a statistically significant difference ($p < 0.05$)..... 48
- Figure 2-7** NIH-3T3 cells lifting from the surface of an UpCell dish. 49

- Figure 3-1** Nebulized droplet diameters as a function of regulator pressure. Images like these pictured above were analyzed using ImageJ software. The diameter of every whole droplet was measured and the results were averaged. Tabulated data can be seen in the lower right. All pressures result in droplet diameters that lie within an acceptable range for the APPLD system. 59
- Figure 3-2** Contact angle measurements as a function of power. A, pre-wash measurements. B, measurements taken after a 50 °C wash cycle. C, measurements taken after a 4 °C wash cycle. Bars represent the mean \pm standard deviation. White bars represent measurements that were made at 50 °C and the black bars represent measurements made at 4 °C. Bars marked with an asterisk represent a statistically significant difference ($p < 0.05$)..... 60
- Figure 3-3** Contact angle measurements as a function of plasma nozzle height. A, pre-wash measurements. B, measurements taken after a 50 °C wash cycle. C, measurements taken after a 4 °C wash cycle. Bars represent the mean \pm standard deviation. White bars represent measurements that were made at 50 °C and the black bars represent measurements made at 4 °C. Bars marked with an asterisk represent a statistically significant difference ($p < 0.05$)..... 63
- Figure 3-4** DPI chip modified with a 40-wt% solution of NIPAAm. The blue line represents the layer thickness, the green line is the mass per unit area and the purple line shows the surface density of ppNIPAAm. The layer thickness and mass can clearly be seen washing off of the surface with a drop in temperature..... 64
- Figure 3-5** Contact angle measurements as a function of coating time. A, pre-wash measurements. B, measurements taken after a 50 °C wash cycle. Bars represent the mean \pm standard deviation. White bars represent measurements that were made at 50 °C and the black bars represent measurements made at 4 °C. Bars marked with an asterisk represent a statistically significant difference ($p < 0.05$). 66
- Figure 3-6** A, Contact angle measurements after two warm water wash cycles using the 3-pass program. B, Contact angle measurements after one warm water wash cycle and one cold water wash cycle using the CNC spot program. Bars represent the mean \pm standard deviation. White bars represent measurements that were made at 50 °C and the black bars represent measurements made at 4 °C. Bars marked with an asterisk represent a statistically significant difference ($p < 0.05$). 67
- Figure 3-7** Cloud point formation of ppNIPAAm (■), NIPAAm monomer (●) and pNIPAAm (◆) purchased from Sigma-Aldrich..... 69
- Figure 3-8** Left, NIH-3T3 cells grown on the TCPS control. Right, NIH-3T3 cells grown on the APPLD modified ppNIPAAm plates. Cells adhered to and grew on the ppNIPAAm surface without any inhibition 70
- Figure 4-1** Cloud point measurement for the control pNIPAAm (■), film coated pNIPAAm (●), pNIPAAm HV(-) and pNIPAAm HV (+).....81

- Figure 4-2** Contact angle measurement on TCPS slides coated using the CNC spot program. Data is representative of two wash cycles, one at 50 °C (left) and one at 20 °C (right). Bars represent the mean \pm standard deviation. White bars represent measurements that were made at 50 °C and the black bars represent measurements made at 4 °C. Bars marked with an asterisk represent a statistically significant difference ($p < 0.05$). 82
- Figure 4-3** DPI chip modified with a 5-wt% solution of pNIPAAm. The blue line represents the layer thickness, the green line is the mass per unit area and the purple line shows the surface density of the APPLD deposited pNIPAAm. In this experiment the layer thickness, mass and density appear to be stable 83
- Figure 4-4** DPI chip modified with a 5-wt% solution of pNIPAAm. The blue line represents the layer thickness, the green line is the mass per unit area and the purple line shows the surface density of the APPLD deposited pNIPAAm. With an increasing temperature, we can observe decreasing layer thickness and an increasing density. As the temperature decreases, we observe the opposite trend..... 84
- Figure 4-5** DPI chip modified with a 5-wt% solution of pNIPAAm. Mass loss is evident when we narrow the y-axis. This loss is primarily observed at 24 °C. 85
- Figure 4-6** Cellular viability at 24 hr (white bar), 48 hr (gray bar), 72 hr (black bar) and 96 hr (striped bar) time intervals. When compared to TCPS, the growth on the 5-wt% pNIPAAm dishes demonstrated a significant difference ($p < 0.05$) at the 72 and 96 hr time intervals. Bars represent the mean \pm standard deviation. White bars represent measurements that were made at 50 °C and the black bars represent measurements made at 4 °C. Bars marked with an asterisk represent a statistically significant difference ($p < 0.05$) when compared to the TCPS control..... 87
- Figure 4-7** NIH-3T3 cells releasing from the surface of an APPLD deposited pNIPAAm well. Pictures were taken every 15 seconds under 40X magnification. 88
- Figure 4-8** Cellular viability as measured by an MTT assay. No significant difference is observed between the adhered cells on the TCPS plate and the released cells in the cell sheet. Bars represent the mean \pm standard deviation. White bars represent measurements that were made at 50 °C and the black bars represent measurements made at 4 °C..... 89
- Figure 5-1** Synthesis scheme for QA-125.....96
- Figure 5-2** Synthesis scheme for QA-247..... 97
- Figure 5-3** Chemical structure of QA-011 98
- Figure 5-4** DPI analysis of QA-247 measured at a temperature of 24 °C. Thickness (blue), mass (green) and density (purple). Thickness of the QA-247 layer is decreasing over the course of an hour indicating the compound is washing off the surface of the chip. 104

Figure 5-5 DPI analysis of QA-011 measured at 24 °C. Thickness (blue), mass (green), density (purple). This sample did not have any vinyl TMS in the solution. Coating appears to be stable on the surface during this one hour time course.....	106
A-1 ¹ H NMR spectra of NIPAAm.....	117
A-2 ¹ H NMR spectra of pNIPAAm.....	118
A-3 ¹ H NMR spectra of APPLD polymerized pNIPAAm (ppNIPAAm) in triplicate.....	119
A-4 ¹ H NMR spectra of APPLD deposited pNIPAAm. Blue line represents control pNIPAAm, yellow line represents pNIPAAm dissolved in IPA and film coated, green line represents APPLD sprayed pNIPAAm without HV, and orange line represents APPLD deposited pNIPAAm with HV.	120

NOMENCLATURE

1,1,4,7,10,10-Hexamethyltriethylenetetramine	HMTETA
2-(Trimethylsiloxy)ethyl Methacrylate	HEMA-TMS
APPLD Polymerized NIPAAm	ppNIPAAm
APPLD Polymerized NIPAAm	pdpNIPAAm
Atmospheric Pressure Plasma Liquid Deposition	APPLD
Computer Number Control	CNC
Copper (I) Bromide	CuBr
Deionized Water	DI water
Deuterated Chloroform	CDCl ₃
Dual Polarization Interferometry	DPI
Dulbecco's Phosphate Buffered Saline	PBS
Gel Permeation Chromatography	GPC
Glucose Oxidase	GOx
High Voltage	HV
Horseradish Peroxidase	HRP
Isopropyl Alcohol	IPA
Lower Critical Solution Temperature	LCST
N,N-Dimethylacrylamide	DMA
N,N-Dimethylaminoethyl Methacrylate	DMAEMA

N-Dimethylformamide	DMF
N-isopropylacrylamide	NIPAAm
Nuclear Magnetic Resonance	NMR
Number Average Molecular Weight	M_n
Poly(N-isopropylacrylamide)	pNIPAAm
Polydispersity Index	M_n / M_w
Polyvinyl Alcohol	PVA
Post Wash	PW
Quaternary Ammonium	QA
Radio Frequency Glow Discharge	RFGD
Sodium Iodide	NaI
Tetra-n-Butylammonium Fluoride	TBAF
Tetrahydrofuran	THF
Thiazolyl Blue Tetrazolium Bromide	MTT
Tissue Culture Polystyrene	TCPS
Weight Average Molecular Weight	M_w

PREFACE

I would like to express my gratitude to the many people that have in some way helped me through my time in graduate school. First and foremost, I would like to thank Dr. Alan Russell who has been a phenomenal mentor. He has pushed me to succeed even when I didn't think it was possible. Working under him provided me with opportunity to study in Japan, an experience that I could not have imagined and will not soon forget. I would also like to thank Laurie Madeya and Gilliane McShane, the past and present keepers of Dr. Russell's calendar, for making those last minute meetings with my advisor possible. I would like to thank Dr. Masayuki Yamato for his guidance during my internship in Japan and the rest of my committee members, Drs. William Wagner, Kacey Marra and Steven Little for their helpful advice.

I would also like to express my gratitude to Dr. Lesley-Ann O'Hare and Dr. Liam O'Neill for sharing their knowledge of the APPLD system and providing long distance support when problems occurred. I would like to thank Chris Shirk and John Albaugh for their technical assistance with the APPLD system.

I am very thankful to the past and present members of the Russell Lab who have provided valuable support and friendship over the past several years. To Dr. Rick Koepsel for providing assistance as needed on a daily basis. To Dr. Matt Heise for keeping the tissue culture room clean and for providing much needed comic relief. To Dr. Hiro Murata for providing me with numerous chemical compounds and all his help with chemical analysis. To Jonelle Chir, Jill

Andersen, Gemma Asche, Dr. Joie Marhefka, Amanda Daly and Dr. Phil Marascalco for the good lunchtime conversation.

Finally, and most importantly, I would like to thank my family and my finacé Dr. Jason Chang. Your encouragement over these past years has meant the world to me. It has been your love and support that helped me the most when I felt like I was never going to finish graduate school. I will be forever grateful.

1.0 INTRODUCTION

1.1 TISSUE ENGINEERING

Tissue engineering is a multidisciplinary field that holds a great promise in the future of the medical care. It has been defined as “an interdisciplinary field that applies the principles of engineering and the life sciences toward the development of biological substitutes that restore, maintain, or improve tissue function [1].” Tissue engineered constructs can be achieved by direct injection of cell isolates or implantation of scaffold materials, with scaffold design being a major focus. Materials for scaffolds are designed first and foremost to be biocompatible and biodegradable. The materials must be porous to allow for cellular integration. Cellular integration can be done after implantation by the host or prior to implantation using an allogenic cell source.

Scaffolds are made from a variety of materials, including synthetic polymers and natural matrices, both having specific advantages. Synthetic polymers can be customized to meet specific needs of the device. Scaffolds made from polymers can be fabricated into any shape or size. Further, these scaffolds can be designed to have a predetermined degradation rate, porosity and mechanical strength. Polymer scaffolds with ideal physical properties, however, do not always exhibit good cellular adherence. This can be addressed by tailoring the chemistry or by modification of the scaffold surface. Natural matrices are biologically inert. Scaffolds made from these materials effectively allow for cellular integration. Further, they mimic biological

constructs that are seemingly random in nature. However, biological matrices are not customizable.

In the early 1990's another approach was taken to making cellular constructs. This approach used culture surfaces that were temperature responsive and scaffold-less. Cells would grow on these surfaces and could be released as a contiguous sheet. Releasing the cells from the culture surface did not interfere with the cell to cell communication channels and the extracellular matrix deposited by the cells remained intact. This approach has since been termed cell sheet engineering and uses for these cellular constructs have widely varied. These cell sheets can be used as functional tissues when recovered from the culture dish, eliminating the need for any scaffold. The following text will discuss temperature responsive cultureware, its relevance and the emerging technologies in the field.

1.2 CELL SHEET ENGINEERING

Cell sheet engineering is a pioneering technology that allows for tissue replacement products to be made from scaffold-less materials. The concept is simple, a temperature responsive polymer, poly(N-isopropylacrylamide) (pNIPAAm), is immobilized onto tissue culture polystyrene surfaces. This polymer exhibits reversible solubility around a lower critical solution temperature (LCST). At cell culturing conditions, the hydrophobicity of the polymer is not much different than that of tissue culture polystyrene. Cells grow on these surfaces just as they would grow on unmodified TCPS. To release the cells, the temperature is lowered. Harvested cell sheets can then be used for clinical applications.

1.2.1 Temperature responsive cultureware

N-isopropylacrylamide was first synthesized in 1956 [2]. Early research on the monomer detailed polymerization techniques and chemical characterization. In 1967, it was reported that

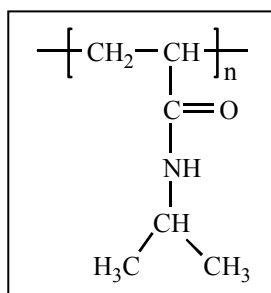


Figure 1-1 Chemical structure of pNIPAAm

poly(N-isopropylacrylamide) (pNIPAAm) exhibited a lower critical solution temperature (LCST) of 31 °C in aqueous media [3], a behavior that proved to be of particular interest to researchers in the fields of chemistry, physics and biology [4]. In the field of biomaterials, pNIPAAm has been immobilized on substrates for the controlled release of drugs [5, 6] and biomolecules [7-9], to create self-cleaning surfaces [10, 11], to fabricate micropatterned surfaces [12, 13] and for the release of cells [12-16].

During culture, cells excrete proteins that bind to the surface of tissue culture polystyrene. Some of these proteins, such as fibronectin, contain cell adhesion sequences, and enable adherent cells to attach to the surface. Once attached, these cells continue to excrete proteins forming an extracellular matrix (ECM) that enables cell to cell communications. Classic cell culturing techniques require degradative enzymes for the removal of adherent cells from the surface of the cultureware. These enzymes denature the ECM proteins eliminating the cell to cell communication channels. Further, the degradative enzymes destroy the focal adhesion sites, causing cells to convert back to a rounded morphology and releasing them from the surface [17].

Immobilization of pNIPAAm onto TCPS has been shown to eliminate the need for trypsin [12-16]. This is possible because the pNIPAAm exhibits both hydrophobic and hydrophilic behavior. At cell culture conditions, pNIPAAm exhibits hydrophobic behavior and is coiled tightly to the TCPS surface. Each pNIPAAm unit can associate with about 25 water molecules at this temperature. Reduction in temperature results in an increase of water molecule association. At 25 °C, about 100 water molecules can associate with one pNIPAAm unit [18]. This increase in water molecule association causes the polymer layer to swell and the surface becomes more hydrophilic. Figure 1-2 shows a schematic of this transition. The abrupt change in surface hydrophobicity enables the release of cultured cells simply by using a temperature stimulus [19].

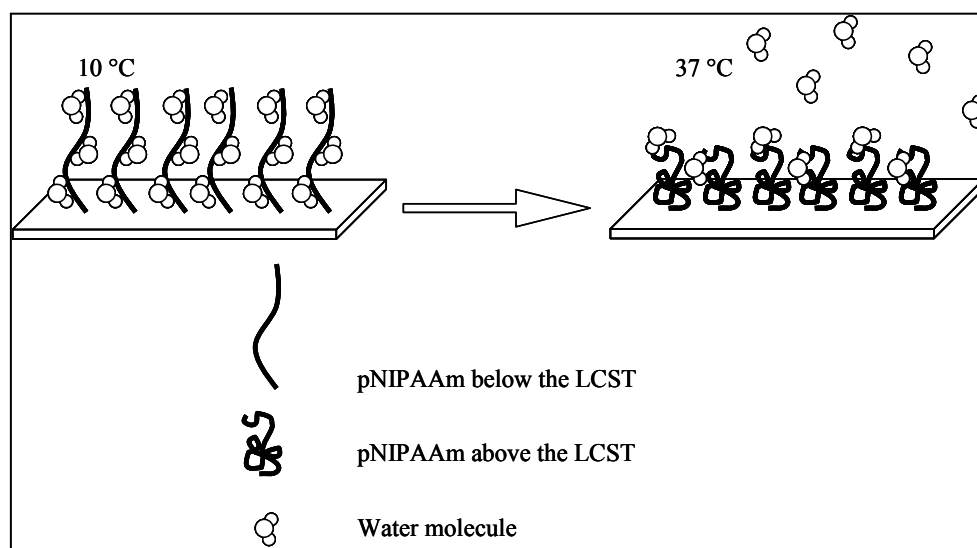


Figure 1-2 Left, pNIPAAm chains associate with many water molecules at 10 °C causing the polymer chains to extend and swell. Right, increasing that temperature to 37 °C, an appropriate temperature for cell culture, the polymer chains shrink, sloughing off most of the previously associated water molecules. The change in the pNIPAAm solubility occurs around a lower critical solution temperature of 31 °C.

Yamada et al initially reported covalently attached pNIPAAm as a temperature responsive surface in 1990. They were able to polymerize the monomer and bind it to TCPS through electron beam irradiation. A 50-wt% solution of the NIPAAm monomer was dissolved in isopropyl alcohol. This solution was placed in the bottom of a culture dish and irradiated with an electron beam [16]. This process breaks the carbon-carbon double bond in the monomer, allowing for polymerization by free radical combination. Further, the energy from the electron beam creates free radicals on the surface of the polystyrene, creating covalently modified surfaces. Contact angle measurements were used to verify the changing hydrophobicity of the surface and the results generated are shown in Table 1-1.

Table 1-1 Contact angle measurements of pNIPAAm modified TCPS as published in Yamada et al . Contact angles are larger at temperatures above the LCST than they are below the LCST demonstrating the switch in surface hydrophobicity of TCPS.

	Contact Angle	
	37 °C	10 °C
pNIPAAm grafted TCPS	48°	30°
Control TCPS	54°	54°

Yamada et al were also able to demonstrate that these surfaces were viable for cell culture and proliferation. Hepatocytes were used in this study, but in general cells would be seeded at a low density onto the cultureware. Over time, cells grow to a confluent monolayer. Reduction of temperature below the LCST causes the polymer to swell and the TCPS surface becomes hydrophilic. Cells release from the edges and can be lifted as a contiguous cell sheet. Figure 1-3 shows a schematic of the cell culturing process.

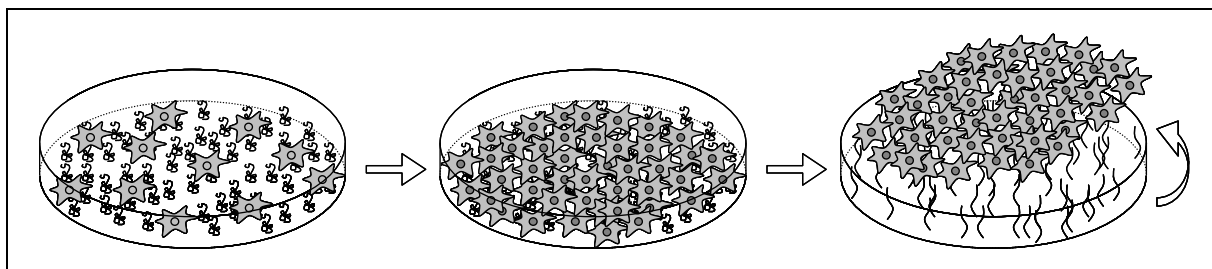


Figure 1-3 Left, cells are seeded onto a modified tissue culture plate and (center) grown to a confluent monolayer. Right, by reducing the temperature, the pNIPAAm chains expand as the film swells with the additional water molecule association. Cells lift away from the edges and off of the surface of the plate with the change in hydrophobicity.

Further, they were able to demonstrate removal of cells by this methodology was not harmful. Hepatocytes are an extremely fragile cell line and are very susceptible to trauma [20]. Removal of hepatocytes from TCPS by trypsinization can cause harm when trying to subculture this cell line. This study showed that 73.3% of the hepatocytes removed from the pNIPAAm dish were successfully transferred to a new dish. This is in contrast to the 14% that were successfully transferred after removal by trypsinization from the control plate [16].

Since the publication of this initial study, a flurry of research has been done in cell sheet engineering [6, 12-14, 16, 19, 21-41]. Much of the early research focused on further developing the technology and the more current literature is focused on animal trials with the intent of progressing toward clinical applications. A start-up company, CellSeed, was also formed and commercially manufactures thermally responsive cell cultureware by electron beam irradiation. Next, we will explore the applications of the more current literature.

1.2.2 Applications of cell sheet constructs

1.2.2.1 Corneal constructs

Approaches have been explored to treat patients that have experienced vision loss or impairment caused by damage done to the outer epithelium layer of the cornea. Corneal cell sheets are subcultured at 37 °C for 2 weeks. The damaged corneal cells are removed from the patient and replaced with the harvested cell sheet [42]. Attachment of the corneal cell sheet to the eye is done without sutures due to the presence of the “sticky” ECM [43]. These cell sheets are autologous in nature. If a patient suffers from damage in just one eye, epithelium cells from the healthy cornea are taken [43]. A methodology has even been developed for cases in which the patient has severe damage in both eyes. In this case, oral mucosal epithelial cells are used [42]. Studies with these constructs have gone to clinical trials and the patients demonstrated recovery from the vision loss that the corneal damage had previously caused [41].

Additionally, constructs have been made to replace the corneal endothelium [26, 39]. These cells do not proliferate *in vivo*, but can be manipulated to proliferate *in vitro*. Cell sheets of endothelium cells made *in vitro* can thus be used to replace the damaged endothelium *in vivo* that the body does not naturally repair. The endothelium cell layer plays an important role in maintaining the thickness and hydration of the corneal stroma. Transplantation of these cell sheets were performed in a rabbit model. This study demonstrated a marked difference in the hydration and thickness of the corneal stroma pre and post-operation, indicating that the implanted endothelium cell sheet was functional [39].

1.2.2.2 Cardiac constructs

Successful culture and harvesting of cardiomyocytes on thermally responsive cultureware has led to the development of cardiac constructs. Beating cardiac tissues can be formed by layering several sheets of cardiomyocytes that resembles native cardiac tissue [38]. Layered cardiomyocyte sheets have been implanted on host hearts. Results have shown that the tissue integrates with the host and that they beat synchronously after 45 minutes [38]. These implants form a well-organized vascular network with the host heart and demonstrate an ability to repair cardiac muscle [30] with a long-term survival of more than one year [36]. Vascularization, however, can be limited. Effective vascularization is observed when 3 or fewer sheets of cardiomyocytes are used. If a thicker graft is required, vascularization can be achieved by multiple implantations of three layer cardiomyocyte cell sheet constructs. After sufficient vascularization of the first construct has occurred, a second construct can be implanted. This process can be repeated until the desired thickness is achieved [37].

Other outlets in cardiac constructs are also being explored. Research with skeletal layered myoblasts is ongoing and initial results demonstrate improved cardiac function [25, 28, 29]. Also, mesenchymal stem cell sheets are being explored for their potential to repair heart damage [31].

1.2.2.3 Esophageal constructs

Methods have been developed to repair esophageal voids from removal of cancerous lesions by implantation of autologous cell sheets. Oral mucosal epithelial sheets are cultured and transplanted by endoscopy. These sheets have been shown to improve wound healing and reduce ulceration, which is commonly seen without the implant [33].

1.2.2.4 Future cell sheet engineered constructs

Cell sheet engineered constructs are moving toward whole organ development, with pulsatile myocardial tubes [35] and miniature liver systems [32] already having been developed. Further work is also being done with periodontal cell sheet constructs and tracheal constructs. The advantages of cell sheet engineered constructs are abundant and the continued exploration of this field could revolutionize the tissue engineering field. Consider first and foremost, that this approach is scaffold-less. Researchers need not worry about potentially harmful degradation products or foreign body responses with the implant of cell sheet devices. Further, many of the cell sheet constructs that have been developed use autologous cell sources thereby eliminating the concern for host rejection. These are very real concerns for devices made with scaffolds

Additionally, cell sheet constructs are unique in that they are devices made from contiguous monolayers of cells. These monolayers have an intact layer of ECM proteins and the cells have formed gap junctions as a means for intracellular communication. The ECM layer is “sticky” allowing for implantation without the need for sutures. Gap junctions allow for the construct to not only communicate with other layers of cells within the construct, but also with the host as was demonstrated by the synchronizing beats of the cardiac constructs. Further, complicated constructs with different cell types, can be made very precisely by layering cell sheets. With these advantages known, there has been an effort to improve upon the methodology for making thermally responsive cultureware. Without compare, the most widely used method has been by electron beam irradiation. This method and methods employed by other groups will be briefly explored in the following section.

1.2.3 Emerging technologies

1.2.3.1 Electron beam irradiation

Electron beam irradiation is the technique utilized by Dr. Teruo Okano's group at Tokyo Women's Medical University, the founder of cell sheet engineering. Briefly, a solution of the NIPAAm monomer is irradiated with an electron beam. Through surface activation and free radical polymerization the polymer is immobilized onto tissue culture polystyrene dishes. Dishes are washed with water to remove any unreacted monomer, dried and then sterilized by low temperature ethylene oxide prior to use [16]. Okano's group has been working on this technology since their first publication in 1990.

Since then, Okano's group has studied the mechanism by which cells release [19] and optimal release conditions. They found that grafted pNIPAAm layers are ideally within the range of 20-30 nm and that cellular adherence is impeded even above the polymers LCST if the graft thickness exceeds 30 nm [21]. They have been able to demonstrate the use of this cultureware for a variety of cell types and have conducted many studies with animal models. Studies with their ocular constructs have even gone to clinical trials with positive results [41].

From this technology a small start-up company was founded. CellSeed is a Japanese company that specializes in commercially manufacturing thermally responsive cultureware. These dishes are made by electron beam irradiation as described by Okano. Dishes from this company are convenient to use, however they are also very expensive to purchase. A case of 6 12-well dishes will cost \$195.00. This high cost may be due to manufacturing or quality assurance problems. Whatever the reason is for this high cost, it has led other to investigate alternative methods for making thermally responsive cultureware.

1.2.3.2 Plasma polymerization by radio frequency glow discharge

Plasma polymerization is a reasonable jump from electron beam irradiation as a means for making thermally responsive cultureware. The reason for this is that the reaction mechanism is the same. Plasma coating surfaces results in an adhesive film that is uniform and free from pinholes [17]. Dr. Buddy Ratner's group has explored the use of radio frequency glow discharge (RFGD) as a means for depositing pNIPAAm onto tissue culture surfaces.

To make thermally responsive cultureware by RFGD, the surfaces are first primed with pure plasma. NIPAAm vapor was gradually introduced into the system as the power was reduced and reacted with the primed surface. Due to the high energy environment of the plasma, samples were chemically analyzed. Plasma polymerization often results in the breaking of bonds randomly therefore the deposited film may no longer chemically retain the monomeric structure. Ratner's group found that they were able to retain the monomeric structure and the LCST [34]. They have had success in culturing bovine aortic endothelium cells on these surfaces and have observed release after a 2 hour incubation at room temperature.

This system is advantageous because it is a solvent free system. The TCPS surface is exposed to only the substrate with which it is being modified by. Further, plasma processes are sterilizing, therefore no additional steps are required. However, RFGD must be done under vacuum conditions. The Ratner group found that there was an inherent variability in the film thickness from batch to batch. However, unlike the electron beam irradiation process, they found that this variability in film thickness did not prevent the adhesion of cells [22, 23].

1.2.3.3 UV crosslinking

UV crosslinking has also been used to make thermally responsive cultureware. By this method a copolymer of 4-(N-cinnamoylcarbamide)methylstyrene and NIPAAm was synthesized. This copolymer was dissolved in solution of toluene and 1-butanol and placed in the bottom of a TCPS well. The solvent evaporated in the dark at room temperature and atmospheric pressure for 2 days before exposure to UV light. Plates were then rinsed with ethanol to remove any unreacted monomer. These plates demonstrated an ability to adhere bovine aortic endothelium cells and successfully release the adhered cells after 3 hours of incubation at 20 °C [40].

NIPAAm immobilization by chemical means has advantages as well. The chemistry of this methodology is more controllable when compared to plasma chemistry and very well defined. Therefore, the resulting film chemistry will be predictable. Further, the chemistry can be specifically tailored such that other biologic molecules could be attached to the surface if desired. However, this multi-step process requires the use of many solvents that are potentially harmful to cells. Further, the UV-crosslinking is not always going to be repeatable, therefore variation is seen layer thickness. This variation, however, did not adversely affect cellular adherence [40].

1.2.3.4 Atmospheric pressure plasma liquid deposition

A new technology has been developed by Dow Corning Plasma Solutions. This technology, known as atmospheric pressure plasma liquid deposition (APPLD), is a plasma system that operates at room temperature. Unlike the RFGD plasma technology previously discussed, vacuum pressures are not required. Further, the APPLD system works as a pulsed plasma, not a continuous wave plasma. Pulsed plasmas have been shown to retain a predictable

film chemistry [44]. In other words, pulsed plasmas target the same bonds that would be targeted in traditional chemical polymerizations. Therefore, APPLD users need not worry that the chemical structure will be adversely affected by this plasma process. Offering all of the benefits of traditional plasma chemistry and a few more, this system may be ideal for the immobilization of pNIPAAm onto TCPS. These benefits include: operation at room temperature while under atmospheric pressure, predictable film chemistry, preservation of sterility, control of deposition and programmability. Plasma technology and more specifically this APPLD technology will be further explored within this thesis.

1.3 PLASMA TECHNOLOGY

Plasma is referred to as the fourth state of matter. It is formed by supplying molecules in the gaseous state with additional energy, resulting in an ionized mixture. This highly reactive mixture contains negatively charged free electrons and ionic species [45]. Plasmas can be divided into two basic types, thermal and nonthermal. Simply put, thermal plasmas are in thermal equilibrium whereas nonthermal plasmas are not. More specifically, the free electrons generated by the energized gaseous mixture are extremely hot. When those electrons are in thermal equilibrium with the other ions in the plasma mixture, a thermal plasma is formed. These plasmas can reach temperatures of several thousands Kelvin [46]. The electron temperature on nonthermal plasmas is still hot, but does not equal the temperature of the ionic species, which remains cool. Therefore, the bulk of the plasma is cool. Nonthermal plasmas operate at ambient temperature and are typically formed under vacuum conditions [47]. Both thermal and nonthermal plasmas will be discussed in more detail.

There are three basic types of electrical discharges that can strike a plasma: corona, glow and arc discharge. Figure 1-4 shows the how these discharges are related to current and voltage. The APPLD system creates a plasma by a glow discharge. This discharge is formed at low currents and intermediate voltages. Glow discharges are nonthermal [46].

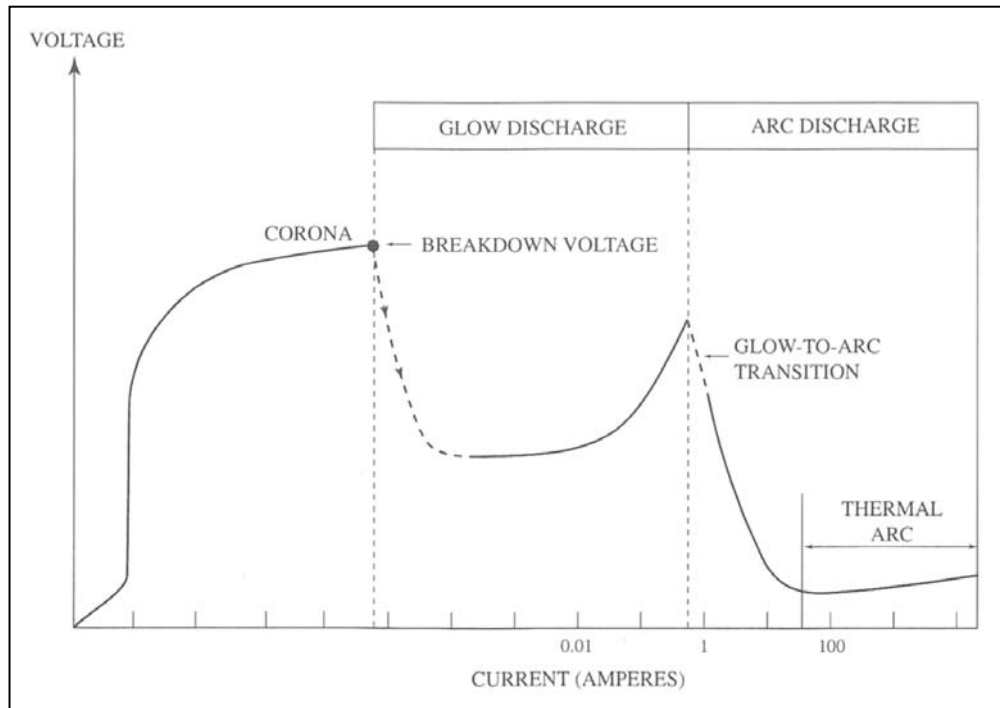


Figure 1-4 Voltage as a function of current as it relates to the generation of three basic types of electrical discharges. Reprinted from [52].

1.3.1 Thermal plasma

Thermal plasmas can be generated by a variety of sources including electric current, radio frequency waves, or microwaves [46]. They are generated at ambient pressure by feeding a carrier gas between a cathode and an anode. A high-energy arc discharge is generated in the gap between the anode and cathode. Plasma is created by flowing a carrier gas through this arc discharge. There are two basic types of thermal plasma generators, the non-transferred arc

plasma and the transferred arc plasma. In a non-transferred arc plasma the cathode is embedded within the walls of the electrode. This is the type of technology used in plasma spray guns. Plasma spray technology introduces fine particulates, which are often times either metallic or ceramic, into the mixture [48]. In the field of biomaterials, researchers have used plasma spray technology to coat metals with hydroxyapatite to improve the biocompatibility and increase cellular adhesion of osteoblasts with an implanted orthopedic device [49].

Thermal plasmas have the highest energy density of all plasmas [50] and are extremely hot. The tip of the plasma flame can reach temperatures of about 2000 K, with the internal core of the plasma flame exceeding temperatures of 30,000 K. Due to such extreme operating temperatures, the plasma jet is able to melt particulates, typically metallic or ceramic, that are introduced into the plasma flame. They are deposited as a thin film onto a substrate. Despite the heat in the plasma flame, a coated substrate rarely reaches temperatures above 150 °C [46]. The substrate is significantly cooler than the plasma flame, but applications of thermal plasma technology in the field of biomaterials are severely restricted. This technology has been used most often in orthopedic and dental research to modify biomaterials, as the substrates being modified are able to withstand the harsh operating temperatures [49].

1.3.2 Nonthermal plasma

Due to the operating temperature, nonthermal plasmas are more commonly used to modify biomaterials. They are able to operate at a lower temperature because the frequency of collision at the atomic level is lower, enabling the bulk of the plasma, or more specifically the ionic species, to remain at or near ambient temperature [51]. The collision frequency is directly

proportional to the plasma density, which is also lower in a nonthermal plasma [52]. Nonthermal plasmas are often ignited under vacuum pressures. Ion temperature increases with system pressure as plasmas trend toward thermal equilibrium seen in Figure 1-5.

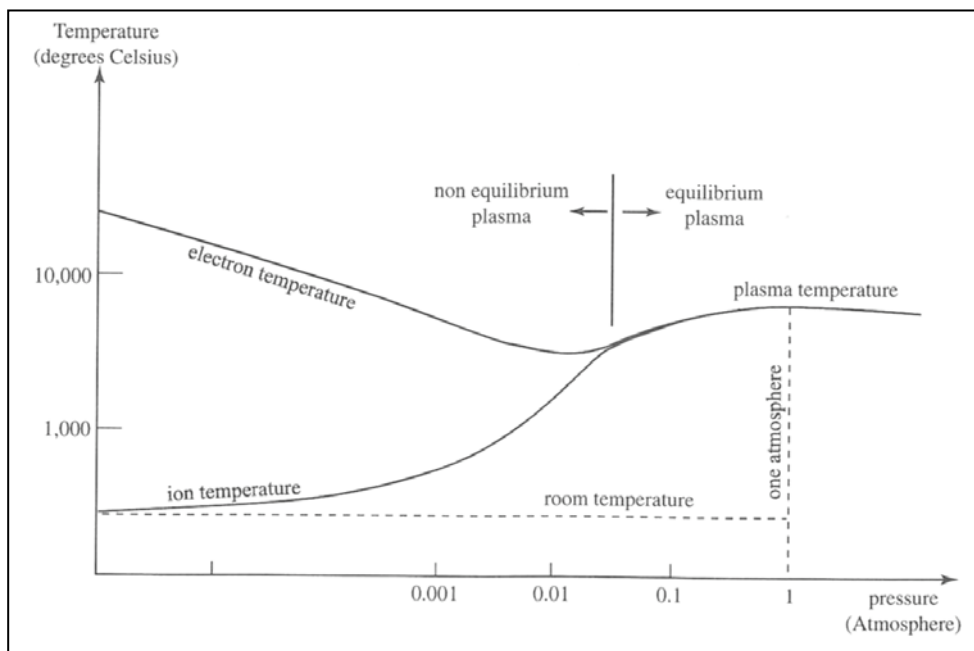


Figure 1-5 Temperature profile of the electron and ion temperature as a function of pressure in both nonthermal and thermal plasmas. As the pressure approaches atmospheric pressure a transition occurs and thermal plasma is generated. Reprinted from [52].

By generating a cold plasma, materials with lower melting temperatures or those that are susceptible to heat damage can be modified. Tissue culture polystyrene, for example, is made more hydrophilic using nonthermal plasma technology [53]. On the contrary, TCPS would melt if thermal plasma spray technology was used.

Additionally, nonthermal plasmas can be used for the plasma polymerization of monomers. Plasma polymerization can result in a film chemistry that is not replicable by traditional synthesis methods. Chemical polymerization schemes are designed to attack specific bonds. Plasma polymerization will nonselectively break bonds in a monomer, forming a

complex, crosslinked polymer that adheres to the surface of a substrate [54]. Glow discharges are commonly used for plasma polymerization [55]. A general schematic for RFGD can be seen below in Figure 1-6. RFGD has also been used to functionalize biomaterial surfaces with reactive groups such as amines [56, 57], hydroxyl groups [58, 59] and carboxyl groups [60, 61]. Functionalizing the surface has enabled the attachment of proteins, peptides and enzymes, as well as other biologic molecules [62]. The glow discharge formed here is the same type of plasma discharge found in the APPLD system.

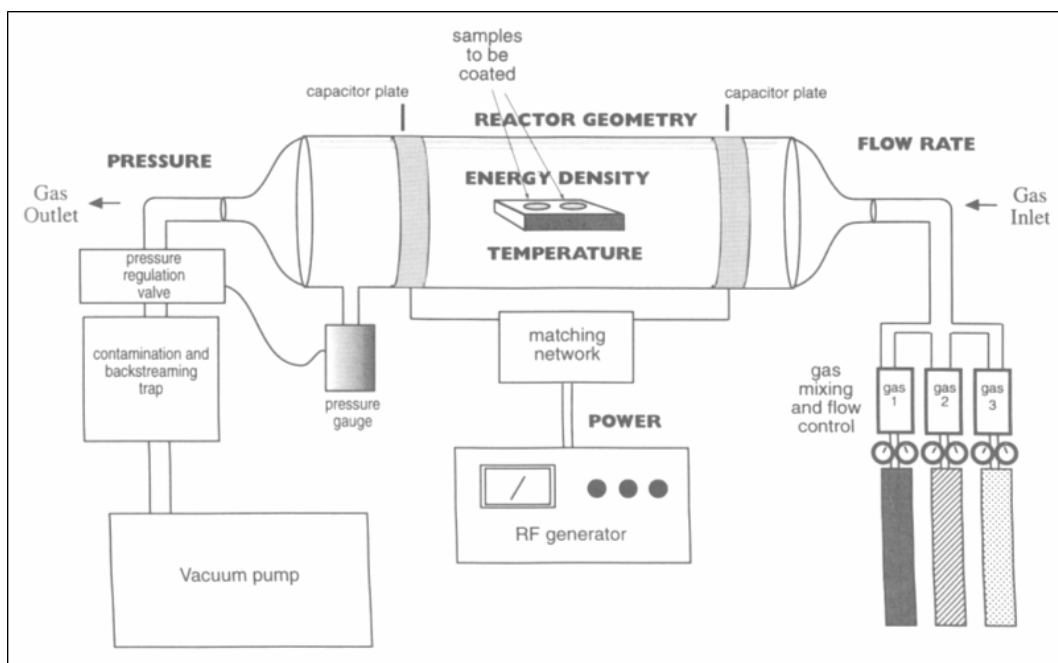


Figure 1-6 Radio frequency glow discharge. The vacuum pump on the left is used to reduce the pressure of the reactor. A radio frequency generator, in the center, is used to supply energy to the gases that are supplied on the right. Samples inside the reactor are modified by glow discharge that is produced. Reprinted from [17].

Nonthermal plasmas have many advantages over thermal plasmas, however, there are some drawbacks to the technology. For instance, the surface modifications must be done in a batch process as vacuum pressures are required [63]. Since modifications have to be made in a batch process, the film chemistry can vary. This is especially true for plasma polymerized

monomers [17]. Also, since the process is done under vacuum, the reactants must be fed in as a vapor to maintain the low pressure.

1.4 ATMOSPHERIC PRESSURE PLASMA LIQUID DEPOSITION

Dow Corning Plasma Solutions developed a system that incorporates the advantages of a thermal plasma, mainly the operating pressure, with that of a nonthermal plasma, mainly the operating temperature. In the APPLD system a liquid precursor is fed through a nebulizer. In the nebulizer, the liquid stream meets with a nebulizing gas stream and aerosolized droplets are formed. Downstream, these droplets combine with a highly charged process gas and undergo a physical change in matter, from a liquid to a plasma. The material reacts in a nozzle and is deposited onto a substrate [47, 63, 64]. In this study we worked with two versions of the APPLD system, the pre-production model, or the beta version, and the SE-2100 PlasmaStream workstation, the first production model. The general operating principles of these two systems were the same, but the system setup was vastly different. These two production models will be looked at in closer detail, but first the general operating principles will be discussed.

The APPLD system operates as a pulsed plasma [47]. Pulsed plasma is created by supplying intermittent waves of energy to the system. Pulses are measured in terms of duty cycle, or the ratio of plasma on-time to the total time in one pulse period. Chemical reaction by free radical polymerization initiates with the first pulse of energy and the polymerization reaction is propagated by each subsequent pulse. Activated monomers can react during the plasma off-time and the reaction is terminated when the plasma is turned off [65]. Pulsed plasma systems have been shown to produce a more predictable and controllable film chemistry when compared

to continuous wave plasmas [66-68]. Limiting the energy supplied to the system increases the probability that the chemical structure of the monomer will remain intact and that the plasma polymerization of that monomer will occur around a reactive chemical group, such as a vinyl group [65]. In the beta version, we had the ability to control the duty cycle. This operating parameter was removed from the production model. Instead, the SE-2100 PlasmaStream workstation allowed users to control the percentage of power used to ignite a glow discharge.

The APPLD system creates a plasma glow discharge by Penning ionization [69]. Helium atoms in an excited, metastable state collide with monomers in solution. This collision results in a transference of energy, with the helium atoms returning to a ground level state and the target monomers becoming activated for reaction by free radical polymerization [70]. It has been shown that a stable glow discharge can be achieved with lower voltages when helium is used as the process gas [71, 72]. For this reason, helium gas will be used in all of the following experiments.

The APPLD system creates a plasma directly from aerosolized liquid droplets, as opposed to the vaporized monomers that are required in vacuum plasma systems. Optimal films are formed with droplets measuring 10 to 50 μm in diameter, although they can be as large as 100 μm . Droplets exceeding this diameter range may not transition entirely from a liquid state to a plasma state, resulting in the deposition of a wet film [73]. Figure 1-7 shows a schematic of the nebulizer from the SE-2100 PlasmaStream workstation and the aerosolized droplets it creates.

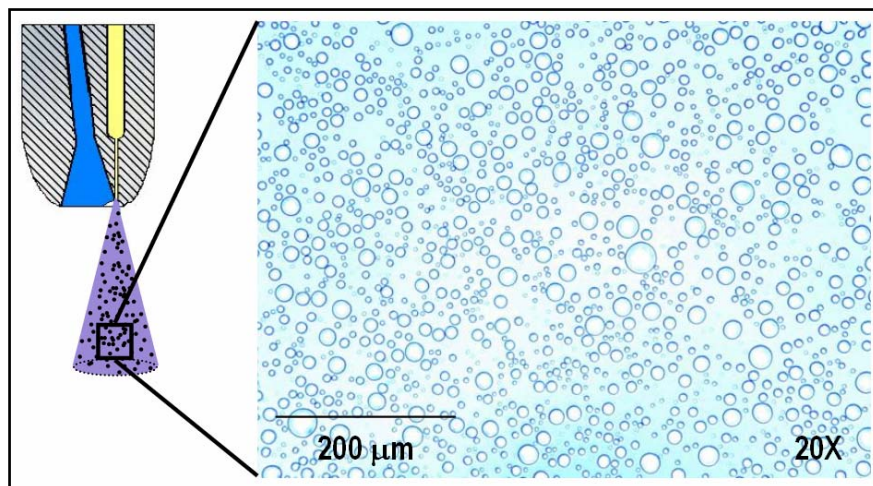


Figure 1-7 Left, schematic of the nebulizer used in the SE-2100 PlasmaStream workstation. Helium is used as the nebulizing gas. It flows down the left side of the nebulizer and the liquid line flows down the right side. The liquid and gas streams meet at the tip and aerosolized droplets are formed. Right, an image of the droplets formed by the nebulizer were captured on a light microscope.

Samples are placed on a table for modification. The plasma head can move in the x-, y- and z- directions over a sample and the user controls the rate at which the plasma head moves. The exact deposition pattern is controlled through the use of computer number control (CNC) programming. This programming uses G-code language and enabled us to develop programs to coat TCPS and glass slides, as well as 6- and 12-well plates.

The APPLD system operates at close to ambient temperatures, typically generating a plasma in the range of 30 °C to 40 °C. The generated plasma can, however, be as cool as 20 °C or as hot as 70 °C [51]. As previously mentioned, the system operates at atmospheric pressure. Power is supplied by a regular 120 V outlet and is run through a high voltage generator. A programmable syringe pump is used to deliver the liquid to the system and the process gas flow rate is controlled by a rotameter.

Both the pre-production model and the SE-2100 PlasmaStream workstation allows for the user to control the liquid solution flow rate, the process gas flow rate, the height of the plasma nozzle and the speed of the plasma head. User controlled parameters independent of the APPLD

system includes the solution concentration, the process gas composition, the pattern of deposition, and the amount of time that the substrate is exposed to the plasma. All of the above parameters can affect the chemistry of the resulting film.

The pre-production model of the APPLD system is pictured in Figure 1-5 and the SE-2100 PlasmaStream workstation is pictured in Figure 1-6. The set-up of these two systems are very different and will be looked at in closer detail.

1.4.1 APPLD pre-production model

The pre-production model of the APPLD system is composed of two main units. In Figure 1-5, the unit on the left houses the high voltage generator, the control panel and the computer for controlling the x-, y- and z- motion of the plasma head. The unit in the center contains the plasma head, the electrode and the programmable syringe pump. The picture on the right is a close-up of the electrode, which is housed within the plasma head.

In this system, a minimum solution volume of 2-mL is required to fill the tubing between the syringe pump and the liquid feed to the electrode. The electrode is composed of two concentric cylinders. The inner cylinder carries the nebulizing gas and the outer cylinder carries the liquid. At the exit of the electrode, the tip of the nebulizing gas line is crimped so that it can aerosolize the liquid feed. The process gas is energized by the high voltage generator creating helium atoms in a metastable state. The aerosolized liquid droplets meet the energized process gas at the letter “h” in Figure 1-8. The plasma reacts in the nozzle and is then deposited onto substrates that are placed on the CNC table.

In this pre-production model, we were able to coat any nonconductive substrate. However, due to the conductive nature of the plasma, materials that were also conductive, such

as silica wafers, would burn. This limitation of the pre-production model was addressed in the SE-2100 PlasmaStream workstation, in which a counterelectrode was included and could be attached to the plasma nozzle. We used the pre-production model to conduct preliminary experiments of NIPAAm monomer polymerization and deposition. We coated substrates using the 3-pass program for TCPS slides and 6-well plates.

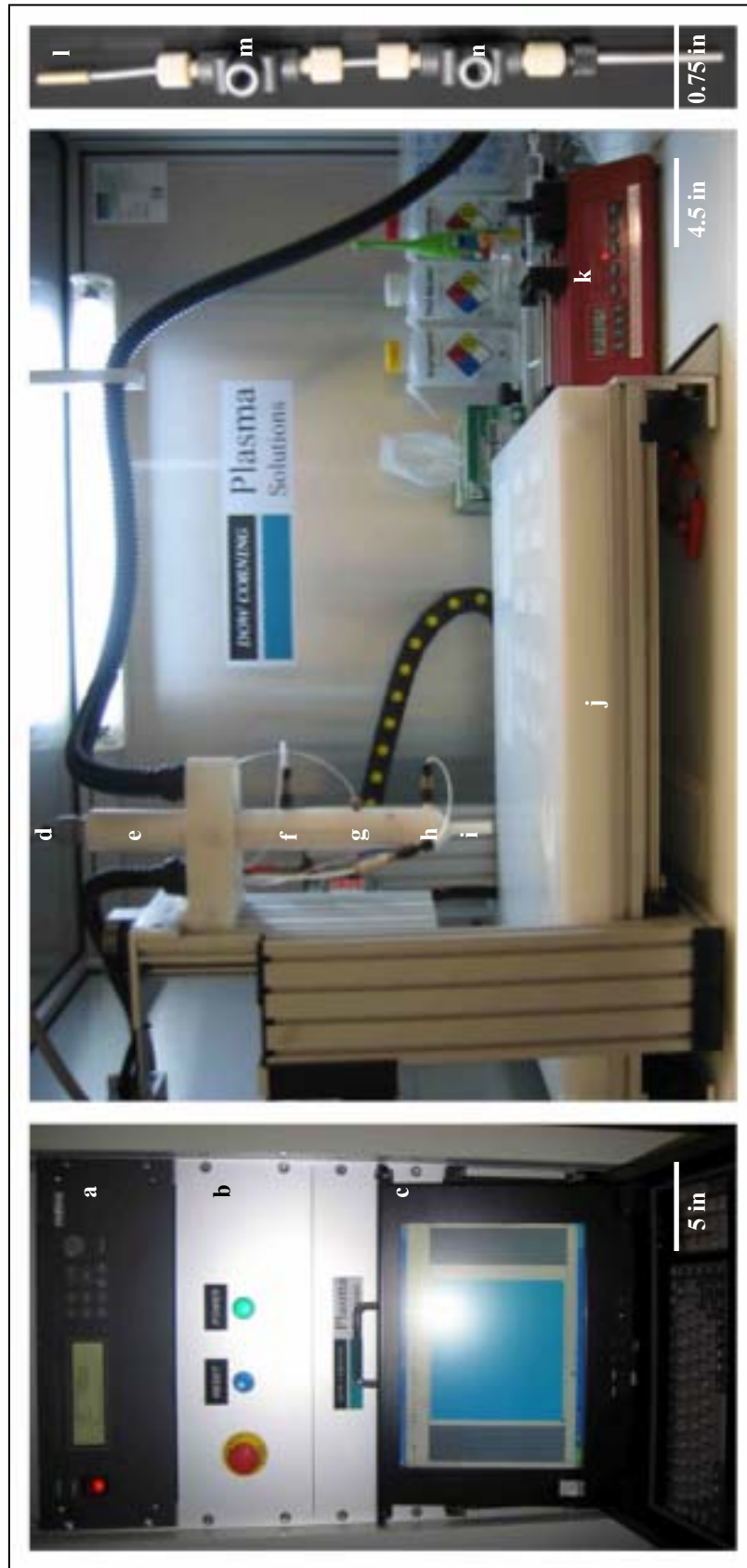


Figure 1-8 Pre-production model of the APPLD system. Left, (a) user control panel, (b) high voltage generator, (c) computer. Center, (d) high voltage input, (e) plasma head, (f) nebulizing gas line, (g) liquid line, (h) process gas line, (i) plasma nozzle, (j) CNC table, (k) programmable syringe pump, (l) high voltage lead, (m) nebulizing gas feed, (n) liquid line feed

1.4.2 APPLD SE-2100 PlasmaStream workstation

The SE-2100 PlasmaStream workstation is housed entirely in one unit. The machine is connected to an external computer by a USB cable. The nebulizers used in this model were purchased from Burgener Research. A schematic of these nebulizers is shown in Figure 1-4. In this system, the liquid feed enters through the top of the nebulizer and the nebulizing gas enters through the side. These two streams meet at the tip and an aerosolized liquid is formed. The process gas is fed into the electrode housing and flows past two parallel electrode pins. The electrode pins are powered with approximately 100 W at 100% power. This energizes the helium and a glow discharge is formed. The aerosolized liquid enters the glow discharge at letter “j” in Figure 1-6. This activates the monomers in solution for polymerization in the plasma nozzle and films are deposited onto substrates.

During the course of this study, two different types of electrode housings were used. The first electrode housing was composed of Teflon, a soft material. This electrode housing was difficult to seal and, as a result, plasma arcing occurred. Plasma arcing can be observed if air, or more specifically oxygen, is introduced into the system. As air leaked through the seal into the system, a plasma arc was formed and channels were bore into the soft electrode housing. With these channels, the electrode was even more susceptible to plasma arcing. To remedy this, a new housing, made from a more robust ceramic material, was used. This electrode housing was redesigned and the parallel electrode pins were made accessible for cleaning without the need to open the housing. In Figure 1-9, the electrode housing pictured is made from a ceramic material.

In general, the SE-2100 PlasmaStream workstation is a more user friendly model of the APPLD technology. It is easier for the user to access the nebulizer, making the system easier to clean, especially when there is a residual build-up on the nebulizer tip. Further, the void volume

in the liquid line is less than 200 μL , making it possible to coat substrates when only a very small amount material is available. Finally, all system parameters are input in the control panel, which is on the outside of the unit. This enables the user to change parameters while the system is operating. This was not possible in the pre-production model.

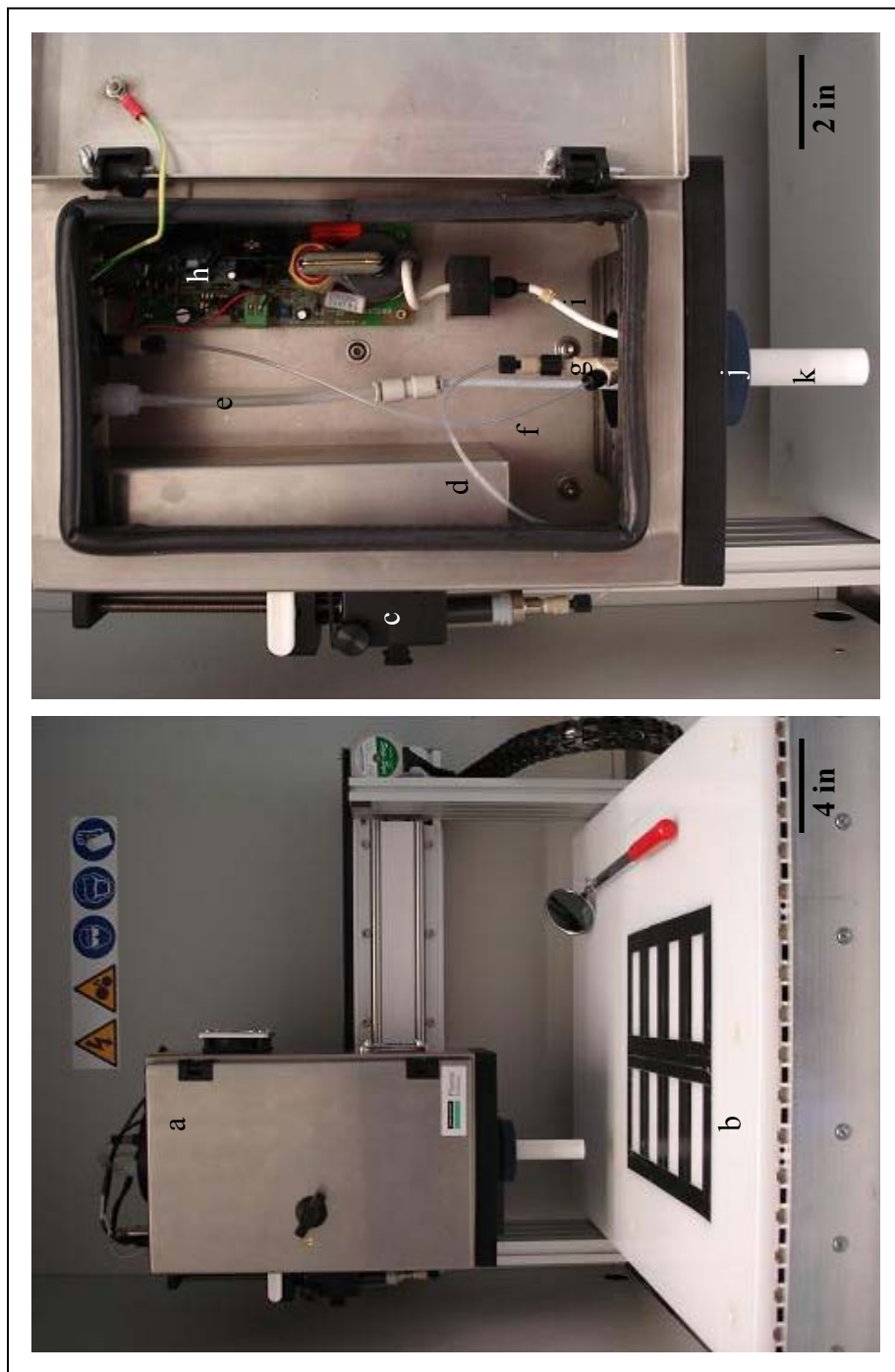


Figure 1-9 SE-2100 PlasmaStream workstation. Left, (a) electrode housing and feed lines, (b) CNC table. Right, (c) programmable syringe pump, (d) liquid feed line, (e) process gas line, (f) nebulizing gas line, (g) nebulizer, (h) high voltage generator, (i) high voltage line, (j) electrode housing and (k) plasma nozzle

1.5 CNC PROGRAMMING

A major benefit to using the APPLD system is the control that the user has over the pattern of plasma deposition. CNC programs can be designed to coat materials regardless of shape and size. In the process of working with the APPLD technology, we developed a fundamental understanding of the G-code programming and were able to modify existing programs and develop basic new programs that were suitable for our applications. Figure 1-10 show the pattern of deposition of basic programs that we used.

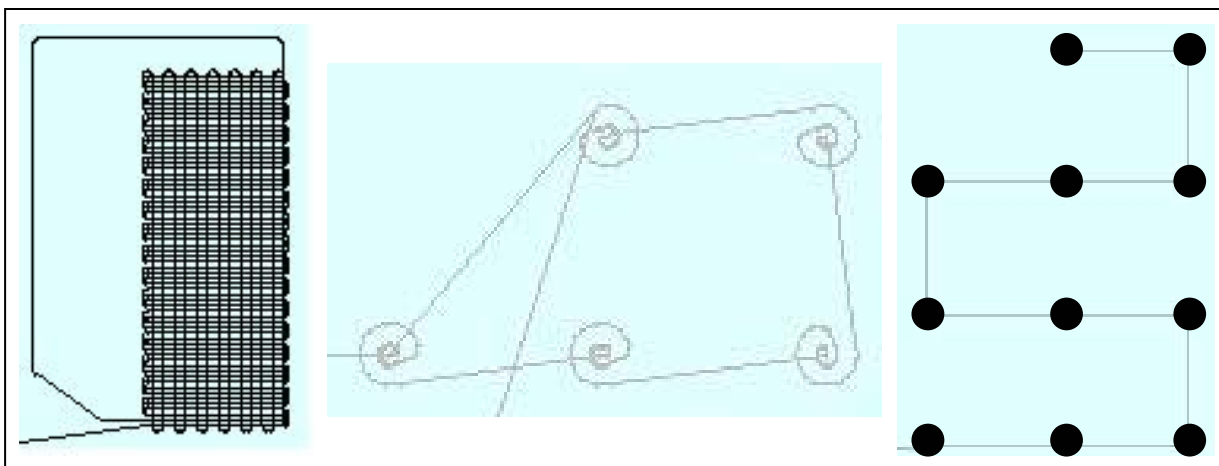


Figure 1-10 CNC programming for coating TCPS or glass slides (left), 6-well plates (center) or 12-well plates (right)

1.5.1 3-Pass program for TCPS or glass slides

The 3-pass program was used to coat any substrate that had dimensions of at most 25 mm \times 75 mm. Our primary use for this program was coating TCPS and glass slides. In the first two passes, the plasma head moved 30 mm across the width of the slide, while in the final pass the plasma head moved 80 mm along the length. No edge effects were seen on these surfaces since the plasma head moved beyond the boundary of the substrates. Modified slides were used

for surface and chemical analysis of the deposited APPLD films. This program was used in both APPLD system production models.

1.5.2 3-Pass program for 6-well plates

We needed to develop program to coat the bottom surface of 6-well plate for cellular studies. We wanted this program to be similar to the 3-pass program used for modifying slides so that reasonable assumptions could be made about the film characterization in the well plates. In the 6-well plate program, the plasma head moved in a spiral motion, starting in the center of the well and moving outward to the wall. Once a well was coated, the plasma head was raised and moved to a neighboring well. All but one well in the plate was coated and then the process was repeated until each well was coated 3 times. This program was used in both APPLD system production models

1.5.3 CNC spot program for 12-well plates

The nozzle of the pre-production model was approximately 1-cm in diameter smaller than the nozzle of production model. This difference in diameter reduced the number of turns the larger nozzle could make per well, thereby reducing the total coating time. Further, the smaller diameter nozzle was able to coat closer to the well wall than the large diameter nozzle. For these reasons, a 12-well plate program was developed for the use with the SE-2100 PlasmaStream workstation. In the 12-well plate program the plasma head was lowered into each well and remained stationary for a predetermined amount of time. The plasma head was then raised and moved to a neighboring well. The program ended when 11 of the 12 wells were coated. One well (A4) was left blank to serve as an internal control. TCPS slides were also coated with this program so that these films could be characterized.

1.6 SPECIFIC AIMS

The current methods for depositing pNIPAAm onto TCPS in order to create thermally responsive cultureware have advantages and disadvantages. For instance, electron beam irradiation system has been the gold standard for 19 years, but the high cost is a drawback. RFGD modifications have proven to be inconsistent with batch to batch variations of the process. And chemical modifications are multi-step processes that require the introduction of highly toxic solvents. The APPLD technology developed by Dow Corning Plasma has the benefits of the RFGD technology and electron beam irradiation in that the process is done in one step. But, unlike RFGD, the APPLD system is operated at atmospheric pressure. Further, like chemical modification schemes, polymerization of the NIPAAm monomer by APPLD could result in a film with a predictable chemistry.

Our hypothesis is that the APPLD technology developed by Dow Corning Plasma Solutions has potential biological applications for modification of surfaces.

The goal of this dissertation is to explore these potential uses and to compare the APPLD deposition system to more traditional methods of surface modification. We propose a model system using tissue culture polystyrene (TCPS) as the substrate for deposition of the monomer N-isopropylacrylamide (NIPAAm). These APPLD coatings will be compared to films formed in a low-pressure plasma deposition system and to those formed by electron beam irradiation. This model system will give us a fundamental understanding of the APPLD system and allow us to

develop other uses for the technology. Based upon these areas of research, the aims for the present study were as follows:

Specific Aim 1: Through APPLD, polymerize the monomer N-isopropylacrylamide and deposit onto tissue culture polystyrene in a manner that enables a desired biological effect. We hypothesized that the NIPAAm monomer could be polymerized by APPLD around the vinyl group without altering the chemical structure of the polymer, thereby preserving the lower critical solution temperature (LCST) of 31 °C. Furthermore, cells could be cultured on tissue culture polystyrene modified with the APPLD polymerized NIPAAm and removed from the surface simply by lowering the temperature below the LCST. This hypothesis was tested by depositing APPLD polymerized NIPAAm onto TCPS slides and culture plates. The polymerization chemistry was characterized by nuclear magnetic resonance (NMR), gel permeation chromatography (GPC) and cloud point measurements. The functionalized surface was characterized by contact angle measurements and dual polarization interferometry (DPI). Further, the biologic functionality of the surface was characterized by growing NIH-3T3 cells to confluence on the modified tissue cultureware and then lowering the temperature to observe the release of cells from the surface.

Specific Aim 2: Use the APPLD system to deposit poly(N-isopropylacrylamide) and contrast the coating functionality with that of the APPLD polymerized NIPAAm films. We hypothesized that poly(N-isopropylacrylamide) (pNIPAAm) could be deposited onto tissue culture polystyrene by APPLD, and that no significant changes in the pNIPAAm chemistry would be observed. Further, the biologic functionality of the coatings would more effective in

removing cells when the temperature is lowered below the LCST because the dispersity of the polymer would not be as broad. To test this hypothesis, TCPS slides and culture plates were modified with pNIPAAm in the same manner that the NIPAAm surfaces were modified. The films were characterized by the same analysis discussed in the previous specific aim. Results of the pNIPAAm characterized films were compared with APPLD polymerized NIPAAm films.

Specific Aim 3: Demonstrate that the APPLD system can be used for other applications in the field of tissue engineering. We hypothesized that the APPLD system could be used to deposit biocidal compounds and that those compounds would retain their ability to kill bacteria. Further, we hypothesized that the APPLD system could be used to deposit biomolecules, such as enzymes, and that those biomolecules would retain their specific biologic activity. This hypothesis was tested by depositing the biocidal compounds onto glass slides and testing their efficacy against *Escherichia coli*. Furthermore, enzymes were deposited onto electrospun polyurethane fibers and their activity assayed.

2.0 APPLD POLYMERIZATION OF N-ISOPROPYLACRYLAMIDE: PRE-PRODUCTION MODEL

2.1 INTRODUCTION

Surface modifications are often made on materials and can range from simple to complex schemes and can be done for any number of reasons including, altering the surface hydrophobicity [74], functionalizing a surface for a chemical reaction [75] or immobilizing biological molecules [76]. In more general terms, surfaces are modified to make materials more biocompatible or to achieve a desired biologic affect. This can be accomplished by a variety of methods like plasma and solvent coating, UV irradiation and chemical reaction. Ideal surface modifications result in a thin film that preserves the bulk properties of the biomaterial. It is also desirable to create a uniform coating across the surface of the biomaterial [17]. Surface modification by plasma technology can easily achieve these two goals [54].

Plasma processes have several advantages over other methods. For example, plasma processing not only results in surface modification, but also in sterilizing, a requirement for any implantable device or cell culture materials [54]. Further, the deposited thin film demonstrates good adhesion to the surface of the biomaterial [77]. The films can have unique chemistries and are not as susceptible to leaching as other chemically reacted or noncovalent coatings are. Advantages of using plasma processes extend beyond the characteristics of the coating itself, as

they can be applied a variety of materials, including polymers, metals and ceramics, regardless of shape [17].

Radio frequency glow discharge (RFGD) is a commonly used plasma technology for making surface modifications. The process is operated at room temperature and low pressure. Due to the operating temperature, RFGD can be used to modify most types of materials, with a limiting constraint of vacuum chamber size [63]. Plasmas generated at atmospheric pressure, such as those generated in a plasma spray torch, are high temperature plasmas. These plasmas can reach temperatures of greater than 8000 K [54]. This operating temperature may be acceptable if a thin metal coating is desired or for modification of a ceramic material, but would not be suitable to modify a polymer that melts at a lower temperature [17].

Dow Corning Plasma Solutions has developed an atmospheric pressure plasma liquid deposition (APPLD) system. This new technology offers all of the same advantages that traditional plasma technology offers and more. The APPLD system generates a “cold” plasma at room temperature. Traditional plasma technology allows the user to choose only one, a nonthermal plasma at vacuum pressures or a thermal plasma at atmospheric pressure. Further, plasma deposition can be patterned using the APPLD system. Patterns are designed by the user to suit individual needs and are precisely controlled by a computer. Traditional plasma technology would require masking in order to achieve specific surface patterning. Dow Corning Plasma Solutions has spent an extensive amount of time in developing uses for this new technology for specific chemical applications. It is our objective to explore this technology for biological applications. Thermally responsive cell culture surfaces have been extensively studied and therefore make an ideal model system [6, 14, 16, 19, 21-23, 34, 40].

In the study described herein, we will explore the use of atmospheric pressure plasma liquid deposition as a means for polymerizing and depositing N-isopropylacrylamide (NIPAAm). Contrary to other plasma polymerization methods, we will create a plasma at atmospheric pressure directly from a liquid solution. We will characterize the surface reactivity of TCPS modified with APPLD polymerized NIPAAm (plasma polymerized or ppNIPAAm) at temperatures above and below the LCST. We will also explore methods for optimizing the adhesion of ppNIPAAm to TCPS and glass surfaces. Eliminating the use of trypsin for the removal of cells from TCPS is beneficial for fragile cell lines [16, 20]. Therefore, this study will evaluate the effectiveness of the ppNIPAAm in removing a confluent monolayer of cells from the surface of TCPS.

2.2 MATERIALS AND METHODS

2.2.1 Selecting APPLD parameters

N-isopropylacrylamide (Aldrich) was purified by recrystallization from n-hexane. Isopropyl alcohol, IPA, (Aldrich) was used as received.

Three parameters in the pre-production model of the PlasmaStream were altered for the polymerization and deposition of NIPAAm, the number of times a substrate was coated, solution concentration and solution flow rate. All remaining parameters were held constant. Power was 160 W, helium flow rate was 20 L/min, CNC head speed was 11.7 mm/s, and the height of the plasma nozzle was 3 mm. Substrates were coated 3 or 5 times at a solution flow rate of 2, 5 or 10 μ L/min. Solutions concentrations ranged from 20-wt% to 60-wt%.

2.2.2 Surface characterization

The change in surface hydrophobicity was observed by measuring contact angles with a VCA Optima using 1.0 μL drop of deionized (DI) water. The contact angles were measured using the sessile drop method at temperatures above and below the LCST. Six measurements were taken per slide for slides modified using the 3-pass program. To remove any unbound materials remaining on the modified surfaces from the APPLD system TCPS slides were washed in DI water at either 50 °C or 4 °C for 1 hour and then dried. Contact angles were reassessed after each wash cycle.

Farfield Scientific has developed an instrument that enabled the measurements of wet layer thickness, mass and density. Traditional methods such as ellipsometry and atomic force microscopy (AFM) could not be used for various reasons. Ellipsometry, for instance, is measured on reflective surfaces like silica wafers, which are also conductive. Such surfaces cannot be modified using the APPLD system due to the high voltages employed. AFM would only allow surface analysis at a temperature below the LCST. Farfield's technology, dual polarization interferometry (DPI), enables measurements at temperatures as high as 40 °C and as low as room temperature. This system gives us an effective means of characterizing the ppNIPAAm layer above and below the LCST.

DPI works by shining a laser through a stacked waveguide and monitoring the changes in the resulting interference patterns. The waveguide, or the DPI chip, is composed of two layers. The bottom layer is the reference layer and contains one channel, channel 2. Channel 2 cannot be modified and is used to indicate if the DPI chip is damaged. The upper layer, known as the sensing layer, is composed of two parallel flow cells. These flow cells will be referred to as channel 1 and channel 3. Changes on the surface of channel 1 or channel 3 will alter the

interference pattern. It is these changes that are traced throughout the timecourse of an experiment. The raw data is measured in terms of two light polarizations, one vertical and the other horizontal. This raw data can be manipulated by the DPI software using Maxwell's equations yielding a discrete data point that reveals the refractive index and the mass of the surface bound molecule that is changing the interference pattern. From this data, wet layer thickness and density can also be calculated.

In these experiments, channel 1 of the DPI chip was modified with ppNIPAAm and channel 3 was left unmodified. Channel 3 was left blank because refractive index is a function of temperature. By leaving this channel blank, these changes in refractive index can be subtracted from the ppNIPAAm data, resulting in a dataset comprised solely of ppNIPAAm surface behavior. A running solution of DI water was flowed across the surface of the chip at a rate of 50 $\mu\text{L}/\text{min}$. The starting temperature of the experiment was 38 $^{\circ}\text{C}$ and was dropped 1 $^{\circ}\text{C}$ every 15 minutes until the temperature reached 26 $^{\circ}\text{C}$. Upon completion of the experiment, the chip was washed with 4 cycles of IPA injections. The instrument was then calibrated with 80% ethanol and DI water. The background data from channel 3 was subtracted from channel 1 and the data was resolved.

2.2.3 Functionalizing surfaces

Glass slides were functionalized with concentrations of vinyl-TMS ranging from 0.01-wt% up to 100-wt%. A solution of 100 mL of toluene was combined with 1 mL of the appropriate concentration of vinyl-TMS and 500 μL of triethylamine. Glass slides were added to the solutions they were heated to 80 $^{\circ}\text{C}$. Slides were removed after 1 hour, rinsed with acetone

and then air dried. Once dry, the vinyl-modified glass was coated using the APPLD system with a 40-wt% NIPAAm solution. Contact angle measurements were evaluated.

Glass slides were functionalized with hydroxyl groups by washing slides in a piranha solution. The slides were then rinsed with water and air dried. Once dry, the hydroxyl-modified glass was coated using the APPLD system with a 40-wt% NIPAAm solution. Contact angle measurements were evaluated.

2.2.4 Sterility analysis

The 3-pass program was used to coat TCPS 6-well plates with helium, helium+high voltage (HV), helium+HV+IPA, and helium+HV+40-wt% solution NIPAAm in IPA. Tryptic soy broth, TSB, (2 mL) was placed in each well of the modified plates. An unmodified TCPS plate was used as a control. The plates were placed in a 37 °C shaker overnight. Tryptic soy agar plates were divided into 6 sections, one section for each well. Three 10 µL drops of the incubated TSB were pipetted onto each section. The agar plates were placed in a 37 °C incubator and bacterial growth was monitored over a 4 day period.

2.2.5 NIH-3T3 cell culture

Culture media consisted of Dulbecco's Modified Eagle Medium, DMEM, (4.5 g/L glucose and sodium pyruvate), with additives of bovine calf serum, BCS, (10%), L-Glutamine (2%, 200 mM) and Pen/Strep (1%, penicillin 100 U/mL, streptomycin 100 mg/mL). Media was sterile filtered through a 0.22 µm polyethersulfone membrane. When a confluent layer of cells was observed, they were washed with Dulbecco's Phosphate Buffered Saline, PBS, (without calcium or magnesium) and removed from the culture flask with Trypsin-EDTA (1X). Removed

cells were used in an experiment, passaged for future experiments or frozen for future cultures. Frozen cells were placed in cryopreservation media and stored in liquid nitrogen.

2.2.6 Cell release studies

Well plates were modified with ppNIPAAm for cell release studies. One well of each plate was left blank and served as an internal control. This blank well was used as a qualitative indication of baseline cell growth for the plate. 6-well plates were coated using the 3-pass well plate program and used immediately for cell culture. After modification, the plates were rinsed with pre-warmed (37 °C) sterile PBS to remove any unbound materials on the surface from the APPLD deposition. NIH-3T3 cells were seeded at an approximate density of 1.0×10^4 cells/cm². The cells were grown to confluence using complete media, as described in the previous section. Once a confluent layer was observed, the cell media was removed and replaced with cold (4°C) PBS. The edges of the wells were scored and the plates were chilled for 30 minutes to observe cell release. Images of the cells were taken at times $t=0$, 15 and 30 minutes. Several control plates were also made for these experiments. These plates included unmodified TCPS plates, along with plates modified by HV and HV+IPA were used as control plates for these experiments.

2.2.7 Statistical analysis

Results are displayed as the mean \pm standard deviation. A two-tailed, paired student t-test was used to determine if the observed difference in the measured contact angles above and below the LCST was statistically different. Contact angle measurements made on each slide were averaged yielding a sample size of 3 or 4.

2.3 RESULTS

2.3.1 Selecting APPLD parameters

Several parameters could be changed in the APPLD system, but at the recommendation of Dow Corning Plasma Solutions only three parameters were investigated. These parameters, the number of times a substrate is coated, solution flow rate and solution concentration, were varied in some preliminary experiments to determine optimal NIPAAm deposition conditions. We first investigated the effect that the solution flow rate and the number of passes had on the thermal responsive behavior of TCPS, keeping the solution concentration constant at 50-wt%. Solution flow rates of 2-, 5- and 10- $\mu\text{L}/\text{min}$ were investigated (data shown in Table 2.1 below). We found that the flow rate of 2- $\mu\text{L}/\text{min}$ resulted in no observable spray from the APPLD system and therefore did not modify the TCPS substrates. As a result, no data was collected at this flow rate. Furthermore, we found that a flow rate of 10- $\mu\text{L}/\text{min}$ resulted in a significant build-up on the nozzle, clogging the APPLD system and resulting in non-uniform coatings. As a result, a flow rate of 5- $\mu\text{L}/\text{min}$ was selected for the pre-production system.

Table 2- 1 Varying system parameters of the pre-production APPLD system. Process parameters varied were the solution flow rate and the number of times of the substrate was coated. Optimal parameters for coating were found to be 5- $\mu\text{L}/\text{min}$ and 3 times coating and are italicized in the table below.

	<i>5-$\mu\text{L}/\text{min}$, 3X</i>		<i>5-$\mu\text{L}/\text{min}$, 5X</i>		<i>10-$\mu\text{L}/\text{min}$, 3X</i>	
	<i>50 °C</i>	<i>4 °C</i>	<i>50 °C</i>	<i>4 °C</i>	<i>50 °C</i>	<i>4 °C</i>
Pre-Wash	<i>26 \pm 1</i>	<i>16 \pm 2</i>	<i>56 \pm 1</i>	<i>53 \pm 2</i>	<i>26 \pm 1</i>	<i>15 \pm 2</i>
Post-Wash	<i>48 \pm 3</i>	<i>46 \pm 3</i>	<i>66 \pm 1</i>	<i>62 \pm 2</i>	<i>60 \pm 1</i>	<i>56 \pm 1</i>

Next, we investigated the number of times a substrate should be coated and compared the results of a 3-pass coating to a 5-pass coating (data shown in Table 2.1 above). Similar to the increased flow rate, the increased number of passes resulted in a greater prevalence of nozzle clogging. For this reason, the 3-pass program was selected for the pre-production system. It is

important to note that the 5- and 10- $\mu\text{L}/\text{min}$ samples coated with the 3-pass program both exhibited a significant change in surface hydrophobicity prior to the samples being washed. After one cold water wash cycle, however, the thermally induced change in surface hydrophobicity was no longer observable.

Solution concentration of NIPAAm significantly ($p < 0.05$) affected the surface hydrophobicity at temperatures above and below the LCST as seen in Figure 2-1. Concentrations of 30-, 40- and 50-wt% demonstrated a visible contact angle switch prior to washing and after one 50 °C wash cycle with DI water. The 20-wt% solution did not significantly modify ($p > 0.05$) the surface of TCPS slides. Data could not be collected for the 60-wt% solution because it was too concentrated causing the atomizer to clog. No significant change was observed in the surface hydrophobicity at any concentration after a 4 °C wash cycle with DI water. As a result, a NIPAAm solution concentration of 40-wt% was used in all future experiments.

From this data, a significant change in the surface contact angles is observed in samples before and after washing. Prior to washing, contact angle measurements are significantly lower. It was hypothesized that these lower contact angles were an artifact of residual, unbound material left on the surface from the APPLD system. Therefore, the surfaces were reassessed after wash cycles. Wash solutions were either at 50 °C, a temperature well above the LCST of pNIPAAm, or 4 °C, a temperature well below the LCST.

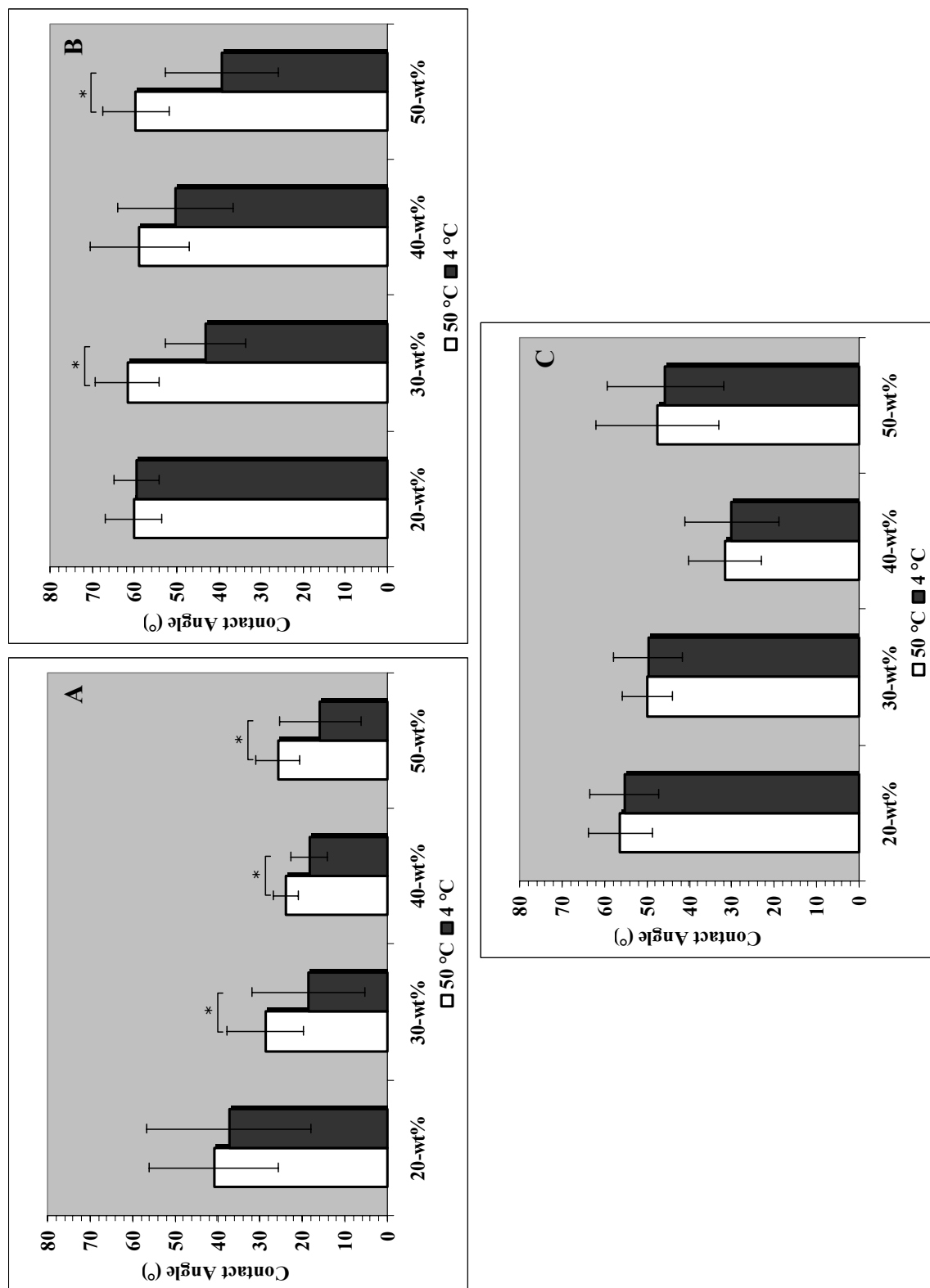


Figure 2-1 Contact angle measurements as a function of NIPAAm monomer concentration. A, pre-wash measurements. B, measurements taken after a 50 °C wash cycle. C, measurements taken after a 4 °C wash cycle. Bars represent the mean \pm standard deviation. White bars represent measurements that were made at 50 °C and the black bars represent measurements made at 4 °C. Bars marked with an asterisk represent a statistically significant difference ($p < 0.05$).

In summary, the following system parameters were used in all of the following experiments with pre-production model of the APPLD system: a power of 160 W, a helium flow rate of 20 L/min, a CNC head speed was 11.7 mm/s, a plasma nozzle height of 3 mm, a NIPAAm solution concentration of 40-wt% and a flow rate of 5 μ L/min, and a 3-pass program.

A DPI study was performed with the optimal system operating parameters to determine the wet layer thickness, mass and density of the ppNIPAAm coatings. Figure 2-2 shows how these parameters change with decreasing temperature. It can be clearly seen that the ppNIPAAm layer washes off of the surface with decreasing temperature. This data complements the contact angle measurement data.

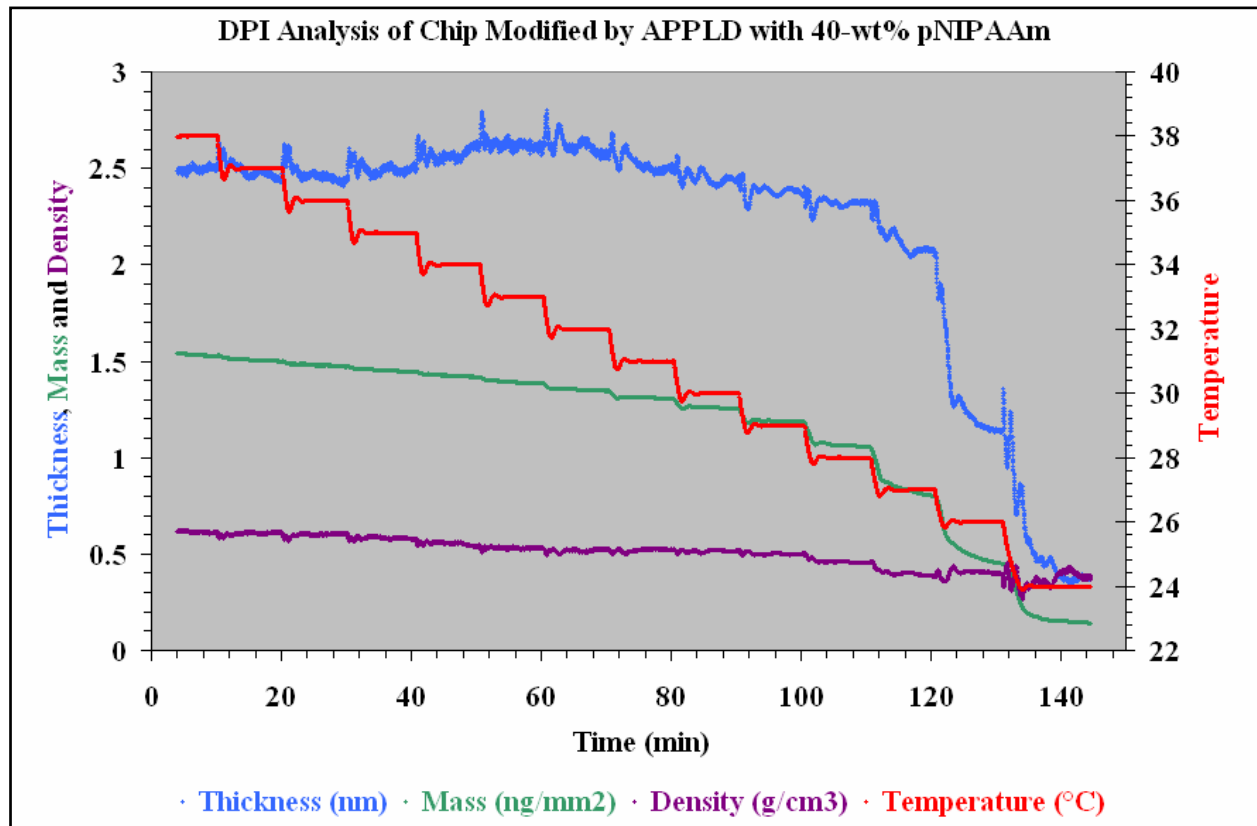


Figure 2-2 DPI chip modified with a 40-wt% solution of NIPAAm. The blue line represents the layer thickness, the green line is the mass per unit area and the purple line shows the surface density of ppNIPAAm. The layer thickness and mass can clearly be seen washing off of the surface with a drop in temperature.

To demonstrate that the observable change in surface hydrophobicity was due to the immobilization of the temperature responsive polymer, contact angles were also measured on TCPS slides as a control. Control slides were made with each experiment and consisted of a plain TCPS slides, TCPS slides exposed to the APPLD high voltage (HV) and TCPS slides exposed to the APPLD high voltage and IPA (HV+IPA). There was no observable change in surface hydrophobicity, as can be seen in Figure 2-3 below, thereby confirming that the observed change in hydrophobicity was due ppNIPAAm immobilization.

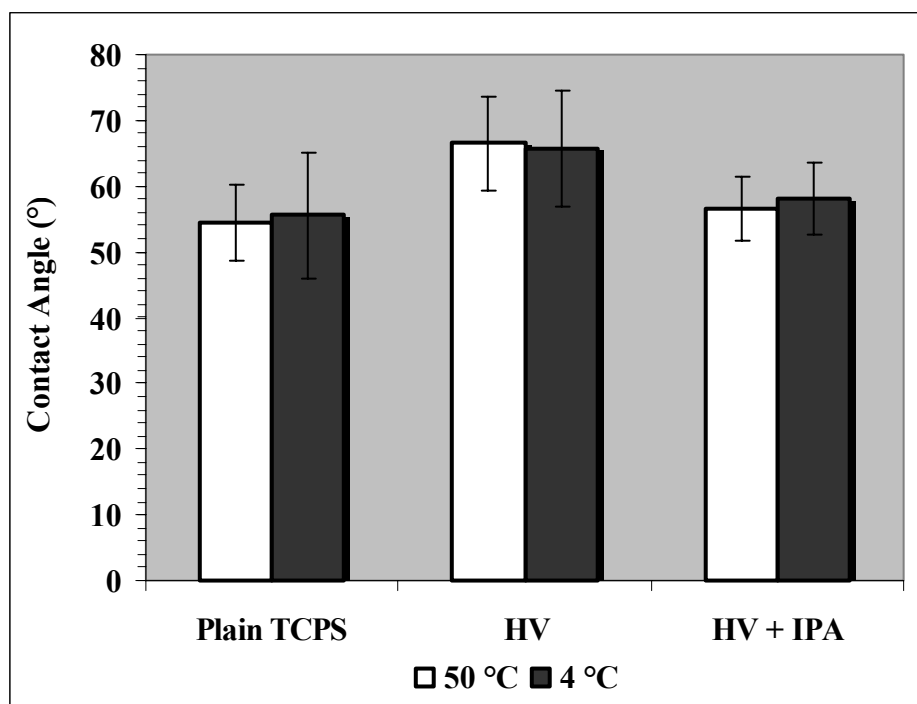


Figure 2-3 Contact angle measurement controls. Bars represent the mean \pm standard deviation. White bars represent measurements that were made at 50 °C and the black bars represent measurements made at 4 °C. No significant difference was observed.

Another significant observation was made when optimizing the system parameters. Contact angle measurements were made prior to and after a 4 °C wash cycle when the solution flow rate and the number of passes were optimized. It was noted that a significant contact angle

switch was observed prior to that cold water wash cycle, but was no longer observable after the wash cycle. When the solution concentration was optimized, the samples were washed with water at 50 °C and contact angles were evaluated. This was followed by a 4 °C wash cycle and a reevaluation of the surface hydrophobicity. A significant contact angle switch was still observed in the 30- and 50-wt% solutions after this wash cycle. However, a cold water wash cycle again eliminated any significant change in surface hydrophobicity. These results further substantiated the DPI data and indicate a limited stability of ppNIPAAm on the surface. In its hydrophobic state, above the LCST, the ppNIPAAm remains stable on the surface, but dropping the temperature below the LCST results ppNIPAAm washing away. This observation led us to investigate whether we could more permanently bind the ppNIPAAm to the surface.

2.3.2 Permanency of APPLD ppNIPAAm coatings

Other groups have had success in developing temperature responsive cultureware by plasma polymerization [22, 24, 34, 78]. One study, of particular interest to us, uses RFGD to deposit NIPAAm [34]. In this system, substrates are first exposed to a high powered glow discharge in order to prime the surface. This step helps to ensure good adhesion of pNIPAAm films. Taking a similar approach, TCPS slides were primed with pure plasma. This was done by first exposing the TCPS slides to the plasma using 3-pass program without flow in the liquid line. Upon completion of the program, the slides were then immediately recoated, again using the 3-pass program, with a 40-wt% NIPAAm solution in an attempt to improve our observed adhesion. Figure 2-4 shows that the immobilized ppNIPAAm remained on the surface after multiple 50 °C water wash cycles. However, despite priming the surface, the ppNIPAAm coating washed off in the 4 °C wash cycle.

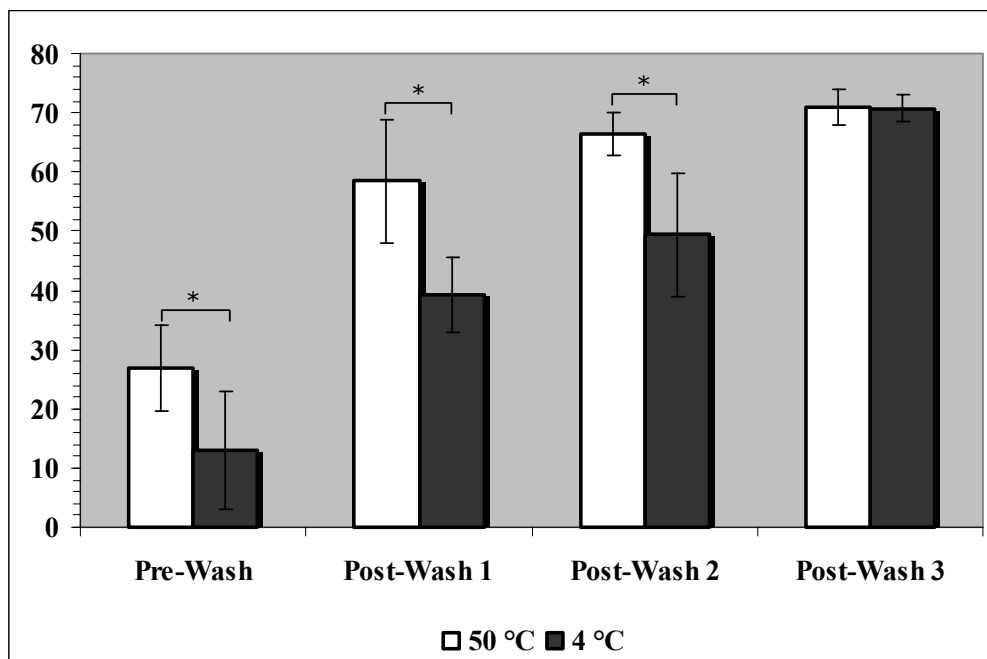


Figure 2-4 The pre-activated TCPS slides modified with a 40-wt% solution of NIPAAm is still rendered inactive after a single cold water wash cycle. Bars represent the mean \pm standard deviation. White bars represent measurements that were made at 50 °C and the black bars represent measurements made at 4 °C. Bars marked with an asterisk represent a statistically significant difference ($p < 0.05$).

Exposing samples to pure plasma is not as effective in priming the surface using the APPLD system, as it is in the RFGD system. This could be explained by free radical stability. The free radicals generated in the plasma system are stable as long as power is being supplied to them [45]. In the RFGD system, the priming of the surface is seamlessly followed by the introduction on the NIPAAm monomer vapor into the vacuum chamber. Therefore, the free radicals formed on the substrate surface are constantly exposed to the high voltage source. However, the APPLD system operates differently. The substrate is modified in very specific regions by a plasma nozzle that moves across the surface. At any one time, the plasma nozzle will cover approximately 0.79 cm² of a slide that has an area of 18.75 cm². In other words, it is impossible to expose the entire slide to plasma at the same time, resulting in areas that are

exposed to the high voltage source while others are not. Free radicals that had been formed on the surface, without exposure to power, return to a lower energy state and are no longer reactive.

Functionalized glass surfaces were also investigated as a means for covalently binding the ppNIPAAm. The APPLD system attacks the vinyl group in the NIPAAm monomer and makes a logical choice for a functionalized surface. We hypothesized that these vinyl groups would act as an anchor for the ppNIPAAm. However, there was no observable change in surface hydrophobicity before or after the wash cycle as can be seen in Figure 2-5 below. Similar results were observed with the piranha washed slides (data not shown). The functionalized surface did not enhance the binding of the ppNIPAAm to the surface. The purpose of this investigation was to determine if functionalized surfaces enable better adherence of the plasma film to the surface. These preliminary studies indicated that the functionalized surfaces would not benefit the APPLD process and would not enhance the permanency of the modification. Glass slide studies were thus discontinued.

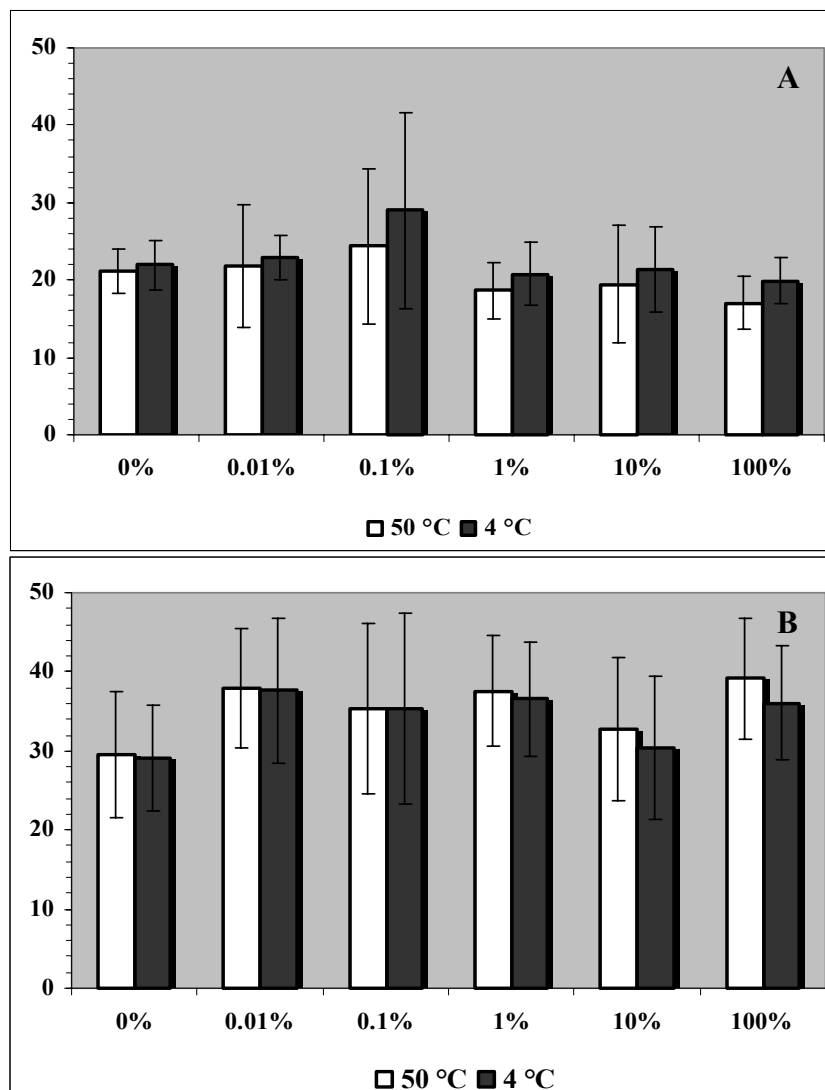


Figure 2-5 Vinyl functionalized glass slides modified with a 40-wt% solution of NIPAAm do not exhibit a change in surface hydrophobicity (A) pre-wash or (B) post-wash. Bars represent the mean \pm standard deviation. White bars represent measurements that were made at 50 °C and the black bars represent measurements made at 4 °C. Bars marked with an asterisk represent a statistically significant difference ($p < 0.05$).

2.3.3 CellSeed analysis

These observations led us to investigate how permanent the pNIPAAm coating is on the commercially available cultureware. UpCell dishes were purchased from CellSeed and contact angles were measured. Figure 2-6 shows that prior to washing a change in surface hydrophobicity is observed. However that change is eliminated when they are washed with cold

water. This data conflicts with the data reported by CellSeed, seen in Figure 2-6 below under the reported measurements title. The reported contact angle measurements are made using the capture bubble method as opposed to the sessile drop method described herein. In the capture bubble method, the surface hydrophobicity is determined by floating the sample on water. A small air bubble is injected and trapped by the sample. The surface hydrophobicity is determined by the angle that this air bubble makes with the modified surface. For the reported measurements, the sample was allowed to equilibrate in water for 1 hour. After that time, the measurements were made and an observable difference in surface hydrophobicity was noted. This is the same amount of time that we used to wash the samples, after which no change in surface hydrophobicity was observed. It could be that the coating was exposed to vast changes in temperature during shipment, rendering the pNIPAAm coating unstable.

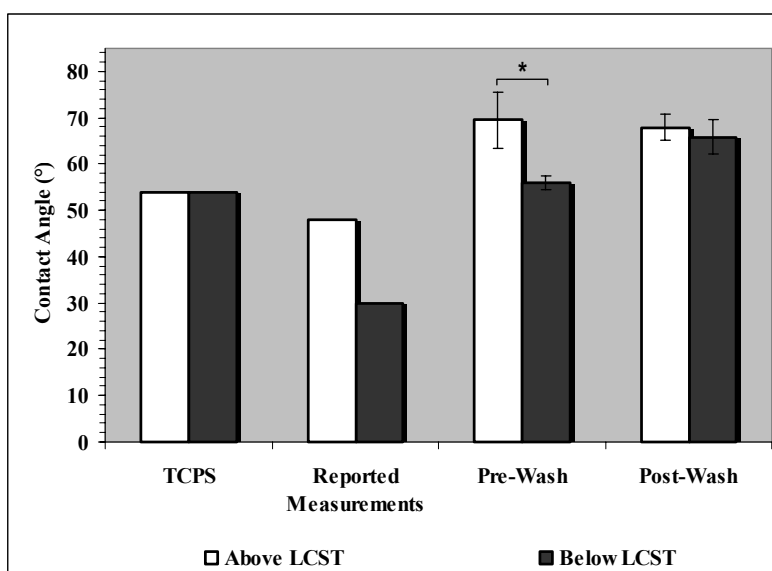


Figure 2-6 Contact angle measurements of commercially available pNIPAAm modified TCPS dishes from CellSeed. Exposure to one cold water wash cycle eliminates the temperature switch in surface hydrophobicity. Bars represent the mean \pm standard deviation. White bars represent measurements that were made at 50 °C and the black bars represent measurements made at 4 °C. Bars marked with an asterisk represent a statistically significant difference ($p < 0.05$).

NIH-3T3 cells were grown on the CellSeed dishes and were successfully removed by lowering the temperature (Figure 2-7). Though these dishes did not demonstrate a change in surface hydrophobicity after washing, they were still able to lift cells with a temperature stimulus. Likewise, we hypothesized that the APPLD modified plates would be able to lift cells despite the ppNIPAAm not being covalently bound.

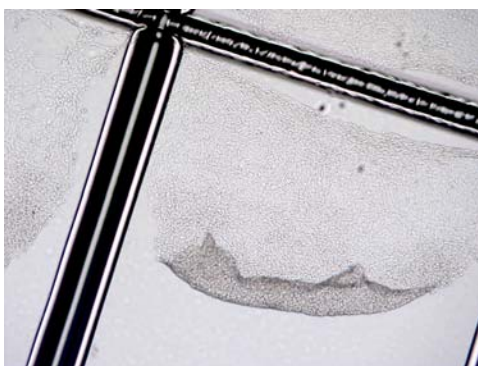


Figure 2-7 NIH-3T3 cells lifting from the surface of an UpCell dish.

2.3.4 Cellular release studies

Prior to using these dishes for cellular release, the sterility of the surface was analyzed. We found that after 4 days of culture the plates were free from bacteria. This indicates that the APPLD system did not contaminate the sterile culture dishes. No additional sterilization methods needed to be employed and the plates were directly used from modification for cellular release studies.

Cells were seeded at a density of approximately 1×10^4 cells/mL. They were grown on average for four days, until a confluent monolayer was observed. In addition to the APPLD modified plates, several control plates were also used in these experiments: plain TCPS, TCPS+HV and TCPS+HV+IPA. At the time of release, the complete media was replaced with

cold PBS. As per the protocol outlined by CellSeed, cellular release should be observed within 10 minutes if the plates are stored at 4 °C. Further, CellSeed recommends an incubation time of 30 minutes for release if the plates are stored at 25 °C. Release from the APPLD modified plates was observed at 4 °C. These plates were observed at times $t = 0, 15$ and 30 minutes. Despite observing significant changes in surface hydrophobicity, cell release was not observed in neither the APPLD ppNIPAAm dishes nor any of the control plates.

While it was not expected to see release in the control plates, it was surprising that no release was observed in the modified plates. Contact angle measurements demonstrate a clear change in surface hydrophobicity and the DPI data revealed that at temperatures above the LCST a clear layer of ppNIPAAm was immobilized on the surface. Though these surface characterization methods indicated that the coating was unstable at temperatures below the LCST, the same observation was noted in our study of the CellSeed dishes. However, unlike in the CellSeed dishes, the APPLD modified dishes were not cell releasing.

2.4 DISCUSSION

The APPLD technology was developed as a means to covalently bind liquid precursors to a wide range of materials, regardless of size or shape. The pre-production model of this technology fell short of that goal. The ppNIPAAm deposited by APPLD can clearly be seen washing off the surface, as has been demonstrated by contact angle measurements and DPI studies. This may have been overcome by optimizing other tunable parameters in this system.

One parameter, in particular, that may have helped achieve a covalently bound layer of ppNIPAAm was duty cycle. The duty cycle is defined as the ratio of plasma “on” time to plasma

“off” time. In other words, the duty cycle describes the pulses of power that supply energy to the plasma. Studies have shown that pulsed plasmas polymerize monomers around specific bonds, such as vinyl groups, more like traditional chemical polymerization schemes [65-68]. As the duty cycle approaches infinite, i.e. the power is always on, a continuous wave plasma would be generated. These plasmas have a higher energy and break bonds randomly resulting in unpredictable film chemistry. The duty cycle that was used in the pre-production model may have been too low. Increasing the duty cycle, or the plasma “on” time, may have supplied the plasma with enough energy to activate both the liquid precursor and the TCPS surface that was being modified.

Though covalent binding of ppNIPAAm was not achieved by APPLD, it is not entirely clear that it is required. Like the CellSeed dishes, a significant change in surface hydrophobicity was observed on the APPLD modified TCPS surfaces. Further, both surfaces were shown to no longer exhibit a change in surface hydrophobicity after a cold water wash cycle. However, unlike the CellSeed dishes, no cellular release was observed on the APPLD modified TCPS surfaces. This may be due to the increased hydrophilicity of the APPLD modified surfaces or an insufficient layer thickness deposited by the APPLD system.

The pre-wash surface of the CellSeed UpCell dishes were measured to have a contact angle of 70° above the LCST and 56° below the LCST, compared to the APPLD modified surfaces that exhibit a 27° contact angle above the LCST and 12° below the LCST. The APPLD surfaces are considerable more hydrophilic than the UpCell dishes. Further, they are considerably more hydrophilic than unmodified TCPS, which has been reported to have a surface contact angle of 54°. Though both surfaces demonstrate approximately a 15° change in contact angle above and below the LCST and good cell adhesion, cell release was only observed on the

UpCell surface. This result may be due to the difference in the initial hydrophobicity of the surface.

Further, Akiyama et al have reported that the optimal cellular release is observed with a grafted layer of pNIPAAm ranging in thickness from 20-30 nm [21]. The ppNIPAAm layer deposited by the APPLD system is only 2.5 nm thick. This difference in thickness may not only explain why cellular release is not observed, but may also explain the apparent difference in the initial surface hydrophobicity. Increasing the grafted layer thickness of APPLD modified surface may result in cellular releasing surfaces.

Layer thickness can be increased a couple of different ways. First, layer thickness is affected by the speed with which the plasma nozzle moves across the surface, or the CNC speed. Decreasing the CNC speed will result in thicker layers. A delicate balance exists when determining the CNC speed. The nozzle should move slowly enough to achieve the desired layer thickness, but not so slowly that oxygen is introduced into the plasma. Further, layer thickness can be increased, to an extent, by increasing the liquid flow rate. Again, a balance exists with the liquid flow rate. A flow rate should be chosen that is high enough to achieve the desired layer thickness, but not so high that the plasma does not have enough time or energy to activate the liquid droplet.

2.5 CONCLUSIONS

We have demonstrated that the APPLD system can be used to deposit NIPAAm onto TCPS and that a significant change in surface contact angle can be observed. However, the modification has a limited surface stability and is not covalently bound to the surface. Despite

the change in surface hydrophobicity, a confluent monolayer of NIH-3T3 cells was not able to lift from the surface via a temperature stimulus. We have noted the differences in the APPLD surfaces compared to the commercially available UpCell dishes and will work toward creating a surface that has a greater layer thickness and an increased surface hydrophobicity. To achieve these goals, we will begin working with the new production model of the APPLD system.

3.0 APPLD POLYMERIZATION OF N-ISOPROPYLACRYLAMIDE: SE-2100 PLASMASTREAM

3.1 INTRODUCTION

During the course of this study, we collaborated with Dow Corning Plasma Solutions to optimize the design of the atmospheric pressure plasma liquid deposition system. The new model, the SE-2100 PlasmaStream, included many more tunable parameters, including carrier gas flow rate and composition, liquid flow rate, CNC speed, power and height of plasma nozzle. Ability to tune these parameters gives the user additional control over the plasma chemistry. Further, the atomization mechanism of this new model was much more sophisticated. Atomization of the liquid substrate is a key process in the APPLD technology. The plasma is formed as a direct conversion of the atomized liquid droplets. Droplets that are too large in diameter cannot be completely converted to plasma, resulting in the deposition of a wet film. Finally, the production model of the APPLD system had a much larger nozzle diameter, approximately 2-cm. This larger nozzle allowed for the development of a new CNC program.

The objective of this study was to explore the production model of the APPLD system as a means for polymerizing and depositing NIPAAm onto tissue culture polystyrene. The chemical structure of the deposited films was analyzed and compared to commercially available pNIPAAm. Further, we characterized the surface reactivity of the TCPS modified with the ppNIPAAm at temperatures above and below the LCST. Cellular studies will also be performed to evaluate the potential to use these surfaces as cell releasing surfaces. Results from the

production model surfaces were compared to the pre-production model. Further, we contrasted the APPLD modified surfaces with the commercially available CellSeed cultureware.

3.2 MATERIALS AND METHODS

3.2.1 Optimization of APPLD parameters for effective deposition

N-isopropylacrylamide (Aldrich) was purified by recrystallization from n-hexane. Isopropyl alcohol, IPA, (Aldrich) was used as received.

In the production model, the system parameters of power, solution flow rate and concentration, carrier gas flow rate and composition, plasma nozzle height and coating time were all systematically determined. Parameters of the pre-production model were used as a starting point. A Burgener MiraMist nebulizer, with a capillary size of approximately 70 μm , was used to aerosolize the NIPAAm solutions. A solution of HFDFA, a nonvolatile solvent, was aerosolized without the power so that the droplet size could be analyzed. Droplets were sprayed onto a glass slide at 60, 80 and 100 psi. Pictures were taken on a light microscope. The size of the aerosolized droplets was determined by use of ImageJ software.

An optimal voltage was first determined by varying the input power from 60% to 100%. The solution flow rate and carrier gas flow rate and composition were next determined. Solution flow rates of 10, 15 and 25 $\mu\text{L}/\text{min}$ were evaluated. A carrier gas composition of just helium was evaluated at flow rates of 1, 5 and 10 L/min . Introduction of nitrogen to the carrier gas stream was also explored with flow rates of 6.5 L/min helium gas and 100 mL/min nitrogen gas. Nitrogen gas absorbs some energy from the plasma and can help yield a stable glow discharge. The height of the plasma nozzle was varied from 1 mm to 10 mm.

The larger nozzle diameter of the production APPLD system allowed for the development of additional CNC programming. The nozzle diameter was nearly the same diameter as that of the wells in a 12-well plate. Therefore, a program was designed such that the nozzle would be lowered into each well and remains stationary while the surface is coated. For this program, the coating time needed to be optimized. Coating times were varied from 10 seconds up to 5 minutes.

3.2.2 Chemical characterization

One milliliter of 4 °C deionized (DI) water was placed into each well of a modified 12-well plate. The plate was placed in the refrigerator for 18 hours. The water was removed, frozen and lyophilized. The product that remained was ppNIPAAm and it was chemically analyzed. To confirm the chemical structure of the ppNIPAAm, ^1H NMR spectra were recorded on a Bruker Avance (300 MHz) spectrometer in CDCl_3 . A Waters 600E Series gel permeation chromatography (GPC) system was used to determine the number average molecular weight (M_n) and polydispersity index (M_w/M_n). The GPC was equipped with three polystyrene columns (Waters styragel HR1, HR2 and HR4) through which DMF with 50 mM LiBr flowed at a rate of 1.0 mL/min. Cloud point measurements were recorded on a Perkin-Elmer Lambda 2 at a wavelength of 490 nm. Absorbance of a ppNIPAAm solution in DI water (4 mg/mL) was measured every degree from 29 °C to 40 °C.

3.2.3 Surface characterization

The change in surface hydrophobicity was observed by measuring contact angles with a VCA Optima using a drop size of 1.0 μL of DI water. The contact angles were measured using

the sessile drop method at temperatures above and below the LCST. Six measurements were taken per slide if the slide was modified using the 3-pass program and 4 measurements were taken per spot if the slide was modified using the CNC spot program. TCPS slides were washed in DI water at 50 °C, 4 °C or room temperature for 1 hour and then dried. Contact angles were reassessed after each wash cycle.

Wet layer thickness, mass and density were measured with a Farfield Dual Polarization Interferometer (DPI). Channel 1 of the DPI chip was modified with ppNIPAAm and channel 3 was left unmodified. A running solution of DI water was flowed across the surface of the chip at a rate of 50 $\mu\text{L}/\text{min}$. The starting temperature of the experiment was 38 °C and was dropped 1 °C every 15 minutes until the temperature reached 26 °C. Upon completion of the experiment, the chip was washed with 4 cycles of IPA injections. The instrument was then calibrated with 80% ethanol and DI water. The background data from channel 3 was subtracted from channel 1 and the data was resolved.

3.2.4 Cell release studies

Well plates were modified with ppNIPAAm for cell release studies. One well of each plate was left blank and served as an internal control. The 6-well plates were coated using the 3-pass well plate program and the 12-well plates were coated with the CNC spot program. After modification, the plates were rinsed with sterile PBS and cells were seeded at an approximate density of 1.0×10^4 cells/cm². NIH-3T3 cells were grown to confluence. Cell media was removed and replaced with PBS. The edges of the wells were scored and the plates were chilled for 10 minutes to observe cell release. Unmodified TCPS plates, along with plates modified by HV and HV+IPA were used as control plates for these experiments.

3.2.5 Statistical analysis

Results are displayed as the mean \pm standard deviation. A two-tailed, paired student t-test was used to determine if the observed difference in the measured contact angles above and below the LCST was statistically different. Contact angle measurements made on each slide were averaged yielding a sample size of 3 or 4.

3.3 RESULTS

3.3.1 Optimization of APPLD parameters for effective deposition

As was previously stated, the atomization of the liquid precursor is key for the APPLD process to be optimum. Droplets formed should ideally be in the range of 10 to 50 μm in diameter [64]. Droplets were examined by atomizing a nonvolatile solution onto a glass slide. Images were taken on a light microscope and analyzed using ImageJ software. Pictures were enlarged and the diameter of each whole droplet was measured. Sample images and tabulated values of the average droplet diameter are seen in Figure 3-1 below. It was determined that the droplets formed at each psi were all within an acceptable range for the APPLD system and a helium pressure of 60 psi would be used for all experiments.

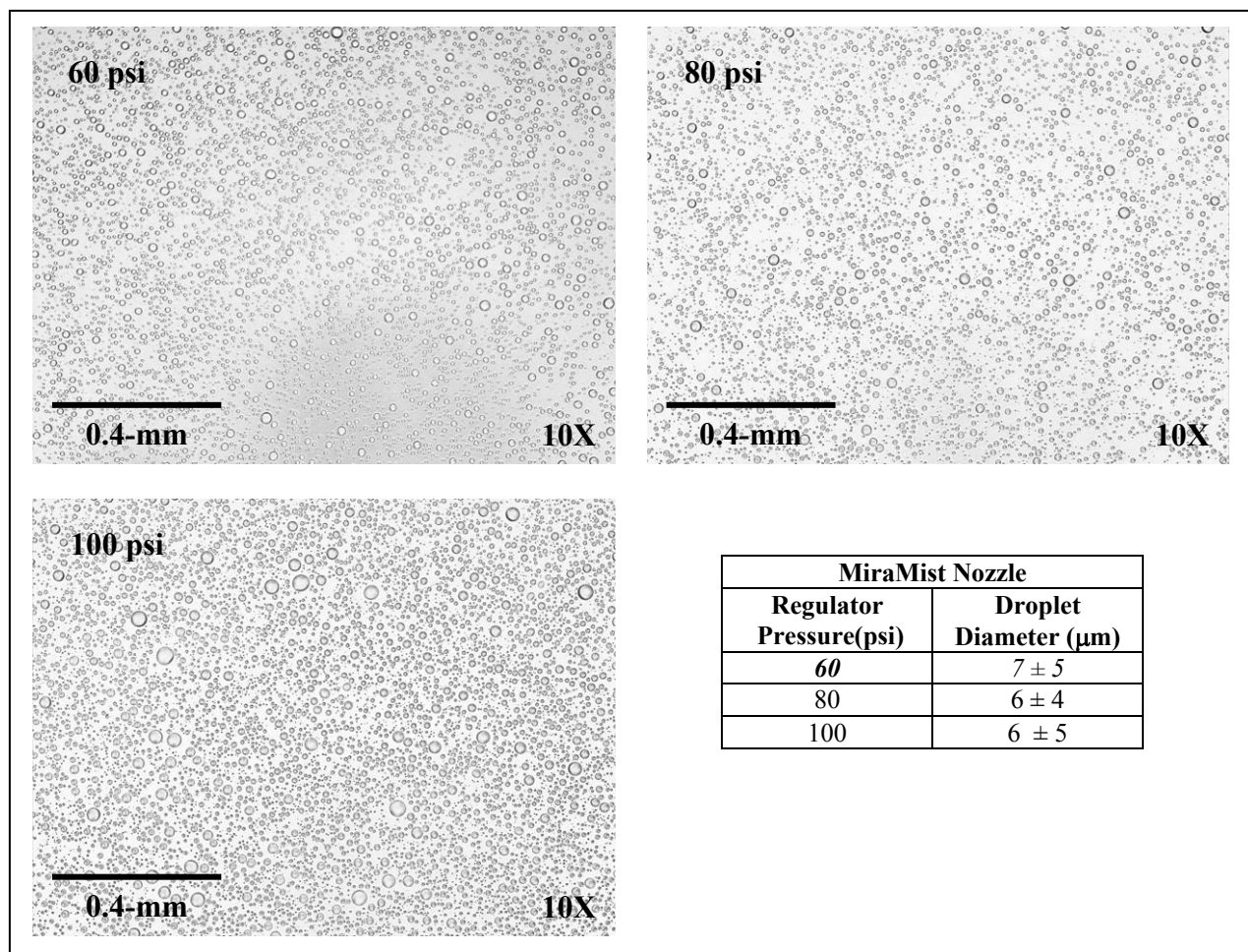


Figure 3-1 Nebulized droplet diameters as a function of regulator pressure. Images like these pictured above were analyzed using ImageJ software. The diameter of every whole droplet was measured and the results were averaged. Tabulated data can be seen in the lower right. All pressures result in droplet diameters that lie within an acceptable range for the APPLD system.

The first system parameter to be evaluated was power. Power was evaluated by maintaining the previously established system parameters from the pre-production model. We found that a significant change in contact angle was observed in the 100% power sample prior to washing and after two wash cycles, one hot (50 °C) and one cold (4 °C). The 80% power sample demonstrated a change in surface hydrophobicity prior to washing, but this effect was eliminated after washing the sample. The 60% power sample did not demonstrate any change in surface hydrophobicity. Data can be seen in Figure 3-2.

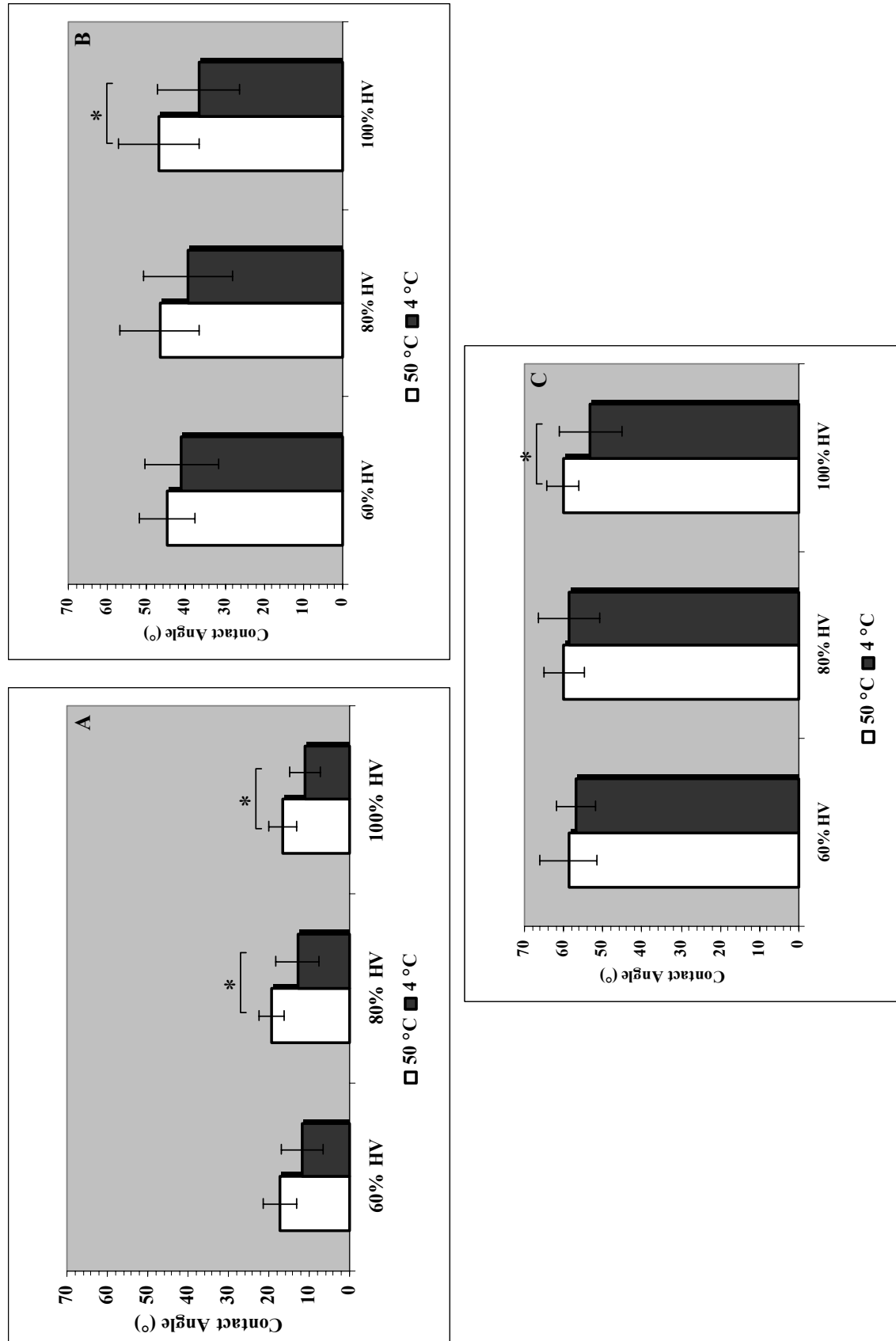


Figure 3-2 Contact angle measurements as a function of power. A, pre-wash measurements. B, measurements taken after a 50 °C wash cycle. C, measurements taken after a 4 °C wash cycle. Bars represent the mean \pm standard deviation. White bars represent measurements that were made at 50 °C and the black bars represent measurements made at 4 °C. Bars marked with an asterisk represent a statistically significant difference ($p < 0.05$).

Using 100% power, the solution flow rate and carrier gas flow rate and composition were investigated. These results are shown in Table 3-1 below. A significant change in surface hydrophobicity is observed only in two samples: one was coated with a liquid flow rate of 15 $\mu\text{L}/\text{min}$ and the other had a liquid flow rate of 25 $\mu\text{L}/\text{min}$ and both samples were coated with a carrier gas composition of strictly helium at a delivery rate of 1 L/min. As was observed in the pre-production model, the higher liquid flow rate did exhibit a greater prevalence for clogging at the tip of the nebulizer. For this reason, a liquid flow rate of 15 $\mu\text{L}/\text{min}$ and a carrier gas composition of strictly helium at a rate of 1 L/min were chosen for all experiments. It was not surprising that the samples coated with the mixed helium/nitrogen gas composition surfaces did not exhibit thermal responsive behavior. The nitrogen gas absorbs energy away from the plasma. As the power study indicated, 100% power was required to see the best surface response. An additive to the plasma that would absorb power would only hinder the surface response. Further, clogging was observed in the samples coated with the higher helium flow rates. The sophistication of the nebulization mechanism may be the reason for this. As was previously shown, the aerosolized droplets formed were an average of 7 μm in diameter. Increasing the gas flow rate will cause the IPA to volatilize more rapidly, thereby increasing the chance that clogging will be observed.

Table 3- 1 Varying system parameters of the production model APPLD system. Process parameters varied were the solution flow rate and carrier gas flow rate and composition. Optimal parameters for coating were found to be liquid delivery at 15- μ L/min and a carrier gas composition of strictly hydrogen at a delivery rate of 1 L/min, italicized below.

A	40-wt% NIPAAm solution at 10 μ L/min					
	Pre-Wash		Post-Wash (50 °C)		Post-Wash (4 °C)	
	50 °C	4 °C	50 °C	4 °C	50 °C	4 °C
He (6.5 L/min) + N ₂ (100 mL/min)	18 \pm 4	11 \pm 3	32 \pm 9	25 \pm 6	51 \pm 9	49 \pm 12

B	40-wt% NIPAAm solution at 15 μ L/min					
	Pre-Wash		Post-Wash (50 °C)		Post-Wash (4 °C)	
	50 °C	4 °C	50 °C	4 °C	50 °C	4 °C
<i>He (1 L/min)</i>	20 \pm 6	14 \pm 4	51 \pm 9	42 \pm 10	50 \pm 10	52 \pm 12
He (5 L/min)	17 \pm 6	17 \pm 10	47 \pm 6	44 \pm 7	64 \pm 4	63 \pm 6
He (10 L/min)	23 \pm 15	24 \pm 14	48 \pm 7	47 \pm 7	56 \pm 5	54 \pm 8

C	40-wt% NIPAAm solution at 25 μ L/min					
	Pre-Wash		Post-Wash (50 °C)		Post-Wash (4 °C)	
	50 °C	4 °C	50 °C	4 °C	50 °C	4 °C
He (1 L/min)	33 \pm 11	12 \pm 3	55 \pm 8	41 \pm 9	60 \pm 4	56 \pm 10

Finally, the plasma nozzle height was considered. Prior to any wash cycles a significant change in surface hydrophobicity was observed in two samples, one in which the nozzle stopped 1 mm above the sample, and the other sample was 7.5 mm above the sample (Figure 3-3). However, after a hot water wash cycle this change was observed only in the sample coated at a plasma nozzle height of 1 mm. For this reason, the 1 mm plasma nozzle height was selected for all experiments.

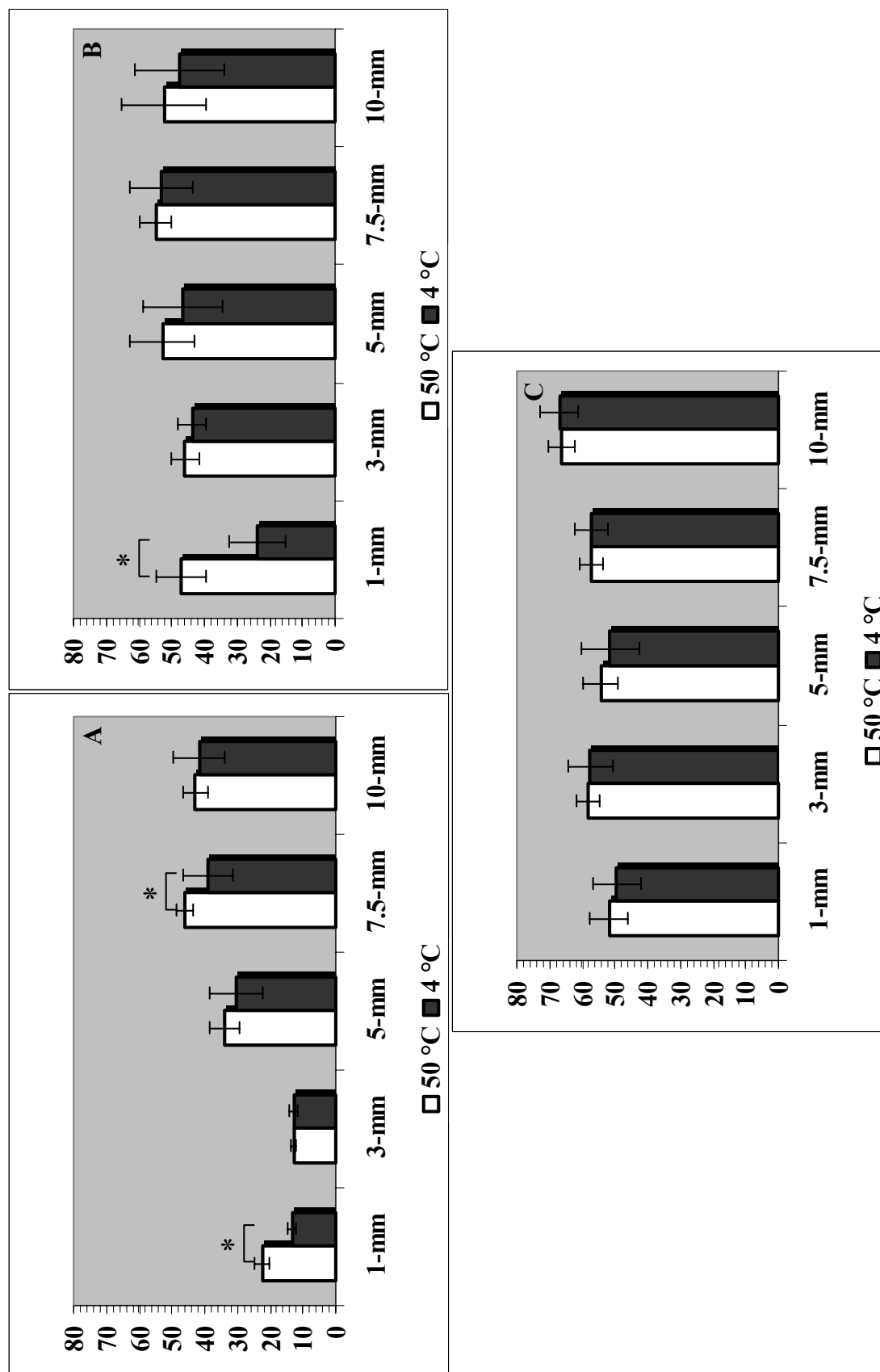


Figure 3-3 Contact angle measurements as a function of plasma nozzle height. A, pre-wash measurements. B, measurements taken after a 50 °C wash cycle. C, measurements taken after a 4 °C wash cycle. Bars represent the mean \pm standard deviation. White bars represent measurements that were made at 50 °C and the black bars represent measurements made at 4 °C. Bars marked with an asterisk represent a statistically significant difference ($p < 0.05$).

In summary, the following system parameters were used in all of the following 3-pass program experiments with the SE-2100 PlasmaStream: a helium flow rate of 1 L/min, NIPAAm concentration of 40-wt% delivered at a rate of 15 $\mu\text{L}/\text{min}$, a CNC head speed of 25 mm/s, a plasma nozzle height of 1 mm and 100% power.

3.3.2 Surface characterization and cellular release on 6-well plates

A DPI study was performed with the optimal 3-pass system parameters to determine wet layer thickness, mass and density of the ppNIPAAm coatings. Figure 3-4 shows how these parameters change with decreasing temperature. It can be clearly seen that the ppNIPAAm layer gradually washes off of the surface with decreasing temperature. This data also corroborates the observed contact angle measurements.

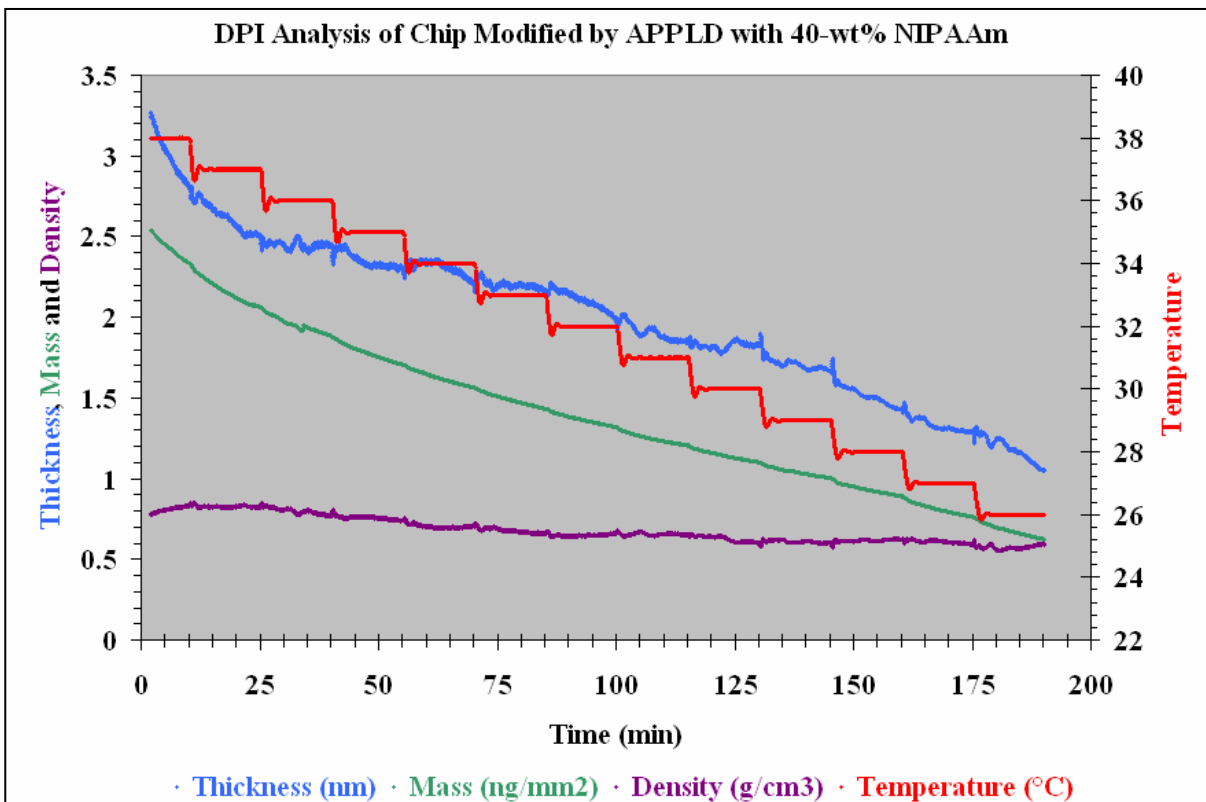


Figure 3-4 DPI chip modified with a 40-wt% solution of NIPAAm. The blue line represents the layer thickness, the green line is the mass per unit area and the purple line shows the surface density of ppNIPAAm. The layer thickness and mass can clearly be seen washing off of the surface with a drop in temperature.

Cellular release studies were also conducted in 6-well plates using the 3-pass program. Despite observing significant changes in the surface hydrophobicity and good cell adhesion and morphology, no cell release was observed. We hypothesized that this may be due to an edge effect. The increased size of the nozzle diameter limited how closely the APPLD system could be programmed to the edge of the wells, without touching the plate. Since the coating pattern is spiral in shape for the well plates, the nozzle will get close to the edge on one side of the well, but not the opposite side. Further, using the larger nozzle required fewer passes in each well resulting in a reduced coating time. To address these issues, a new CNC program was developed.

3.3.3 Development of the CNC spot program

This program was targeted at coating 12-well plates. The new nozzle diameter and that of a well in a 12-well plate were comparable in size and thus the program would bring the nozzle into each well and it would remain stationary for a predetermined period of time. Coating times varied from 10 seconds to 5 minutes and these results can be seen in Figure 3-5 below. A significant change in contact angle was seen in most samples before and after a 50 °C wash cycle. This significance was strongest in the samples coated for 60 seconds (pre-wash $p = 0.02$, post-wash $p = 0.005$) and thus was chosen as the coating time for CNC spot program.

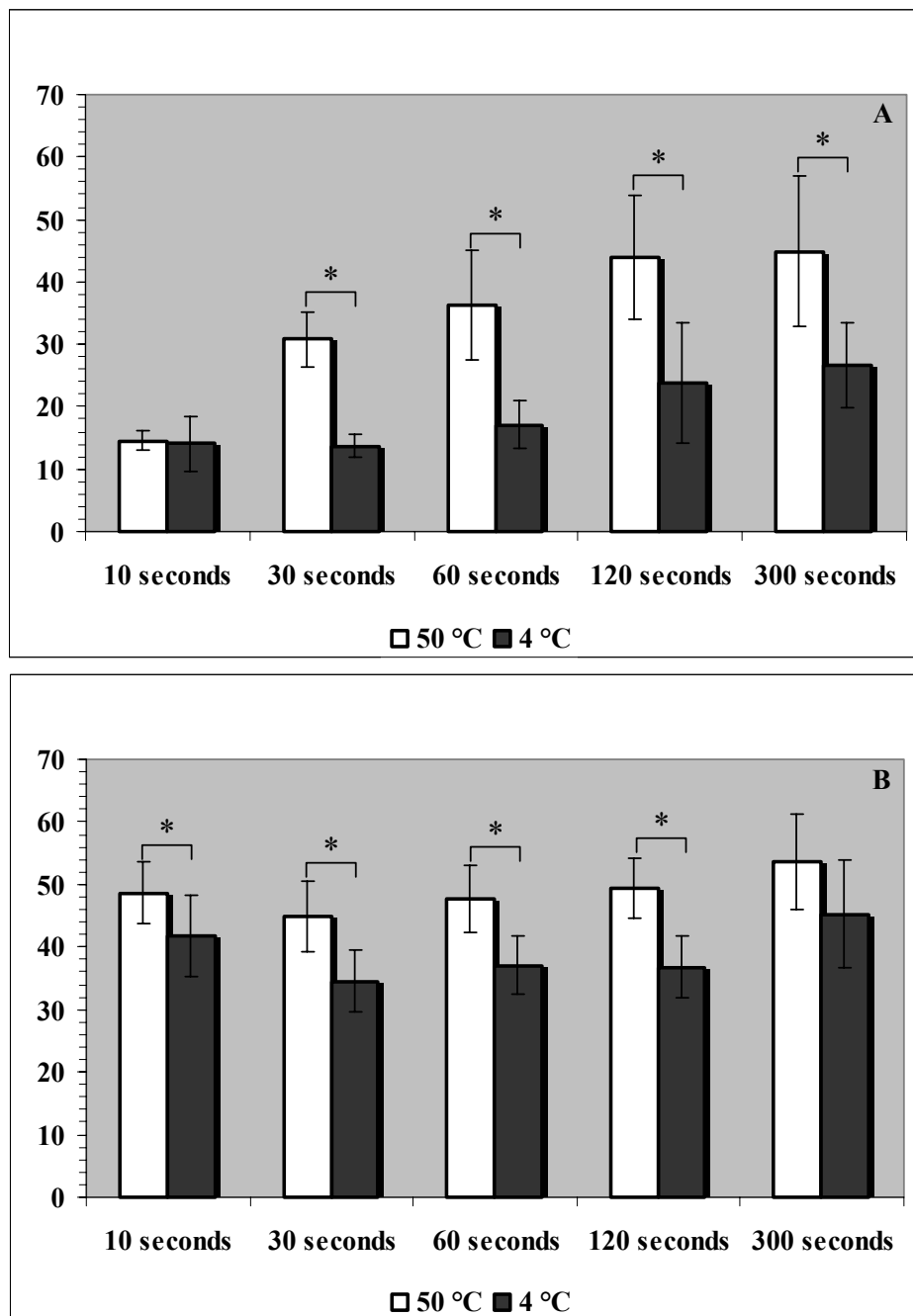


Figure 3-5 Contact angle measurements as a function of coating time. A, pre-wash measurements. B, measurements taken after a 50 °C wash cycle. Bars represent the mean \pm standard deviation. White bars represent measurements that were made at 50 °C and the black bars represent measurements made at 4 °C. Bars marked with an asterisk represent a statistically significant difference ($p < 0.05$).

The thermal responsive behavior of slides coated via the 3-pass program were compared to those coated using the CNC spot program. Though both slide sets were able to withstand

multiple wash cycles, only the CNC spot program samples maintained a surface response after a cold water wash cycle (Figure 3-6). This data suggests that the CNC spot program is more effectively activating the tissue culture polystyrene by creating free radicals on the surface and enabling the free radicals in the liquid precursor solution to covalently bind with those free radicals on the surface. As was previously stated, in order for free radicals to remain stable, a constant stream on energy must be supplied. This is the case in the CNC spot program, where the plasma nozzle rests for a predetermined period of time above one specific location

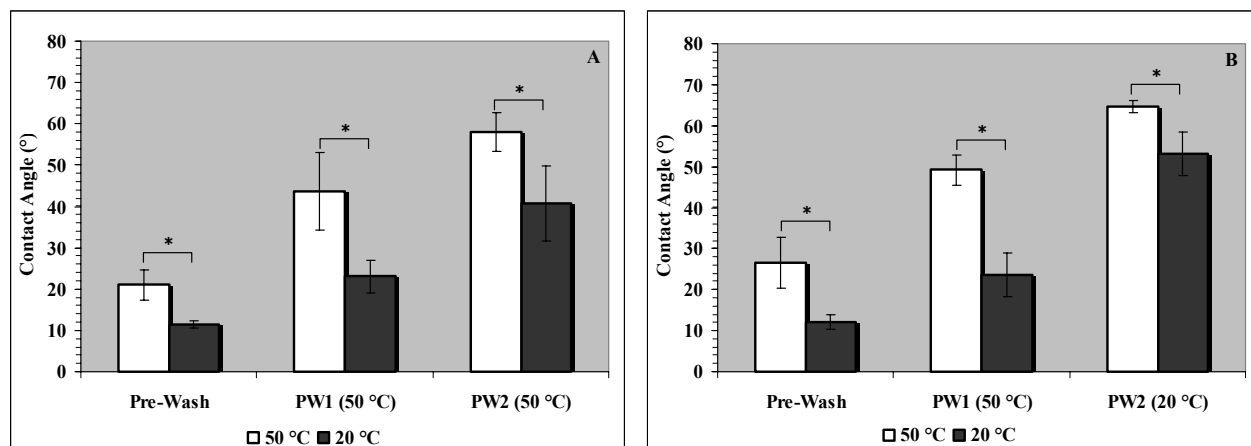


Figure 3-6 A, Contact angle measurements after two warm water wash cycles using the 3-pass program. B, Contact angle measurements after one warm water wash cycle and one cold water wash cycle using the CNC spot program. Bars represent the mean \pm standard deviation. White bars represent measurements that were made at 50 °C and the black bars represent measurements made at 4 °C. Bars marked with an asterisk represent a statistically significant difference ($p < 0.05$).

Additionally, studies were done to compare the ppNIPAAm layer thickness made by the 3-pass program and the CNC spot program. Several attempts were made to analyze a CNC spot coated surface with the 40-wt% solution by DPI, however, the deposited layer was too thick for analysis.

3.3.4 Chemical analysis of ppNIPAAm by the CNC spot program

Though the contact angle data indicates a covalent binding of the ppNIPAAm to the TCPS using the CNC spot program, a decrease in the change in contact angle is observed. This suggests that some of the ppNIPAAm may be more loosely bound to the surface and could be washed off and collected for chemical analysis. Samples of the ppNIPAAm were collected and analyzed for molecular weight, cloud point formation and chemical structure. The M_n of the ppNIPAAm was found to be 754 Da and the polydispersity index (M_n/M_w) was 1.57. This data indicates that the APPLD is synthesizing more oligomer than it is polymer. The ^1H NMR spectra of ppNIPAAm revealed that a mixture of monomer and polymer was present. The ppNIPAAm spectra along with the control spectra of the NIPAAm monomer and pNIPAAm can be found in Appendix A. The cloud point formation is shown in Figure 3-7. The ppNIPAAm does not exhibit a sharp transition indicating that the polymer has a disperse molecular weight [79].

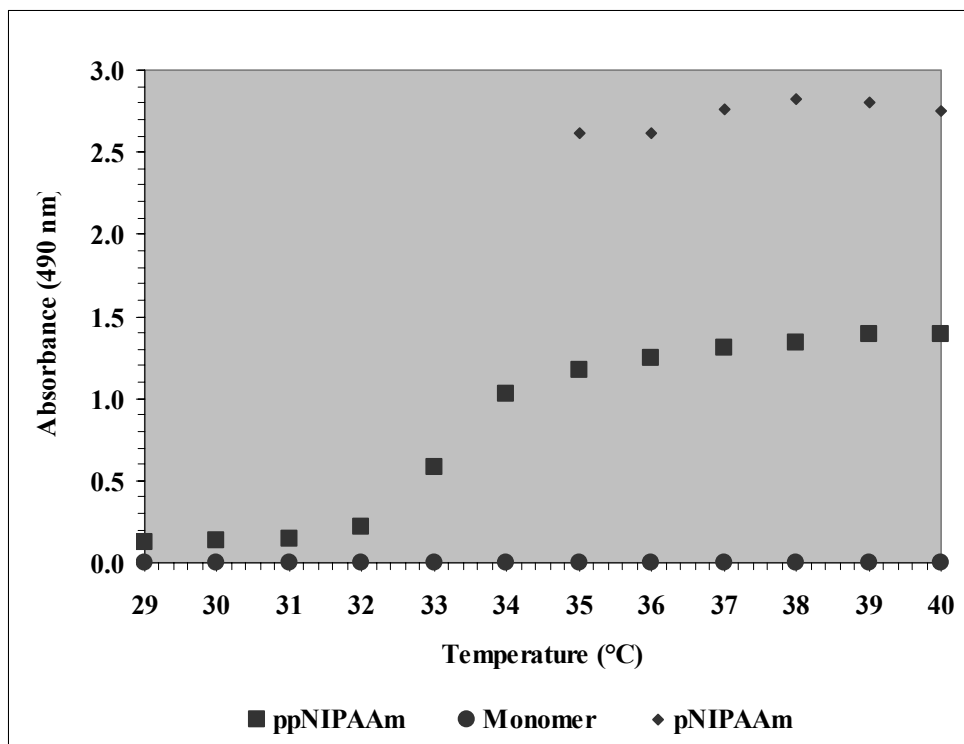


Figure 3-7 Cloud point formation of ppNIPAAm (■), NIPAAm monomer (●) and pNIPAAm (♦) purchased from Sigma-Aldrich

The chemical analysis reveals a surprising result. The APPLD system was designed to both polymerize and covalently deposit a liquid precursor to a desired surface. This analysis reveals that the polymerization of the monomer is extremely limited. We previously stated that the layer thickness and initial surface hydrophilicity may be responsible for the lack of cellular release. This phenomenon may also be attributed to the poor polymerization.

3.3.5 Cellular release studies on 12-well plates

Cells were grown in the 12-well plates modified using the CNC spot program. NIH-3T3 cells were able to adhere to the surface and grew to confluence. We attempted cell release at 10 °C. Very patchy release was observed occasionally in the ppNIPAAm wells. This release was not consistent and is not significant. The same controls were done in these cellular release studies that were done previously with the pre-production PlasmaStream. Again, no cell release was observed from any of the control plates. Figure 3-8 shows NIH-3T3 cells grown on TCPS and the ppNIPAAm plates. The morphology of the cells is similar, demonstrating that the dishes are not harming the fibroblasts. Despite observing a change in surface hydrophobicity after a cold water wash cycle, cell release was still not observed.

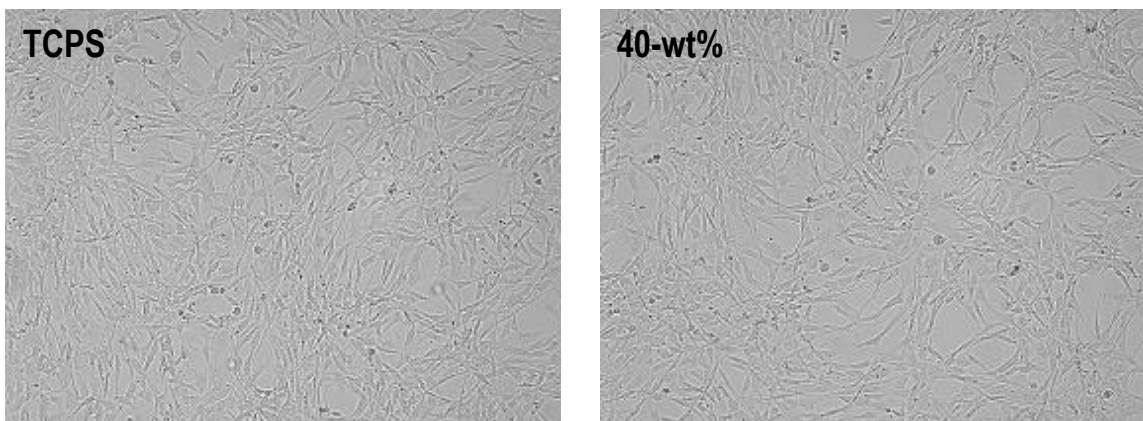


Figure 3-8 Left, NIH-3T3 cells grown on the TCPS control. Right, NIH-3T3 cells grown on the APPLD modified ppNIPAAm plates. Cells adhered to and grew on the ppNIPAAm surface without any inhibition

3.4 DISCUSSION

The 3-pass program using the SE-2100 PlasmaStream yielded similar results to the pre-production model. Both machines were used to modify TCPS slides and those surfaces were found to have a limited ppNIPAAm film stability. Contact angle data reveals that the surface is rendered inactive after washing with cold water. This observation is further substantiated by the DPI data, which clearly shows a decreasing layer thickness and mass on the surface with decreasing temperature. Further, despite an initial significant change in surface hydrophobicity, cellular release is not observed. The SE-2100 PlasmaStream deposited a layer a thickness that initially measured approximately 3.5 nm. This layer was slightly thicker than that deposited by the pre-production model. However, this film thickness is not close to the reported ideal thickness, ranging from 20 to 30 nm.

A vast improvement was observed in the system performance, however, when the CNC spot program was employed. In this program, just one specific spot is modified and the plasma nozzle does not move at all during that modification. This lack of movement means that the spot being modified is constantly supplied with power. Slides modified with the CNC spot program demonstrated a significant change in surface hydrophobicity, even after the slides were exposed to a cold water wash cycle. This data indicated that the ppNIPAAm is covalently bound to the surface. The covalent binding of the ppNIPAAm is likely due to the lack of movement by the plasma nozzle. With the plasma nozzle stationary, the TCPS surface to be modified was exposed to the plasma for a longer period of time than it was using the 3-pass program. Two thought processes can be followed to explain why this resulted in a covalent binding of the ppNIPAAm.

First, and more simply, the extended exposure time was required to form radicals on the TCPS surface. The 3-pass program may not have exposed any given area the target substrate to plasma for a suitable period of time in order to form radicals. Second, the extended exposure time continuously supplied energy to the radicals formed on the TCPS surface, thereby stabilizing them. This stabilization increased the chance that the radicals formed on the TCPS surface would interact with the liquid precursor radicals, resulting in covalent binding. This mechanism is comparable to priming the surface with pure plasma discussed Chapter 2. In the 3-pass program, radicals may have been formed on the TCPS surface, but since the nozzle moved they would not be stabilized. Therefore, the radicals formed on the surface would have to almost instantaneously come into contact with the liquid precursor radicals. Otherwise, they would return to a lower energy state and covalent binding would not occur.

Despite the observed covalent binding of ppNIPAAm using the CNC spot program, cellular release was still not inducible by temperature reduction. Unfortunately, the layer thickness of the ppNIPAAm formed by the CNC spot program could not be assessed. Traditional means of measuring layer thickness, such as ellipsometry could not be used with the APPLD system. Ellipsometry requires the use of reflective surface, such as silica wafers. These electrically conductive surfaces are damaged when exposed to the high voltage in the plasma system. Other methods, such as atomic force microscopy, did not allow for surface analysis at temperatures above and below the LCST. The DPI can only resolve surface layer thicknesses of 100 nm or less. The ppNIPAAm deposited by CNC spot program on the DPI chip interfered with the measurable light patterns. It remains a possibility that the layer thickness was actually too large to observe cellular release. This is, however, unlikely as it has been reported that cells do not adhere to surfaces with a pNIPAAm layer thickness exceeding 30 nm. This was not the

case in the 12-well plate experiments performed. Good cellular adherence and morphology was observed. Given this result, it is unlikely that the layer thickness exceeded the operating range of the DPI, but rather that the concentration of the solution and the plasma process affected the surface of the DPI chip.

It still remains a possibility that cellular release was not observed due to the limited polymerization of the NIPAAm monomer by the APPLD system. The ppNIPAAm film was composed primarily of oligomers and the NMR spectrum shows that there is some unreacted monomer present. Further, a broad cloud point observed is indicative a broad molecular weight polymer. This further substantiates the limited polymerization by the APPLD system. Starting the process with a polymer is a viable means to overcome the limited polymerization, provided that the plasma process does not interfere with the chemical structure. Future experimentation will consider such a strategy.

3.5 CONCLUSIONS

We have demonstrated that the new APPLD system is comparable to the pre-production model when using the same 3-pass program. These coatings result initially in a significant change of surface hydrophobicity. However, both systems yield a surface that is not covalently bound and are not cell releasing. Vast improvement in the SE-2100 PlasmaStream performance is observed when the CNC spot program is used. This program yields surfaces that are covalently modified with ppNIPAAm, but are still not cell releasing. We have hypothesized that these surface are not cell releasing because of the limited polymerization by the APPLD system.

Experimentation will be done to demonstrate that a higher molecular weight polymer immobilized on the surface will result in cell releasing surfaces.

4.0 APPLD DEPOSITION OF POLY(N-ISOPROPYLACRYLAMIDE): SE-2100 PLASMASTREAM

4.1 INTRODUCTION

The APPLD technology was designed specifically as a one-step system for the polymerization and deposition of monomers. In the previous chapter we demonstrated that film chemistry produced by APPLD is predictable, but that the polymerization is limited. Even with this limited polymerization we were able to see a change in surface hydrophobicity, but we were not able to release cells by inducing a temperature stimulus.

Previous publications have reported success in removing cells from surfaces by using the NIPAAm monomer as the starting material [6, 16, 19, 21-23]. These methods require that the monomer be polymerized during deposition. Though these studies have been successful in applying a temperature stimulus to lift cells, the surfaces made are not always consistent, reporting batch to batch differences in layer thickness. These differences in layer thickness may be due to the inconsistent nature of the polymerization.

An early study of temperature responsive cell cultureware by Takezawa et al used pNIPAAm as a starting material. Unlike the procedures that start with the monomer, pNIPAAm was physically adsorbed onto tissue culture polystyrene. It was found that fibroblasts would not adhere to a physisorbed pNIPAAm surface. However, when they modified surfaces, again by physical adsorption, with a mixture of collagen and pNIPAAm cell release was observed. This

release was more a function of dissolving the collagen layer, than a functionally responsive pNIPAAm [14].

We hypothesized that polymerization was the limiting factor in the APPLD process described in the previous chapter. Therefore, we decided to look at the direct deposition of pNIPAAm by APPLD. By using pNIPAAm as our starting material, we eliminate the need for the SE-2100 PlasmaStream workstation to polymerize the monomer. The pulsed plasma operation of the APPLD process should not destroy the chemical structure of the pNIPAAm, thereby preserving the LCST. Based on these, we would expect to see cell removal by a temperature stimulus if the APPLD can immobilize pNIPAAm onto the surface of TCPS. In this study, we investigated the deposition of pNIPAAm by APPLD and determined if this was a viable method for making temperature responsive cell cultureware.

4.2 MATERIALS AND METHODS

4.2.1 Substrate modification

Poly(N-isopropylacrylamide) and IPA were used as received from Sigma-Aldrich.

The system parameters used for pNIPAAm deposition were the same as those used in the monomer study, with the exception of solution concentration. Again, the operating conditions found to be optimal were: a helium flow rate of 1 L/min, pNIPAAm concentration of 5-wt% and a flow rate of 15 μ L/min, CNC head speed of 25 mm/s, plasma nozzle height of 1 mm and 100% power (100 W). Substrates were coated using the CNC spot program and coating a time of 1 minute.

4.2.2 Chemical characterization

One milliliter of deionized (DI) water was placed into each well of a modified 12-well plate. The plate was placed in the refrigerator for 18 hours. The water was removed, frozen and lyophilized. The product that remained was APPLD deposited pNIPAAm (pdpNIPAAm) and it was chemically analyzed. ^1H NMR spectra were recorded on a Bruker Avance (300 MHz) spectrometer in CDCl_3 to confirm the chemical structure. A Waters 600E Series gel permeation chromatography (GPC) system was used to determine the number average molecular weight (M_n) and polydispersity index (M_w/M_n). The GPC was equipped with three polystyrene columns (Waters styragel HR1, HR2 and HR4) through which DMF with 50 mM LiBr flowed at a rate of 1.0 mL/min. Cloud point measurements were recorded on a Perkin-Elmer Lambda 2 at a wavelength of 490 nm. Absorbance of an pdpNIPAAm solution in DI water (4 mg/mL) was measured every degree from 29 °C to 40 °C. Controls for the chemical characterization were: pNIPAAm, a film coating of 5-wt% pNIPAAm dissolved in IPA and a 5-wt% coating of pNIPAAm plasma deposited without HV.

4.2.3 Surface characterization

The change in surface hydrophobicity was observed by measuring contact angles with a VCA Optima using a drop size of 1.0 μL of DI water. The contact angles were measured using the sessile drop method at temperatures above and below the LCST. Four contact angle measurements were made per spot (2 spots per slide). TCPS slides were washed in DI water at either 50 °C or room temperature for 1 hour and then dried. Contact angles were reassessed after each wash cycle.

Wet layer thickness, mass and density were measured with a Farfield Dual Polarization Interferometer (DPI). Channel 1 of the DPI chip was modified with pdpNIPAAm and channel 3 was left unmodified. A running solution of DI water was flowed across the surface of the chip at a rate of 50 $\mu\text{L}/\text{min}$. The starting temperature of the experiment was 38 $^{\circ}\text{C}$ and was dropped 1 $^{\circ}\text{C}$ every 15 minutes until the temperature reached 26 $^{\circ}\text{C}$. Upon completion of the experiment, the chip was washed with 4 cycles of IPA injections. The instrument was then calibrated with 80% ethanol and DI water. The background data from channel 3 was subtracted from channel 1 and the data was resolved.

A modified version of this DPI experiment was also run. The modified protocol requires that the experiment temperature start at 24 $^{\circ}\text{C}$. After 1 hour, the temperature is raised in 4 $^{\circ}\text{C}$ or 6 $^{\circ}\text{C}$ increments until a temperature of 38 $^{\circ}\text{C}$ is reached. The temperature is then lowered back down to 24 $^{\circ}\text{C}$. Upon completion of the experiment, the chip was washed with 4 cycles of IPA injections. The instrument was then calibrated with 80% ethanol and DI water. The background data from channel 3 was subtracted from channel 1 and the data was resolved.

4.2.4 Cell release studies

NIH-3T3 cells were used for these studies and were cultured as previously described in section 2.2.5. We modified 12-well plates with pdpNIPAAm using the CNC spot program and a coating time of 1 minute. One well (A4) of each plate was left blank and served as an internal control. After modification, the plates were rinsed with sterile PBS and cells were seeded at an approximate density of 1.0×10^4 cells/ cm^2 . NIH-3T3 cells were grown to confluence. Cell media was removed and replaced with PBS. The edges of the wells were scored and the plates

were chilled for 10 minutes to observe cell release. Unmodified TCPS plates, along with plates modified by HV and HV+IPA were used as control plates for these experiments.

4.2.5 Cellular viability assay

NIH-3T3 cells were grown on TCPS plates, and TCPS plates modified by HV, HV+IPA and HV+IPA+5-wt% pNIPAAm. Cellular viability was assayed every 24 hours for 4 days. A stock solution of thiazolyl blue tetrazolium bromide, MTT, (5 mg/mL) was diluted 10 fold with PBS to make a working solution. The cultured cells were washed with pre-warmed PBS. The PBS was removed and replaced with 1 mL of the MTT working solution. Cells were incubated for 30 minutes. The MTT solution was removed and the dye was solubilized with 1 mL acidic isopropanol (0.04 M HCl in pure IPA). Absorbance was measured on a Perkin-Elmer Lambda 2 at a wavelength of 570 nm and the background absorbance was measured at 650 nm.

A modification to this protocol was made when assaying the cellular viability of cell sheets. In this case, the adhered cells were washed with 1 mL PBS and then chilled to release the cell sheet. 0.1 mL of stock solution was added to each well with a floating cell sheet and incubated for 30 minutes. The MTT was removed and centrifuged for 2 minutes at 13,000 rpm. Acidic IPA was used to solubilize the dye and absorbance was measured.

4.2.6 Statistical analysis

Results are displayed as the mean \pm standard deviation. A two-tailed, paired student t-test was used to determine if the observed difference in contact angle switch above and below the LCST was statistically significant. One-way analysis of variance (ANOVA) was used to determine significance in the MTT data.

4.3 RESULTS

4.3.1 Chemical characterization of APPLD deposited pNIPAAm

We examined the film chemistry of the pdpNIPAAm and several controls. The molecular weights seen in Table 4-1 were determined by GPC. No significant changes were observed in the molecular weight data when comparing the APPLD deposited pNIPAAm to the controls.

Table 4-1 Molecular weights determined by GPC of pNIPAAm deposited by APPLD and pNIPAAm controls.

	M_n	M_w	M_n/M_w
pNIPAAm Control	47,270	173,280	3.67
pNIPAAm Film Coating	45,130	187,200	4.15
pNIPAAm HV (-)	52,980	187,900	3.55
pNIPAAm HV (+)	52,090	171,800	3.3

The ^1H NMR spectrum of pdpNIPAAm is very similar to the spectra of the controls. These spectra can be seen in Appendix A. This chemical characterization data indicates that pNIPAAm exposure to the high voltage of the APPLD plasma does little, if anything, to affect the chemical structure. Further, the cloud point formation is shown in Figure 4-1. Sharp transition temperatures are observed in all samples. This sharp transition in solubility is in contrast to the very broad transition that was observed in the previous chapter when the NIPAAm monomer was the starting material.

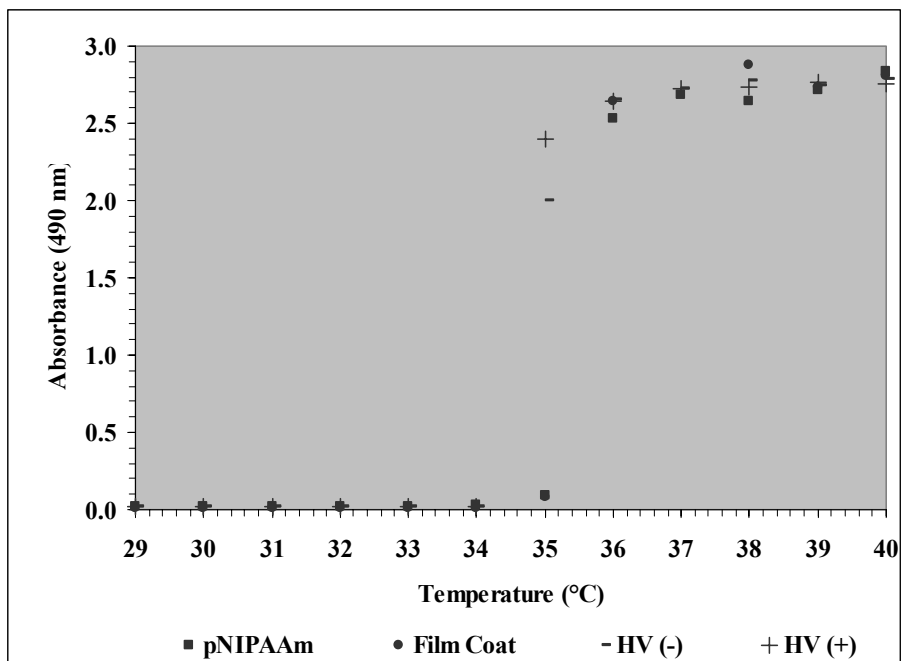


Figure 4-1 Cloud point measurement for the control pNIPAAm (■), film coated pNIPAAm (●), pNIPAAm HV(-) and pNIPAAm HV (+)

4.3.2 Surface behavior at temperatures above and below the LCST

TCPS slides were modified using the CNC spot program and contact angle measurements were taken at temperatures above and below the LCST. This data can be seen in Figure 4-2. The TCPS slides show a significantly different ($p < 0.05$) contact angle measurement at temperatures above the LCST than they show below the LCST. Like we observed previously when analyzing ppNIPAAm films made using the CNC spot program, this significant difference was preserved even after the slides were washed with cold water. This data suggests that the pdpNIPAAm is covalently immobilized on the surface of TCPS. DPI studies were done to determine how the APPLD deposited pNIPAAm films behaved in situ. Figure 4-3 shows that the film thickness is stable in solution and there is no evidence that the coating is washing off of the surface.

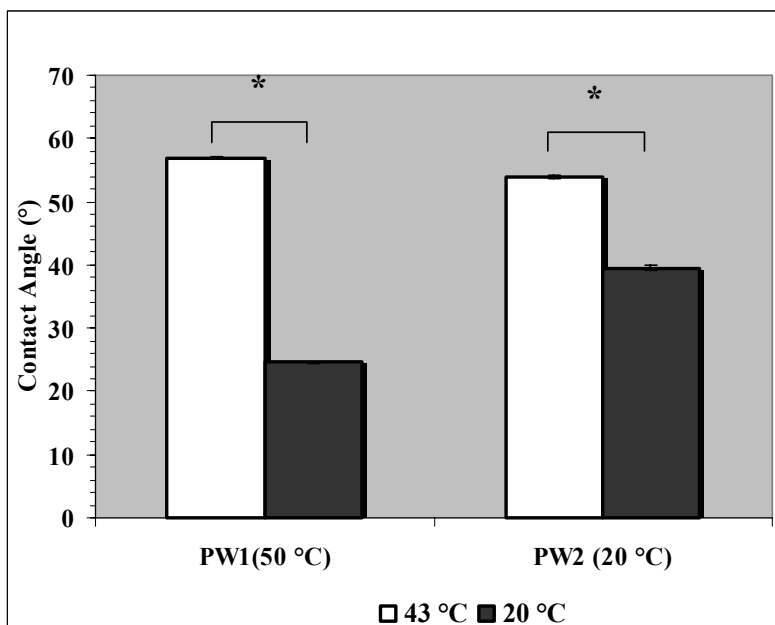


Figure 4-2 Contact angle measurement on TCPS slides coated using the CNC spot program. Data is representative of two wash cycles, one at 50 °C (left) and one at 20 °C (right). Bars represent the mean \pm standard deviation. White bars represent measurements that were made at 50 °C and the black bars represent measurements made at 4 °C. Bars marked with an asterisk represent a statistically significant difference ($p < 0.05$).

Due to the apparent stability of layer thickness, mass and density, the DPI procedure was modified. Figure 4-4 shows the layer thickness, mass and density change as a function temperature. It was observed that the layer thickness (blue line) decreased as the temperature increased. As the temperature dropped, the layer thickness swelled again. Density, on the other hand, follows the opposite trend. With the decreasing layer thickness, we observe an increasing surface density. The mass appears to remain relatively constant in this experiment. However, if we narrow the y-axis and focus on the mass, we can see that minor mass loss is occurring (Figure 4-5). This loss is most evident at the beginning and the end of the experiment when the system temperature is 24 °C, but is trending toward stabilization.

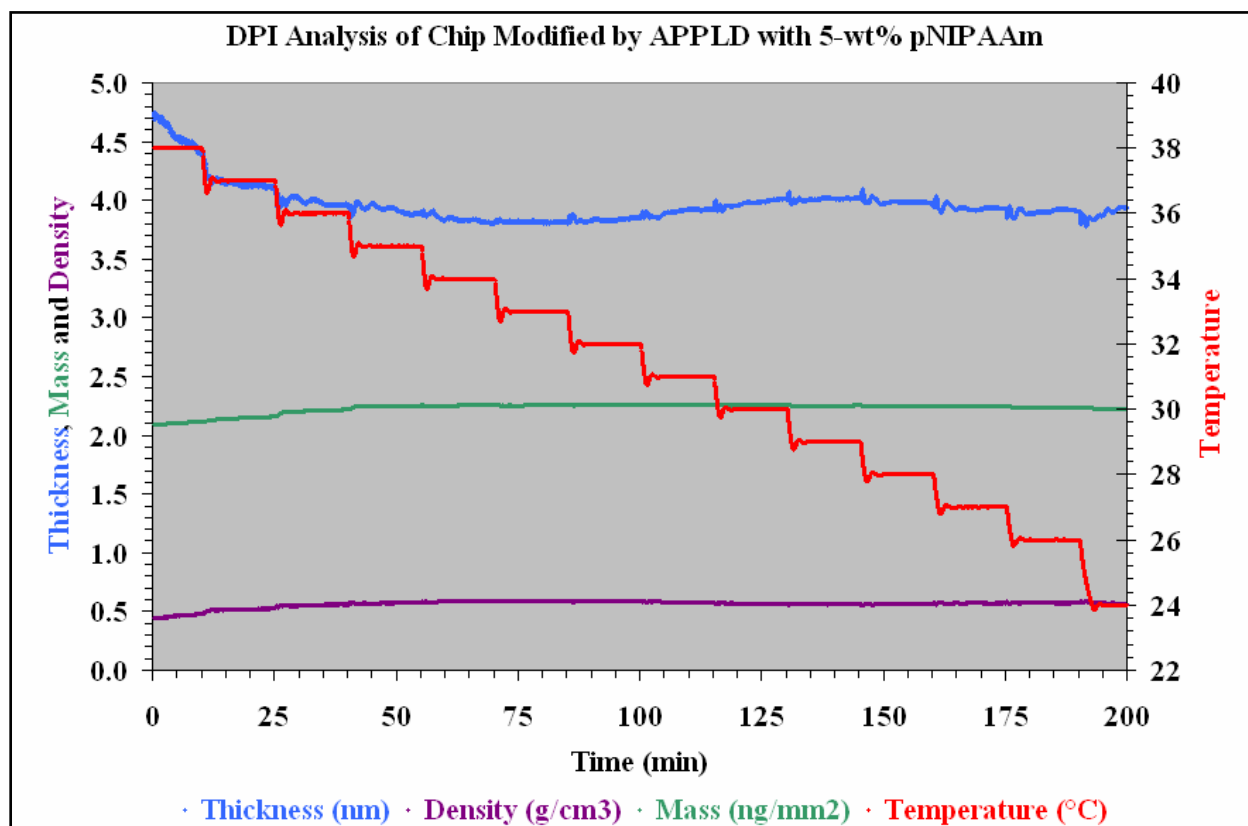


Figure 4-3 DPI chip modified with a 5-wt% solution of pNIPAAm. The blue line represents the layer thickness, the green line is the mass per unit area and the purple line shows the surface density of the APPLD deposited pNIPAAm. In this experiment the layer thickness, mass and density appear to be stable

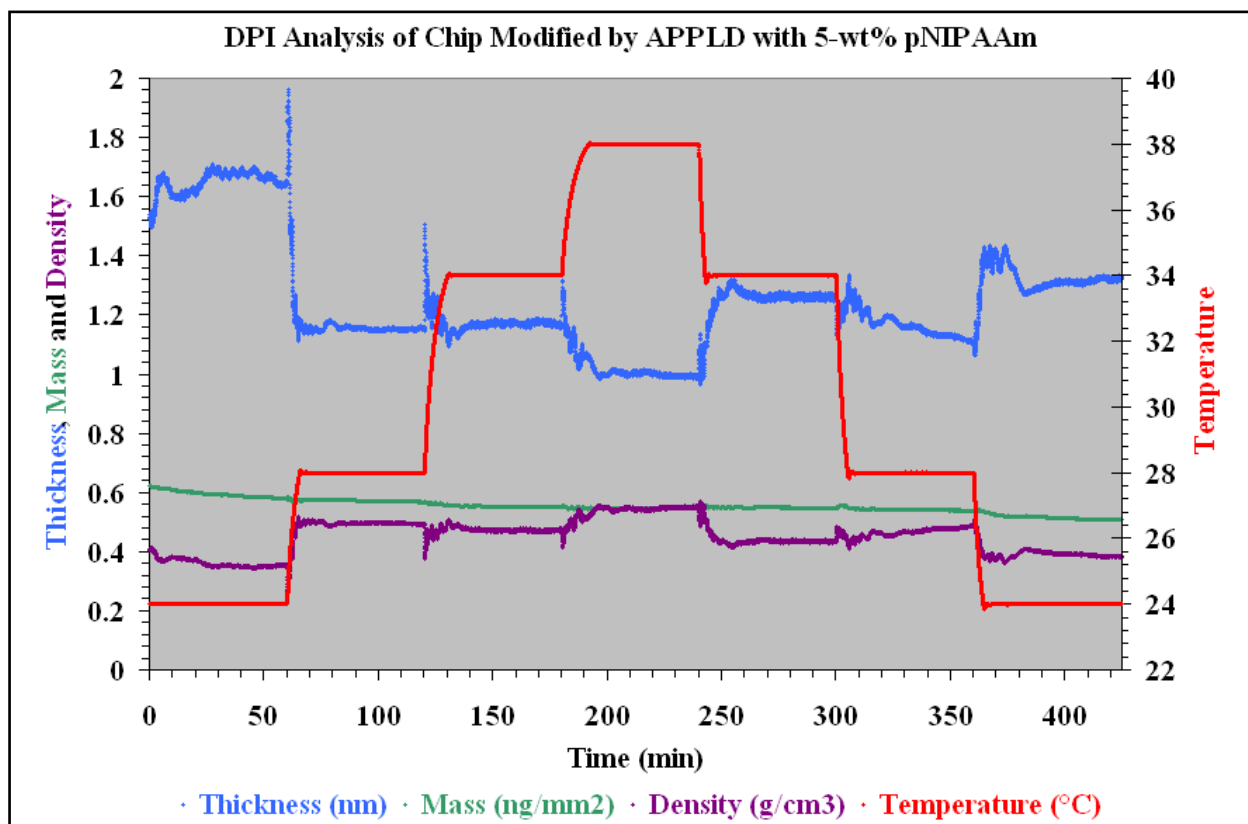


Figure 4-4 DPI chip modified with a 5-wt% solution of pNIPAAm. The blue line represents the layer thickness, the green line is the mass per unit area and the purple line shows the surface density of the APPLD deposited pNIPAAm. With an increasing temperature, we can observe decreasing layer thickness and an increasing density. As the temperature decreases, we observe the opposite trend.

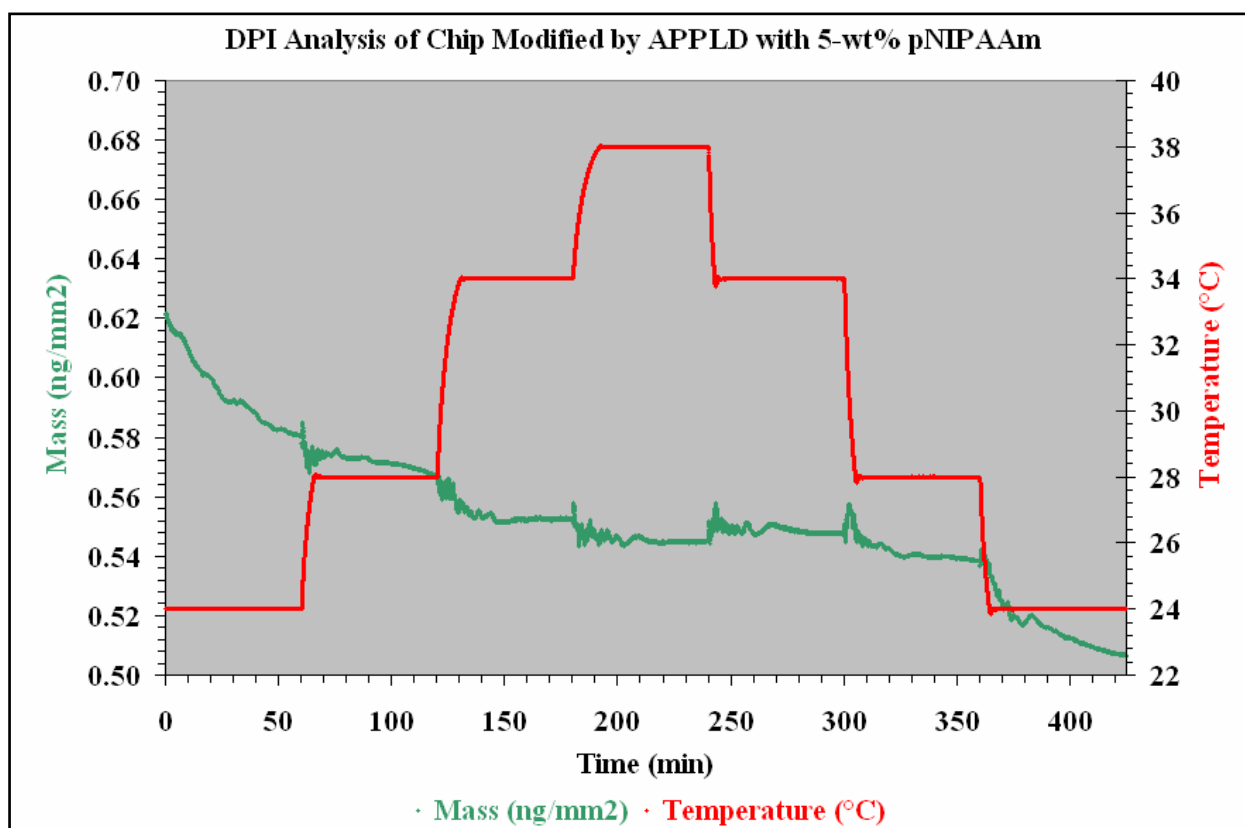


Figure 4-5 DPI chip modified with a 5-wt% solution of pNIPAAm. Mass loss is evident when we narrow the y-axis. This loss is primarily observed at 24 °C.

This DPI data suggests that some of the pdpNIPAAm is loosely bound to the surface and rinses away when the temperature is below the LCST. However, the majority of the pdpNIPAAm layer is covalently bound. Further, it indicates that the pdpNIPAAm films have better adhesion with the TCPS surface than the ppNIPAAm films when deposited by APPLD.

4.3.3 Cellular viability and release studies

We have been able to demonstrate that the APPLD deposited pNIPAAm films are not chemically modified by the plasma process. Further, we have been able to show that the coatings are functional and that the surface hydrophobicity changes with a temperature stimulus. Next, we examine NIH-3T3 cell growth on these surfaces and if they can be released by a

temperature stimulus. Figure 4-6 shows cellular viability data of NIH-3T3 cells grown on TCPS, TCPS+HV, TCPS+HV+IPA and TCPS+HV+5-wt% pNIPAAm. Despite the significant difference in the MTT absorption at the 72 and 96 hour time interval, NIH-3T3 cells did grow to confluence in all wells.

Cellular release studies were done and release was observed in 56 of the 66 pdpNIPAAm wells. No release was observed in any of the control wells. Figure 4-7 shows sequential images of the cells lifting from the surface as a sheet. Pictures were taken every 15 seconds until the cells moved from the field of vision. We also evaluated cellular viability of the released cell sheets by a slightly modified MTT assay and compared the absorbance to a confluent layer of cells grown on TCPS (Figure 4-8). We found that there was no significant difference between the viability of the cell sheets and the cells that were adhered to TCPS.

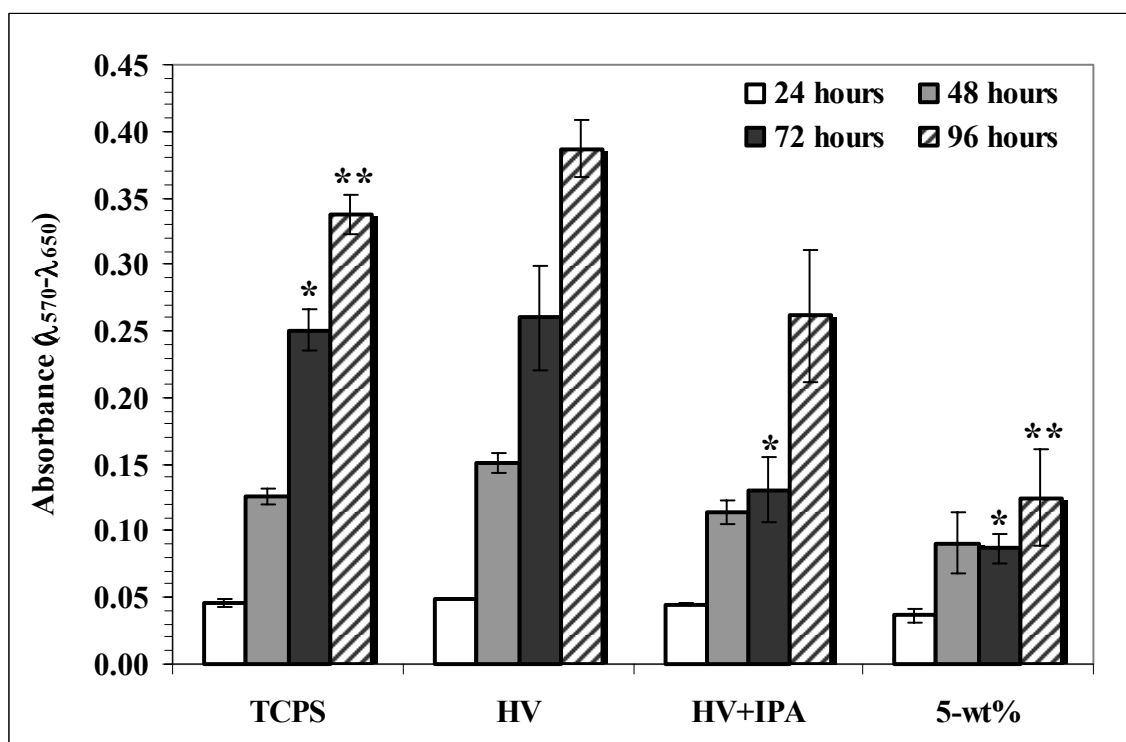


Figure 4-6 Cellular viability at 24 hr (white bar), 48 hr (gray bar), 72 hr (black bar) and 96 hr (striped bar) time intervals. When compared to TCPS, the growth on the 5-wt% pNPAAm dishes demonstrated a significant difference ($p < 0.05$) at the 72 and 96 hr time intervals. Bars represent the mean \pm standard deviation. White bars represent measurements that were made at 50 °C and the black bars represent measurements made at 4 °C. Bars marked with an asterisk represent a statistically significant difference ($p < 0.05$) when compared to the TCPS control.

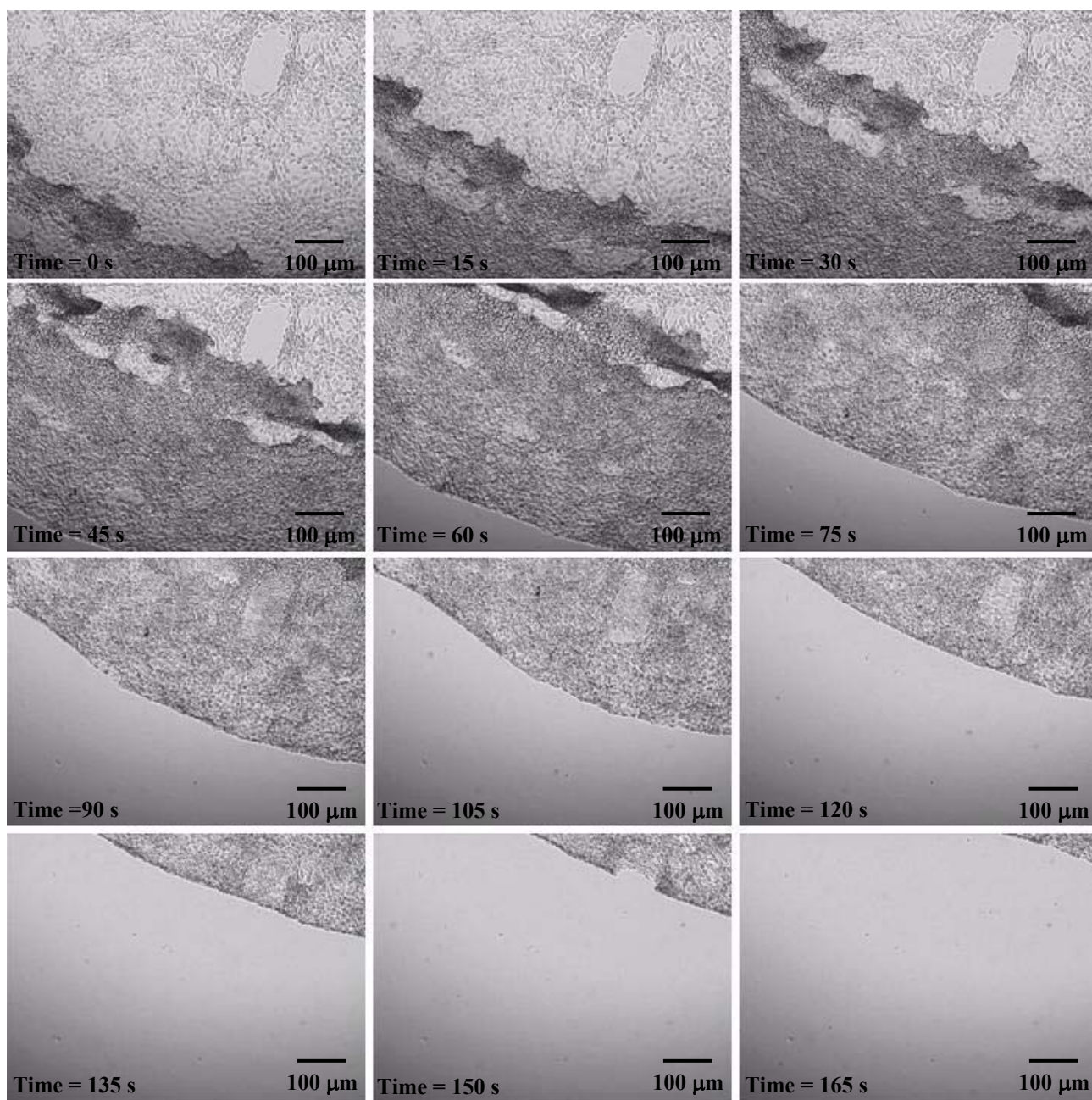


Figure 4-7 NIH-3T3 cells releasing from the surface of an APPLD deposited pNIPAAm well. Pictures were taken every 15 seconds under 40X magnification.

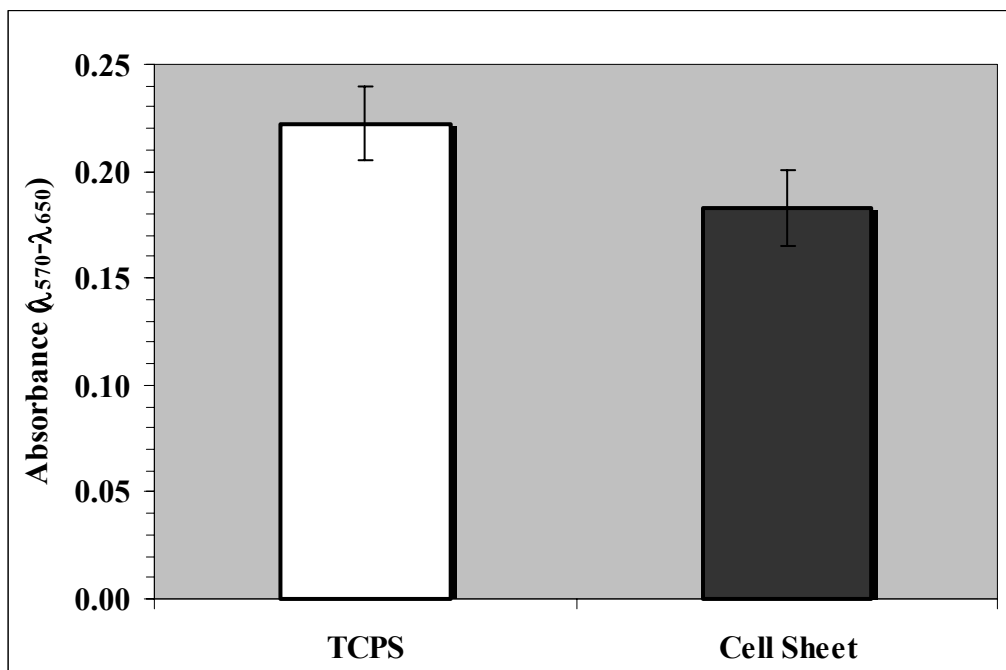


Figure 4-8 Cellular viability as measured by an MTT assay. No significant difference is observed between the adhered cells on the TCPS plate and the released cells in the cell sheet. Bars represent the mean \pm standard deviation. White bars represent measurements that were made at 50 °C and the black bars represent measurements made at 4 °C.

4.4 DISCUSSION

The previous chapters demonstrated that the APPLD process was much more efficient when the CNC spot program was used to modify surfaces when compared to the 3-pass program. With the use of this program, ppNIPAAm was covalently bound to surface of TCPS. However, a weakness of the APPLD system was revealed. This weakness was the systems limited ability to polymerize the monomer. The chemical analysis of the ppNIPAAm revealed a composition of primarily oligomers and the NMR scan revealed trace amounts of monomer still present. Though a disperse molecular weight was expected, this restricted polymerization was not. To overcome this system weakness, the starting material was changed to pNIPAAm.

A starting product of pNIPAAm is different than what had been used in the aforementioned studies, in which the NIPAAm monomer was used. But these studies revealed

that the films formed had batch to batch variations in thickness [21-23, 34]. In one study the variations in thickness affected whether or not cellular adherence was observed [21], while others showed that the batch to batch variations had no effect on adherence [22, 23]. The variation in the deposited layer thicknesses observed in these studies may have been due to the monomer polymerization.

By excluding polymerization as a variable from this system, it was shown that the pdpNIPAAm films remain covalently bound to the surface. Further, with this increased molecular weight polymer immobilized on the TCPS surface, cell release was observed. This behavior of cell release was similar to the behavior of the commercially available plates from CellSeed. The pdpNIPAAm plates have a quick release time of 10 minutes at 4 °C and a slightly longer release time at room temperature, approximately 25 minutes. These release times are on the order of the release times observed with the CellSeed dishes. They are, however, much quicker than the 2 [22, 23] or 3 [40] hour release times observed in other studies. Quicker release times are beneficial, especially when culturing fragile cell lines.

Very thin layers of pdpNIPAAm are observed on the APPLD modified surfaces. Compared to the study done by Akiyama, cell release should not be observed on these surfaces [21]. However, the DPI data demonstrates the surface response as a function of temperature with observable differences in layer thickness and density. These differences are due to the films uptake and release of water and are dependent on the structure of the polymer. At lower temperature polymer swelling indicated that the polymer structure was in a hydrophilic conformation exposing the amine groups. Increasing the temperature decreased layer thickness and water molecule association as the polymer conformation changed exposing the more hydrophobic isopropyl groups [18]. No correlation to cell release and molecular weight has been

made with other pNIPAAm modified surfaces. It would be interesting to determine if the inconsistencies observed are in fact due to the extent of polymerization and if they could be eliminated by using a starting material of pNIPAAm instead.

Cells were able to adhere and proliferate on the plasma modified substrates. Despite the significant difference observed in the time course MTT assay, cells did grow to confluence in the pdpNIPAAm coated wells. Comparative MTT assays were not done on the CellSeed dishes. These studies should be considered in the future to determine if the immobilized pNIPAAm affects the sensitivity of this assay. When cells were released as a sheet from the surface, no significant difference was observed in the viability when compared to a confluent monolayer of NIH-3T3 cells grown on TCPS. This data supports the observation that cells grow to a confluent monolayer on the pdpNIPAAm surfaces and suggest that some data skewing may be

4.5 CONCLUSIONS

Deposition of pNIPAAm by APPLD proved to be an effective means for making temperature responsive tissue cultureware. Data of this study indicates that the pdpNIPAAm was covalently immobilized onto TCPS when using the CNC spot program. Further, by eliminating the polymerization variable, cell release was observed. This is in contrast to the data described in the previous two chapters that used the NIPAAm monomer as the starting material and demonstrated limited polymerization by the APPLD system. This study strongly suggests that the lack of cell release was due to the limited polymerization of the monomer in the APPLD system. We are, therefore, able to conclude that the extent of polymerization is an important factor in the observation of cell release by a temperature stimulus.

Further, we were able to demonstrate that the APPLD process did not affect the chemical structure of the pNIPAAm. NMR spectra of the pNIPAAm and pNIPAAm controls are all very similar. Likewise, the GPC data and the observed LCST of the pNIPAAm and the pNIPAAm controls are all in good agreement. Therefore, we can conclude that the APPLD system is an effective system for depositing polymers onto substrates.

5.0 APPLD DEPOSITION OF BIOCIDAL MOLECULES

5.1 INTRODUCTION

Biomaterials are required to be compatible with the environment in which they will be implanted. Ideally the surrounding tissue will integrate into the device, providing a first line of defense against possible infection. But biomaterials are often composed of inert materials that bacterial microbes can colonize. Competition exists between tissue integration of the surface and bacterial colonization. This competition has been described as a “race for the surface” [80] a race that researchers hope can be won by the integrating tissue. Yet, infection of biomaterials still remains a very real problem. The infection rates of implantable devices per operation are in the range of 1-2%, but can be higher. Take, for example, urethral catheters where infection rates near 100% after an implantation time of one month [81]. Many complications can arise from infection, including recurrent infections, reoperation, amputation or death and are often costly to both the patient and the medical care [80, 82, 83].

The need for biocidal biomaterials has been realized. Researchers have studied the immobilization of chemical compounds and biologic molecules to prevent the bacterial colonization of devices. Different mechanistic approaches have been explored. For example,

biomaterials have been surface modified with poly(ethylene glycol) to increase surface hydrophobicity and prevent the adhesion of cells on the surface of the biomaterial [84-86]. This type of surface modification has been shown to reduce the adhesion of *Staphylococcus aureus* (*S. aureus*) on titanium oxide surfaces [87]. Others have looked at impregnating biomaterials with antibacterial molecules, such as silver [88, 89] or antibiotics [90, 91]. Silver has been a very popular antimicrobial as it has been proven to be effective against a wide range of microbes and has demonstrated anti-inflammatory properties. Concentrations must remain low, however, as silver is toxic not only to bacterial microbes, but to mammalian cells as well [92, 93]. Coating materials with antibiotics is nontoxic to mammalian cells, but increasing antibiotic resistance could make this approach ineffective [83, 94]. This has led some groups to develop custom antimicrobial materials, made from cationic compounds. These compounds have been shown to kill bacteria by disrupting the surface charge of the membrane envelope [95].

We propose that the APPLD technology could be an ideal method for coating biomaterials with antimicrobial agents and took a two-fold approach in the study described herein. Much work has been done in our lab studying quaternary ammonium (QA) compounds and their biocidal activity [95-100]. We used the SE-2100 PlasmaStream workstation to deposit synthesized monomers and polymers with functional QA groups. These custom made QA compounds had a vinyl group that would be susceptible to plasma polymerization. The effective antimicrobial activity of the APPLD modified substrates was evaluated against *E. coli*.

5.2 MATERIALS AND METHODS

5.2.1 Materials

QA synthesis materials: *N,N*-dimethylaminoethyl methacrylate (DMAEMA), ethyl 2-bromoisobutyrate, 1,1,4,7,10,10-hexamethyltriethylenetetramine (HMTETA), 2-(trimethylsiloxy)ethyl methacrylate (HEMA-TMS), copper (I) bromide (CuBr), 1-bromododecane, 11-bromo-1-undecene, anisole, potassium fluoride (KF), acryloyl chloride, tetra-*n*-butylammonium fluoride (TBAF), acetone, acetonitrile, chloroform, methanol, 1,2-dichlorobenzene, *N,N*-dimethylformamide (DMF), *N,N*-dimethylacrylamide (DMA) and tetrahydrofuran (THF) were purchased from Sigma-Aldrich Chemical Co.

Enzyme system materials: Glucose oxidase (GOx) (100 U/mg), horseradish peroxidase (HRP) (1500 U/mg), glucose, sodium iodide (NaI) and polyvinyl alcohol (PVA) were all purchased from Sigma-Aldrich.

5.2.2 Synthesis of antimicrobial quaternary ammonium compounds

Synthesis of MAQAC12: 1-bromododecane (35 mL, 133.7 mmol) was added to a solution of DMAEMA (21.4 mL, 127.2 mmol) in acetonitrile (100 mL) and chloroform (50 mL), and stirred at 40 °C overnight. The resulting residue was precipitated into diethyl ether and filtered. The obtained monomer was dried in vacuo. This monomer will be referred to as QA-125. **QA-125**; yield 44.1 g (86 %). This monomer will be referred to as QA-125.

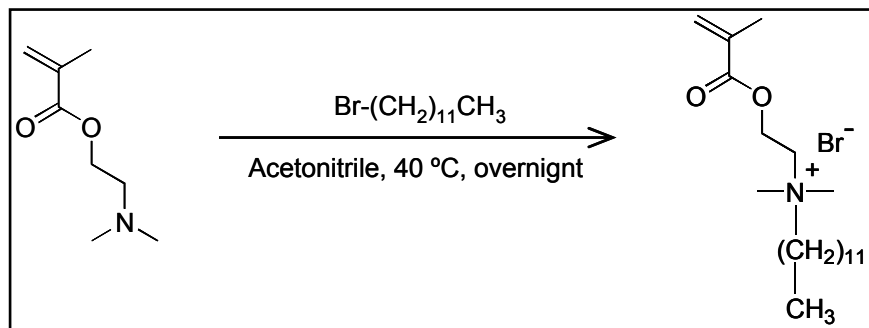


Figure 5-1 Synthesis scheme for QA-125

Preparation of poly(DMAEMA): DMAEMA (17.5 mL, 104 mmol), HMTETA (283 μ L, 1.04 mmol), ethyl 2-bromoisobutylic acid (152 μ L, 1.04 mmol), 1,2-dichlorobenzene (100 mL) were placed in a polymerization tube. The monomer solution was degassed by five freeze-pump-thaw cycles and then Cu(I)Br (149 mg, 1.04 mmol) was added under flowing nitrogen. The polymerization was carried out at 50 °C for 16 h. The resulting mixture was diluted with 20 mL of 1,2-dichlorobenzene and passed through basic activated aluminum oxide to remove any trace copper. The obtained polymer was precipitated with *n*-hexane (1 L). The *n*-hexane-insoluble part was filtered off and the polymer was dried overnight in vacuo; **poly(DMAEMA)**; yield 11.0 g (67 %), M_n ; 4,300 g/mol and the distributions (M_w / M_n) 1.619

Quaternization of poly(DMAEMA) with 1-bromododecan and 11-bromo-1-undecene: 2 mL of 11-bromo-1-undecene and 18 mL of 1-bromododecane were added to a solution of 5.0 g of poly(DMAEMA) in 50 mL of acetonitrile and 50 mL of CHCl_3 . The mixture was stirred at 55 °C for 20 h. The residue mixture was precipitated in *n*-hexane and the solid was filtered, washed with ether and dried in vacuo. This polymer will be referred to as QA-247. **QA-247**; Yield; 12.6 g (96.9 %), M_n ; 18,200 g/mol and the distributions (M_w / M_n) 1.83.

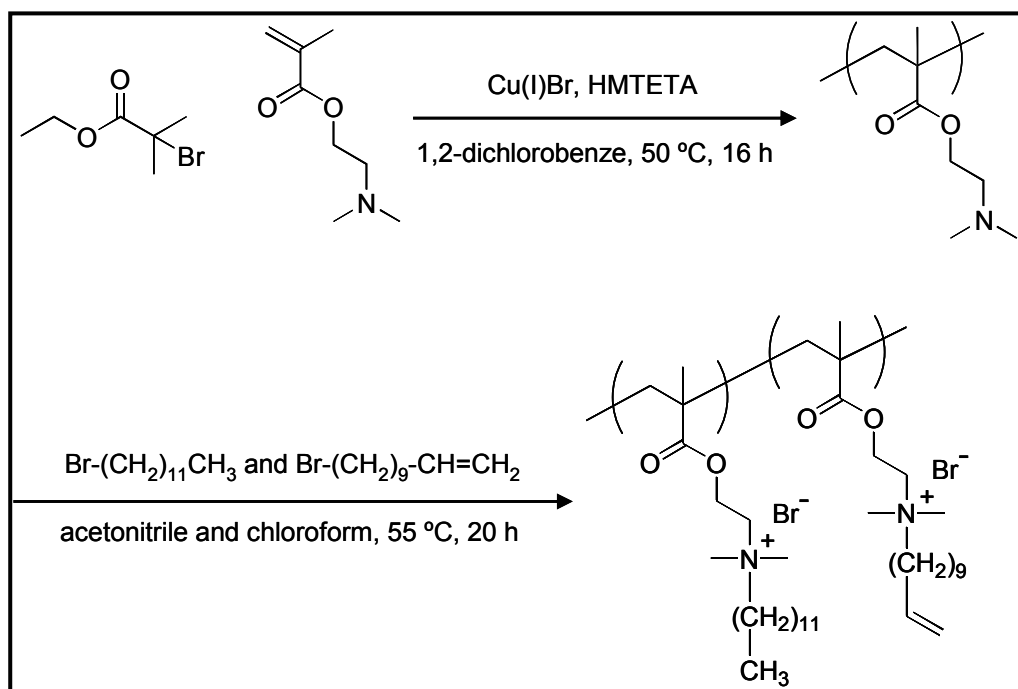


Figure 5-2 Synthesis scheme for QA-247

Synthesis of p(HEMA-TMS-co-DMAEMA): Cu(II)Cl_2 (10.0 mg, 0.074 mmol), HMTETA (80.7 μL , 0.297 mmol) and anisole (2.8 ml) were added to a 25 mL Schenk flask containing DMAEMA (5.0 mL, 29.7 mmol) and HEMA-TMS (1.62 mL, 7.42 mmol). The solution was degassed by three freeze-pump-thaw cycles and CuCl (22.0 mg, 0.0233 mmol) was added under flowing nitrogen. Once the reaction mixture reached room temperature, an anisole solution of *p*-toluenesulfonyl chloride (0.5 mL, 0.74 mmol) was injected into the flask. The polymerization was carried out at $35\text{ }^{\circ}\text{C}$ for 37.3 h. The resulting mixture was diluted with THF and filtered through a neutral alumina column. The polymer was precipitated with *n*-hexane and dried under vacuum at room temperature. About 5 g the purified polymer was dissolved in acrylonitrile and 15 mL bromohexane was added. Quaternization was done overnight at $40\text{ }^{\circ}\text{C}$. The resulting **p(HEMA-TMS-co-QDMAEMA)** was precipitated in hexane dried under vacuum. **p(HEMA-TMS-co-QDMAEMA)**; Yield; 57.3%, M_n ; 52,490 g/mol and the distributions (M_w / M_n) 1.09.

Synthesis of p(HEMA-A-co-QDMAEMA): A solution of p(HEMA-TMS-co-QDMAEMA) (3.5 g) and THF (24 mL) was combined with a solution of KF (2.54 g), acryloyl chloride (3.6 mL, 0.044 mmol), several drops of a 75-wt% solution of TBAF in water and THF (15 mL). The mixture reacted overnight at room temperature. Triethylamine was added and the reaction was carried out for an additional 2 hours. The polymer was precipitated with n-hexane. This polymer will be referred to as QA-011.

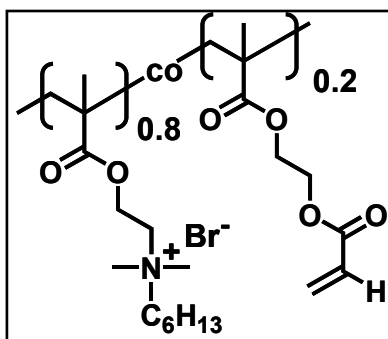


Figure 5-3 Chemical structure of QA-011

5.2.3 Preparation of the APPLD deposited QA substrates

A 7-wt% solution of QA-125, QA-247 and QA-011 were prepared by dissolving in a solution containing DMA (69.1%), IPA (30.7%) and vinyl TMS (0.2%). A second solution of 7-wt% QA-011 was prepared by dissolving in a solution containing DMA (69%) and IPA (31%). Substrates were modified by the SE-2100 PlasmaStream workstation. A Burgener T2100 nebulizer, with a capillary size of 750 μm , was used to aerosolize the QA solutions. Plain glass slides were modified using the CNC three pass program. The helium flow rate remained constant at 10 L/min, the QA solution flow rate was 15 $\mu\text{L}/\text{min}$, and the height of the plasma nozzle was 3 mm for all samples. Power was varied from 70% to 90% and the CNC head speed

was varied from 15 mm/s to 25 mm/s, for a total of 6 sample groups. Control slides were also made using the solvent mixture.

5.2.4 Fluorescein staining

Surface accessible quaternary ammonium groups can be quantified by calculating the amount of fluorescein sodium salt that binds to the surface. A plasma modified sample measuring $1 \times 1 \text{ cm}^2$ was placed in a 10 mL solution of 1-wt% fluorescein. After 10 minutes, the samples were removed and rinsed extensively with DI water. They were then placed in 3 mL of 0.1% solution of cetyltrimethylammonium chloride and shaken for 20 minutes at 300 rpm. A 0.9 mL aliquot of the aqueous solution was removed and 0.1 mL of phosphate (pH 8.0, 100 mM) was added. The absorbance of the desorbed dye was measured at 501 nm on a Perkin Elmer Lambda 2.

5.2.5 Dual polarization interferometry

DPI was used to determine the wet layer thickness, mass and density of QA compounds bound to the surface after the APPLD modification. Channel 1 of the DPI chip was modified with QA compounds and channel 3 was left blank. A running solution of DI water was flowed at a rate of 50 $\mu\text{L}/\text{min}$ for 1 hour at 24 °C. The chip was washed with IPA to remove any of the QA compounds still bound to the surface and then calibrated with 80% ethanol and water. The background data from channel 3 was subtracted from channel 1 and the raw data was resolved.

5.2.6 Biocidal activity

The biocidal activity was determined by a modified version of the ASTM standard: *E2149-01 Standard test method for determining the anti-microbial activity of immobilized antimicrobial agents under dynamic contact conditions*. A colony of *E. coli* K12 was cultured in Luria broth overnight at 37 °C. Cells were diluted in Sorensen's phosphate buffer (pH 6.8, 0.3 mM KH₂PO₄) and the total number of cells used in an experiment was determined by serial dilutions. Plasma modified QA samples, measuring 1 × 2.5 cm², were placed in a 50-mL conical tubes containing 5 mL of the bacterial cell suspension. The conical tubes were incubated at 300 rpm and 37 °C for 2 hours. Plain glass and APPLD glass modified with the solution were used as controls for this study. Samples were diluted and plated on Luria agar plates. Results are reported as a percentage rendered harmless compared to an untreated blank.

Biocidal activity was also measured on washed slides. Prior to following the procedure as described above, the APPLD modified slides were washed by vortexing for 1 minute. These samples were then exposed to the *E. coli* and the percentage rendered harmless was determined.

5.3 RESULTS

5.3.1 Evaluating APPLD coatings of QA compounds

Synthesized QA compounds were deposited on glass surfaces using the following system parameters: a helium flowrate of 10 L/min, solution flow rate of 15 µL/min, solution concentration of 7-wt%, and a plasma nozzle height of 3 mm. The parameters of power and CNC were varied. Contact angles, percentage kill and the solvent accessible charge per unit area are expressed for all sample groups in Table 5-1 through 5-4.

Table 5-1 The effect of system parameters on QA-247

	QA-247-v Pre-Wash ^a				QA-247-v Post-Wash ^a			
	Contact Angle (°)	Killing Percentage (%)	Solvent accessible charge/cm ²	Contact Angle (°)	Killing Percentage (%)	Solvent accessible charge/cm ²	Contact Angle (°)	Solvent accessible charge/cm ²
70% Power, 15-mm/s	32.8	50%	4.38×10 ¹⁵	76.4	46%	2.08×10 ¹⁵		
80% Power, 15-mm/s^b	37.7	100%	3.08×10 ¹⁵	79.4	87%	9.54×10 ¹⁴		
90% Power, 15-mm/s	38.2	39%	5.91×10 ¹⁴	81.3	n/a ^c	5.74×10 ¹⁴		
70% Power, 25-mm/s	33.4	22%	1.26×10 ¹⁵	68.0	36%	5.65×10 ¹⁴		
80% Power, 25-mm/s	43.2	n/a ^c	1.03×10 ¹⁵	77.4	n/a ^c	7.29×10 ¹⁴		
90% Power, 25-mm/s	33.5	n/a ^c	2.06×10 ¹⁵	79.6	n/a ^c	7.14×10 ¹⁴		

^a Solution mixture contains 0.2-wt% vinyl TMS^b Coating conditions used for a DPI study^c Number of cells rendered harmless was greater than the number of cells on the untreated blank**TABLE 5-2** The effect of system parameters on QA-125

	QA-125-v Pre-Wash ^a				QA-125-v Post-Wash ^a			
	Contact Angle (°)	Killing Percentage (%)	Solvent accessible charge/cm ²	Contact Angle (°)	Killing Percentage (%)	Solvent accessible charge/cm ²	Contact Angle (°)	Solvent accessible charge/cm ²
70% Power, 15-mm/s	12.4	n/a ^c	3.36×10 ¹⁴	48.5	n/a ^c	3.15×10 ¹⁴		
80% Power, 15-mm/s	15.0	n/a ^c	3.63×10 ¹⁴	47.1	0%	3.09×10 ¹⁴		
90% Power, 15-mm/s	n/a	68%	1.47×10 ¹⁵	n/a	40%	4.00×10 ¹⁴		

^a Solution mixture contains 0.2-wt% vinyl TMS^b Coating conditions used for a DPI study^c Number of cells rendered harmless was greater than the number of cells on the untreated blank

TABLE 5-3 The effect of system parameters on QA-011 with vinyl TMS

	QA-011-v Pre-Wash ^a				QA-011-v Post-Wash ^a			
	Contact Angle (°)	Killing Percentage (%)	Solvent accessible charge/cm ²	Contact Angle (°)	Killing Percentage (%)	Solvent accessible charge/cm ²	Contact Angle (°)	Solvent accessible charge/cm ²
70% Power, 15-mm/s	13.8	100%	8.93×10^{14}	65.0	0%	3.58×10^{14}		
80% Power, 15-mm/s	17.3	9%	7.05×10^{14}	55.9	n/a ^c	3.55×10^{14}		
90% Power, 15-mm/s	12.7	100%	8.53×10^{14}	60.5	n/a ^c	4.22×10^{14}		
70% Power, 25-mm/s	10.5	100%	1.17×10^{15}	54.4	54%	4.38×10^{14}		
80% Power, 25-mm/s	13.6	100%	1.08×10^{15}	65.7	95%	3.57×10^{14}		
90% Power, 25-mm/s	14.0	100%	9.44×10^{14}	66.4	12%	4.07×10^{14}		

^a Solution mixture contains 0.2-wt% vinyl TMS

^b Coating conditions used for a DPI study

^c Number of cells rendered harmless was greater than the number of cells on the untreated blank

TABLE 5-4 The effect of system parameters on QA-011 without vinyl TMS

	QA-011 Pre-Wash				QA-011 Post-Wash			
	Contact Angle (°)	Killing Percentage (%)	Solvent accessible charge/cm ²	Contact Angle (°)	Killing Percentage (%)	Solvent accessible charge/cm ²	Contact Angle (°)	Solvent accessible charge/cm ²
70% Power, 15-mm/s	11.1	100%	1.43×10^{15}	51.4	71%	2.92×10^{14}		
80% Power, 15-mm/s	10.7	100%	9.06×10^{14}	49.5	87%	2.67×10^{14}		
90% Power, 15-mm/s^b	18.7	100%	1.36×10^{15}	51.4	100%	3.00×10^{14}		
70% Power, 25-mm/s	10.1	5%	8.3×10^{14}	53.6	11%	3.21×10^{14}		
80% Power, 25-mm/s	10.5	100%	9.33×10^{14}	50.2	28%	3.02×10^{14}		
90% Power, 25-mm/s	9.1	100%	1.07×10^{15}	51.3	36%	3.06×10^{14}		

^b Coating conditions used for a DPI study

^c Number of cells rendered harmless was greater than the number of cells on the untreated blank

Compounds QA-011 and QA-247 were polymers and compound QA-125 was a monomer. QA-125 was deposited at limited coating conditions because polymerization occurred at the tip of the nebulizer, resulting in clogging. This clogging was observed regardless of the system parameters used. Eventually complete nebulizer clogging was observed. In general, when compared to the deposited polymers, the surface charge density of the monomer was low and the surfaces were not effective in killing bacteria. This observation is not unlike what we have seen previously with the APPLD technology, in that the system appears better equipped for depositing polymers rather than monomers.

Compound QA-247 was found to be most effective when coated at 80% power and a CNC speed of 15 mm/s. Prior to washing, a high surface charge density was observed and 100% of the bacterial cells were killed during the 2 hour shake test. After washing, we do observe a decrease in the surface charge density and in the ability of the surface coating to kill bacteria, which was reduced to 87%. A DPI chip was coated to observe how the APPLD deposited QA-247 film behaved in situ and is shown in Figure 5-4.

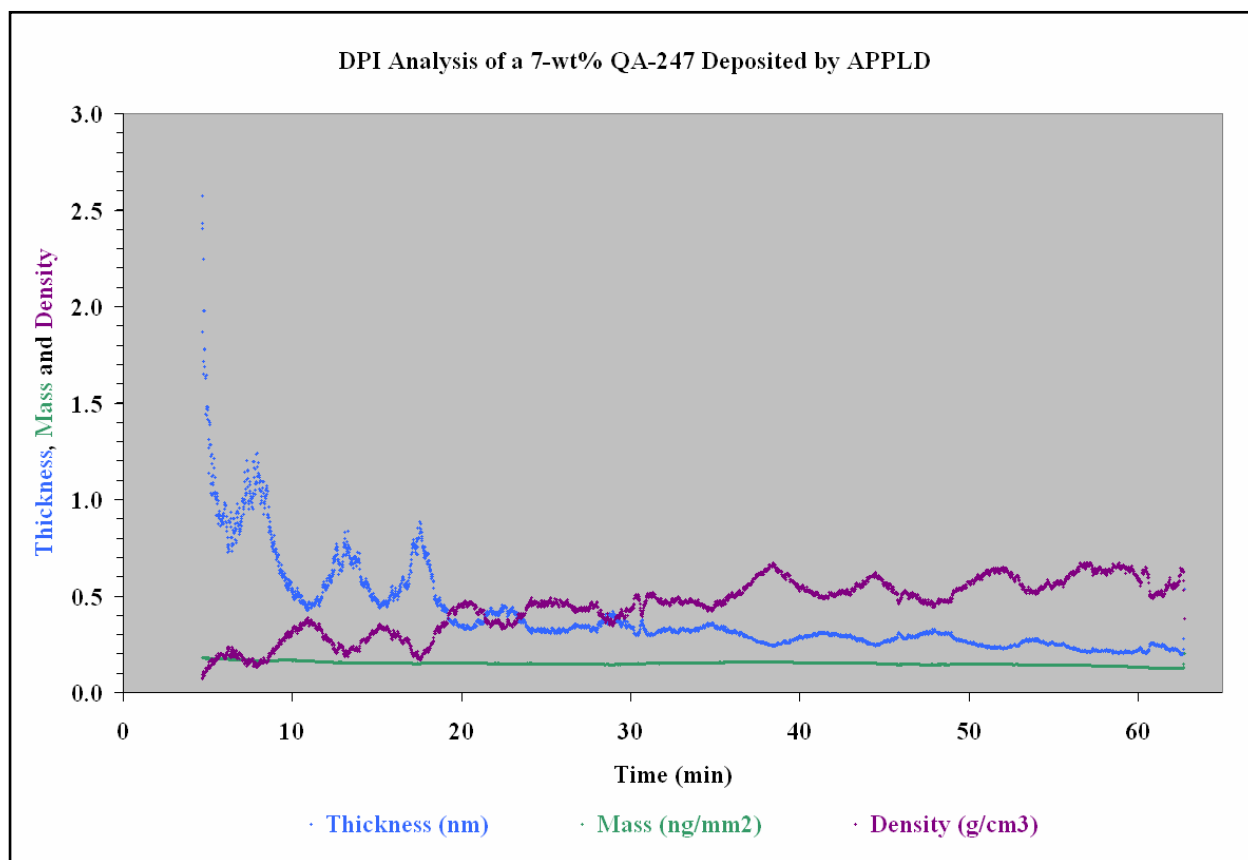


Figure 5-4 DPI analysis of QA-247 measured at a temperature of 24 °C. Thickness (blue), mass (green) and density (purple). Thickness of the QA-247 layer is decreasing over the course of an hour indicating the compound is washing off the surface of the chip.

Compound QA-011 was deposited by APPLD with and without vinyl TMS in the mixture. We had done some preliminary studies with QA-011 and found that it was effective in killing bacteria prior to being washed, but the surface was rendered biologically inactive after washing. We used a wider variety of coating conditions in this study when compared to the preliminary screening of QA-011, with the hope of retaining biocidal activity after washing. In the preliminary study we did not include vinyl TMS in the solvent solution. Therefore, we prepared two solutions of QA-011 for coating. Vinyl TMS is a film former and was added to the solutions with the intention that it will help form a more uniform and covalently bonded coating.

We have observed that compound QA-011 is effective at killing bacteria in almost all samples prior to washing. In the solution mixture that contains vinyl TMS, we have observed that biocidal activity is retained in sample group coated at a speed of 25 mm/s, but not in the sample group coated at 15 mm/s. We have also noticed that, prior to washing, the surface charge density of QA groups is higher in the group coated at 25 mm/s than in 15 mm/s. Looking at the solution without vinyl TMS, we observe the opposite trend. Surfaces are more effective at killing bacteria before and after washing when a CNC speed of 15 mm/s is used. A DPI chip was coated to observe how the APPLD deposited QA-011 film behaved in situ and the data is shown in Figure 5-5.

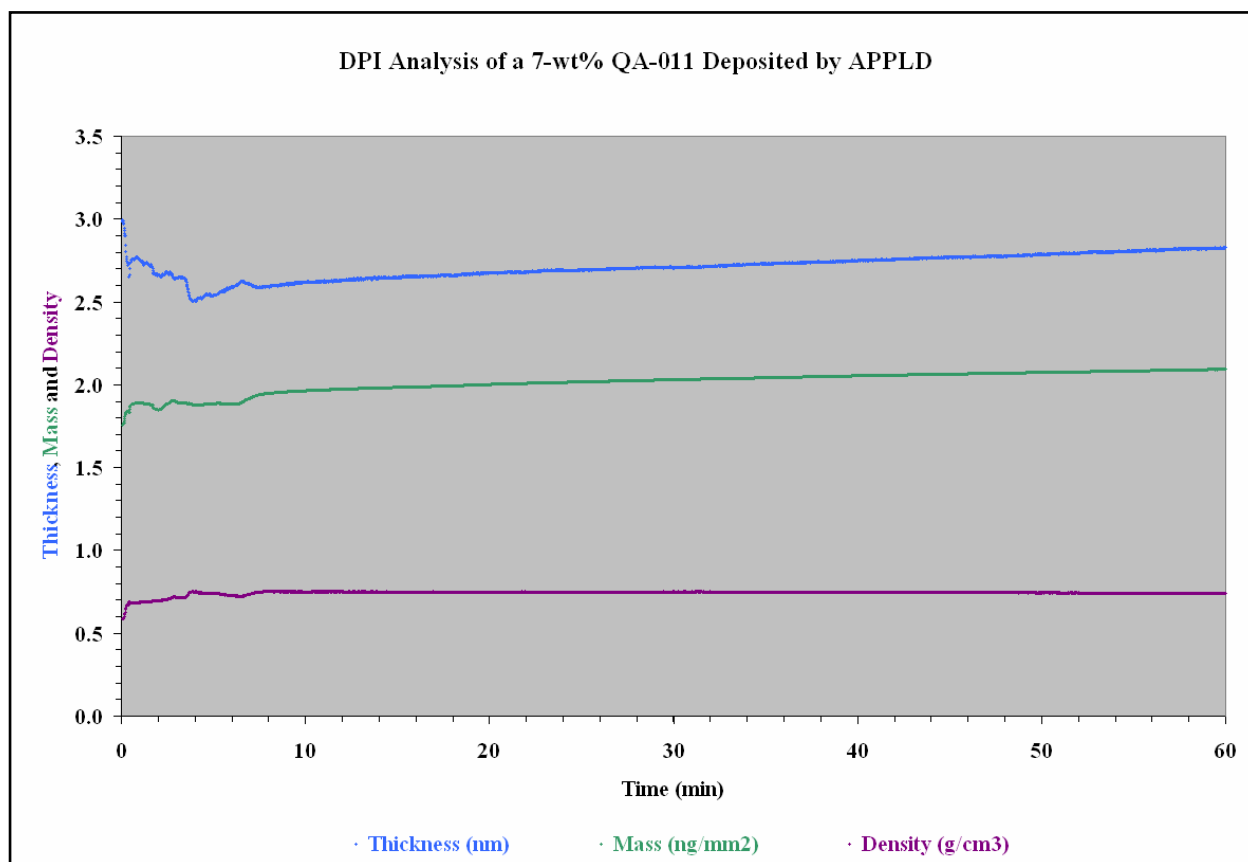


Figure 5-5 DPI analysis of QA-011 measured at 24 °C. Thickness (blue), mass (green), density (purple). This sample did not have any vinyl TMS in the solution. Coating appears to be stable on the surface during this one hour time course.

The DPI data reveals that the coating is stable on the surface. This is likely to be the reason we see such a high retention of kill in the QA-011 samples when compared to the QA-247 samples.

5.4 DISCUSSION

Parallels can be drawn between the APPLD deposition of the temperature responsive compound NIPAAm and these biocidal compounds. We will begin with the monomer

comparisons. Just as we observed in the previous chapters with the NIPAAm, the biocidal monomer was successfully deposited onto surfaces. This monomer was slightly more challenging to deposit, however, since there was a higher concentration of reactive groups not only in the monomer, but also the solvent mixture. We found that in order to successfully deposit this highly reactive mixture, power had to be decreased from 100%. Films made by monomer deposition showed some resistance to washing as evidence of biocidal kill was observed both prior to and after a wash cycle. The ability of the surface to kill was reduced after washing. This was also seen in the NIPAAm modified surfaces, where the change in surface hydrophobicity was reduced after wash cycles. In general, the monomer films deposited by APPLD do not exhibit the same stability and are not as adherent to surfaces as the polymer films.

Similarly, we deposited biocidal polymers by APPLD and we observed more efficient kill by these surfaces. It is likely that this increased efficiency in kill is due to the higher molecular weight. We demonstrated in the previous chapters that the APPLD system did not effectively polymerize the NIPAAm monomer and hypothesized that the same was true of the biocidal monomer. Starting with a few biocidal polymers, we were able to identify several process parameters that enabled 100% kill of all of the *E. coli* to which the surface was exposed. After washing the samples, we were able to identify one polymer and one set of system parameters that enabled the retention of this biocidal effect. It is this repeated kill after wash cycles that we strived to attain. Likewise, it was not until we started with the polymer precursor pNIPAAm that we were able to observe the desired effect of cell release in the previous chapters.

5.5 CONCLUSIONS

The APPLD system was not successful in the polymerization and deposition of the biocidal monomer QA-125. More success was seen in the deposition of QA polymers. This result is not unlike what we observed in the previous two chapters. The APPLD system produced far better coatings when pNIPAAm was used as a starting material than when NIPAAm was. QA-011 proved to be better biocide than QA-247 and was found to be a more robust coating when it came to washing the samples. DPI data revealed that QA-011 was stable on the surface, whereas QA-247 was observed to wash off the surface over the course of 1 hour.

6.0 SUMMARY

6.1 PRE-PRODUCTION MODEL OF THE APPLD SYSTEM

Dow Corning Plasma Solutions developed the atmospheric pressure plasma liquid deposition system as a one step system for polymerizing and depositing monomers onto substrates of various sizes and shapes. We studied the polymerization and deposition of the NIPAAm monomer extensively with this system. More specifically, we studied this deposition using a 3-pass program on flat TCPS surfaces. These surfaces were characterized by contact angle measurement and dual polarization interferometry. Two parameters, solution concentration and flow rate were varied to determine optimal deposition conditions. It was found that ppNIPAAm was successfully deposited onto surfaces, however, it was not covalently bound to the surface. It was also shown that though a significant change in contact angle was observed prior to any wash cycles, no cell release was observed from these surfaces.

Several system parameters could have been altered on this system, but we focused on the three that would most greatly affect the deposition, solution flowrate, solution concentration and the number of passes. One parameter that could have been more carefully examined was power. In the pre-production model, the duty cycle was variable. Increasing the duty cycle may have increased the reactivity of the monomer, binding it more covalently to the surface and enabling

cell release. However, before any additional parameters could be studied, a new version of the technology was released.

6.2 APPLD AS A MEANS FOR MAKING CELL RELEASING SURFACES

The SE-2100 PlasmaStream proved to be a much more effective system for depositing the NIPAAm monomer. This system had more user controlled parameters, and as a result took much longer to optimize. Two basic programs were used with this system, a 3-pass program (the same program used while operating the pre-production model) and a CNC spot program. Of the two, the CNC spot program achieved better films. Surface analysis data revealed that the films formed using the CNC spot program were covalently bound to the TCPS surface and much more robust. Unlike the films formed using the 3-pass program, these films were able to withstand multiple wash cycles with both hot (50 °C) and cold (4 °C) wash cycles, but cellular release was not observed. In comparison to other publications, the layer thickness observed by the APPLD system is much thinner. Layer thickness has been correlated with cellular adherence and may be a factor in the lack of observable cell release.

Further, chemical characterization revealed a weakness in the APPLD system. Designed to polymerize monomers, GPC data revealed that the ppNIPAAm product was primarily oligomeric. NMR data corroborated the GPC data, revealing a mixture of both monomer and polymer present in the ppNIPAAm product. This limited polymerization was not expected and may have also contributed to the lack of cell release observed.

The results from the chemical characterization shifted our focus and we began to use pNIPAAm as the starting product in the APPLD system. Recalling that the APPLD technology operates as a pulsed plasma and that pulsed plasmas have been demonstrated to preserve the

chemical structure of compounds we hypothesized that polymer deposition could be achieved without affecting the chemical structure.

We were able to deposit pNIPAAm by APPLD using the CNC spot program and observed a significant change in surface hydrophobicity when contact angles were measured above and below the LCST. This change in hydrophobic/hydrophilic behavior was preserved after hot and cold water wash cycles, indicating that this coating was more robust than the coating made with the monomer. Further, DPI studies corroborated this data and enabled the observation of changing polymer structure. DPI studies also revealed that the polymer did not wash off of the surface at temperatures below the LCST, indicating that the polymer was covalently immobilized.

Chemical analysis revealed the pdpNIPAAm was similar in molecular weight to the three control samples, indicating that the plasma process does not break the straight chain pNIPAAm units. Further, cloud point analysis revealed a sharp transition in solubility. This transition is in contrast to the broad transition observed from the ppNIPAAm and is indicative of a high molecular weight polymer. Finally, NMR analysis reveals that the pdpNIPAAm retains a predictable chemical structure. This structure is similar to that of the 3 control samples and demonstrates that the pulsed nature of the plasma is not destructive.

More importantly, we were able to observe the release of NIH-3T3 cells by inducing a temperature stimulus. Confluent layers of cells could be fully removed the bottom of a 12-well plate within 10 minutes of chilling. The cells released from the wells were shown to be viable by an MTT assay.

6.3 APPLD AS A MEANS FOR MAKING BIOCIDAL SURFACES

Similar to the NIPAAm studies, we began the analysis of biocidal compounds with a monomer, QA-125. Deposition of this monomer proved to be more challenging than NIPAAm as it resulted in residual build-up at the tip of the nebulizer almost instantaneously. We were able to coat few samples and observed some biocidal activity with one set of coating conditions. After washing, however, that activity was diminished. The chemical composition of the monomer was only analyzed prior to APPLD deposition and not after deposition. Therefore, correlations cannot be made between the polymerization limitations of the NIPAAm monomer and that of this biocidal monomer.

We also used liquid precursors that contained biocidal polymers and observed positive results by APPLD deposition. QA-011 and QA-247 both demonstrated an ability to kill cells using various coating parameters. This biocidal activity was preserved even after the samples were washed with DI water. QA-011 demonstrated superior biocidal activity to QA-247. DPI analysis of these two films showed that while QA-011 appeared to be stable on the surface for the 1 hour observation time, QA-247 slowly washed off.

Similar to what we observed when depositing the NIPAAm compounds, the APPLD system proved to be more effective when coating surfaces with biocidal polymers than monomers. There is evidence in the data that these coatings are stable and can withstand wash cycles, and still retain the ability to kill.

6.4 LIMITATIONS OF THE APPLD SYSTEM

The APPLD system has many advantages. Probably the most prominent advantage is that this system is capable of generating a “cold” plasma at atmospheric pressure. However, the system does have several limitations. For instance, what was observed in this study to be limited polymerization. The system has been manufactured and advertised as a one step process for polymerization and deposition. However, in these studies, there is no indication that the plasma effectively polymerizes monomers. It is possible that the extent of polymerization could be increased by changing system parameters. However, with the numerous parameters it is difficult to know where to start. One parameter that was not examined was the length of the plasma nozzle. It is possible that by shortening that distance the free radicals present would be more concentrated and more likely to react with each other, resulting in a higher molecular weight polymer.

Additionally, accumulation of solute at the tip of the nebulizer often resulted in clogging. This was a constant problem throughout this study, though mechanisms were devised to cope with this. When depositing the pNIPAAm into the 12-well plates only 3 wells were coated at any one given time. The system was then stopped and the nebulizer cleaned before the next 3 wells could be coated. This system was designed to coat materials of all shapes and sizes, but if persistent clogging is observed the surface area that can be coated is limited. As the nebulizer begins to clog, patchy coatings are deposited. These coatings cannot be described as uniform or pinhole free as typical plasma coatings are. Once the nebulizer completely clogs, no deposition is observed. It was observed that if the system is allowed a sufficient period for warming up, at least 1 hour, nebulizer clogging is less of a problem.

Pattern of plasma deposition is also limited by the nozzle diameter. The increase in the nozzle diameter from the pre-production model to the SE-2100 PlasmaStream limits the patterns that can be designed by the user. The nozzle is almost 2 cm in diameter. Therefore, if a finer pattern is desired by the user a mask will still be required. When compared to vacuum plasma systems, however, the APPLD system still has selective control over where the modification can be made.

Finally, cost is a major limitation of the technology. The cost of the equipment is expensive and for laboratory research the APPLD technology may be out of reach.

7.0 FUTURE DIRECTIONS

7.1 CONTINUED WORK ON THE USE OF THE APPLD SYSTEM FOR THE DEPOSITION OF BIOMOLECULES

Biomolecules are often immobilized on the surface of biomaterials to improve biocompatibility. For instance, RGDS has been linked to a surface by reaction with free amine groups to enhance cellular adhesion. These procedures usually require multiple steps. Preliminary studies on the APPLD have demonstrated that biomolecules retain at least some of their biologic activity when exposed to this high energy system. We propose continuing these studies to determine if biomolecule immobilization can be made permanent. This would provide a one step process for the immobilization of biomolecules. Based on the findings of this study, we propose that the biomolecules chosen for APPLD immobilization be sizable, like whole proteins or enzymes, instead of protein fragments as we have seen positive APPLD results from bulky polymers, but not from monomers.

7.2 USE OF APPLD FOR PATTERNED DEPOSITION

One distinct advantage of the APPLD system for surface modification over other vacuum plasma systems is the control that the user has over the deposition pattern. Other system, such as RFGD, would require the use of a mask in order to achieve a patterned deposition. The current system would have to be slightly altered, however, for ideal patterned deposition. As was previously noted, the plasma nozzle is nearly 2-cm in diameter. Studies would have to be done to determine how narrowing the plasma nozzle affects the deposition. Narrowing of this nozzle

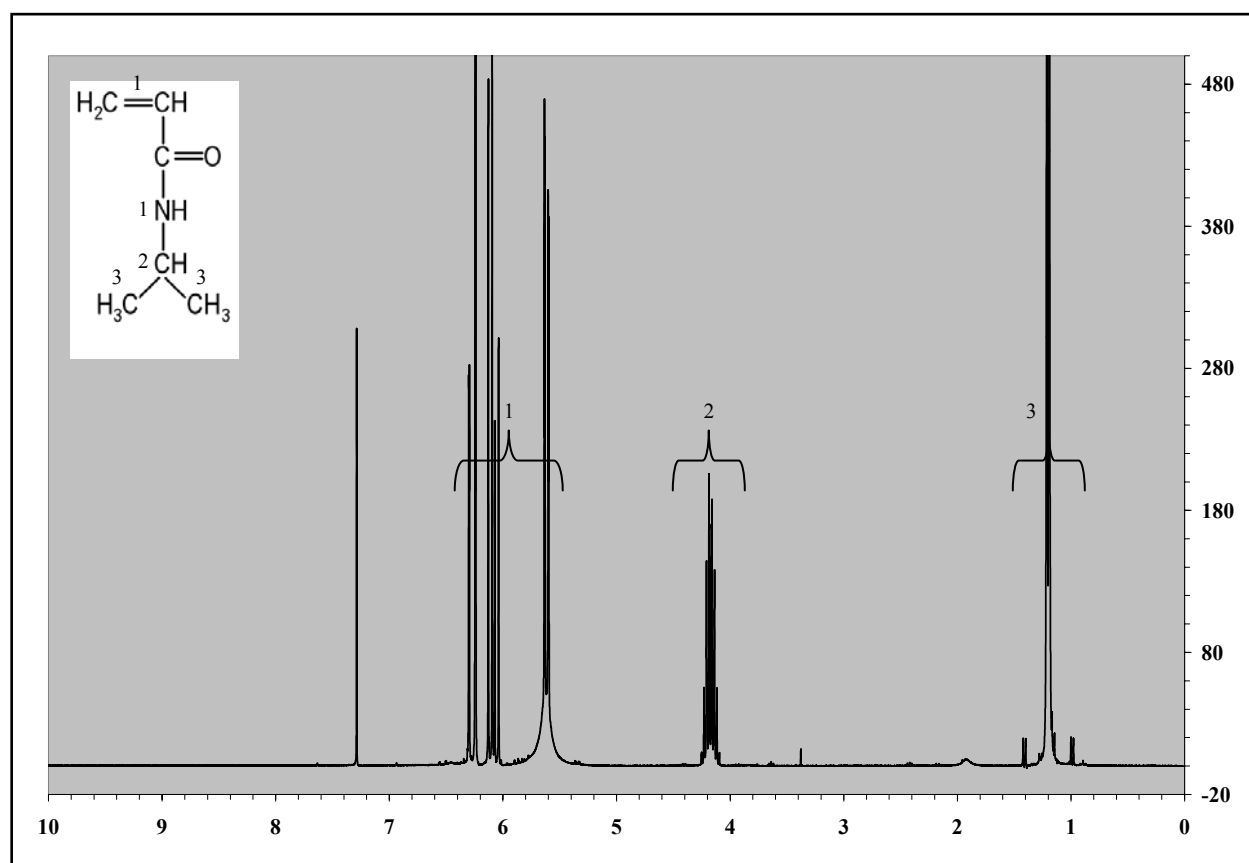
is key to patterned deposition and will likely be the limiting factor in APPLD patterned deposition.

7.3 IMMOBILIZATION OF PNIPAAm BY APPLD ONTO SOFT CONTACT LENSES

Many studies have demonstrated the clinical relevance in using pNIPAAm surfaces for making cell constructs. This technology, however, could be expanded. For instance, contact lenses are prone to biofilm formation, which can lead to infections in the eye. Poly(N-isopropylacrylamide) has been investigated as an anti-biofilm forming compound [10, 11]. Just as it has been shown to release mammalian cells from surfaces, it has also been found to release biofilms. Immobilization of pNIPAAm onto soft contact lenses could potentially prevent biofilm build-up and reduce the risk of infection from wearing soft contact lenses by making the lenses easier to clean. Corneal cells have been successfully grown on pNIPAAm dishes and released as cell sheets for corneal replacements [26, 43]. Poly(N-isopropylacrylamide) nanoparticles have also been used as a drug delivery system for glaucoma drugs [101]. These studies indicate that the immobilization of pNIPAAm on contact lenses would not be harmful to the biologic environment in the eye.

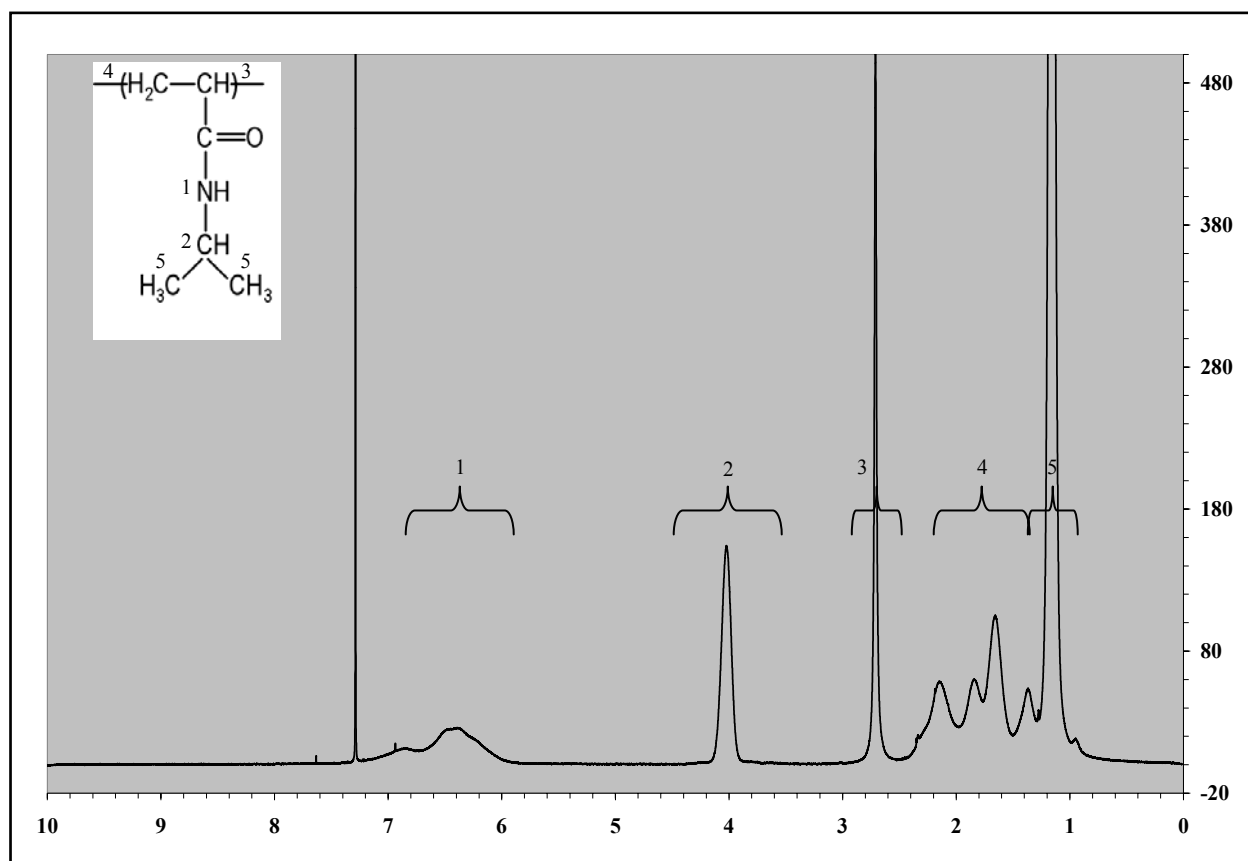
APPENDIX A

A.1 ^1H NMR Spectrum of NIPAAm



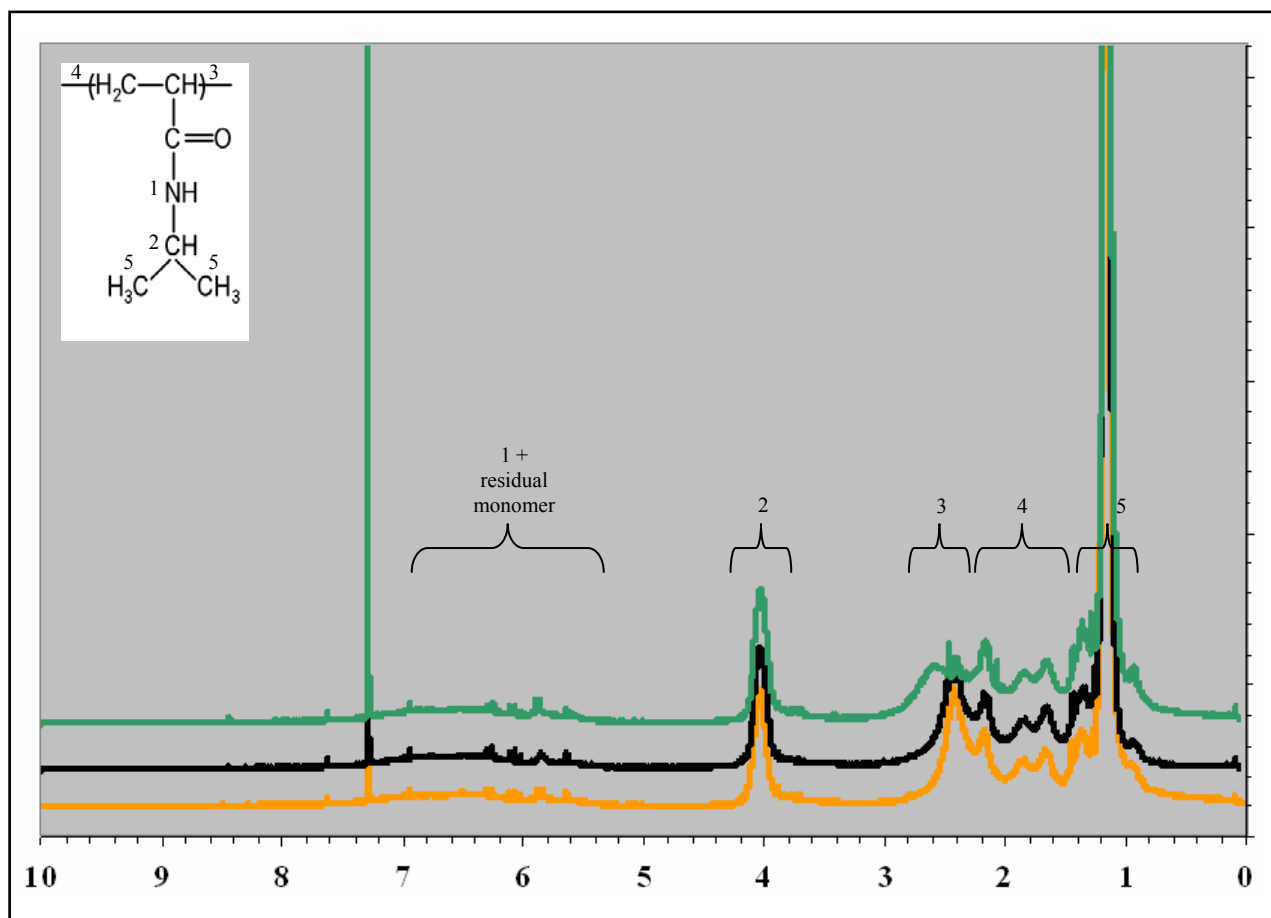
A-1 ^1H NMR spectra of NIPAAm

A.2 ^1H NMR Spectrum of pNIPAAm



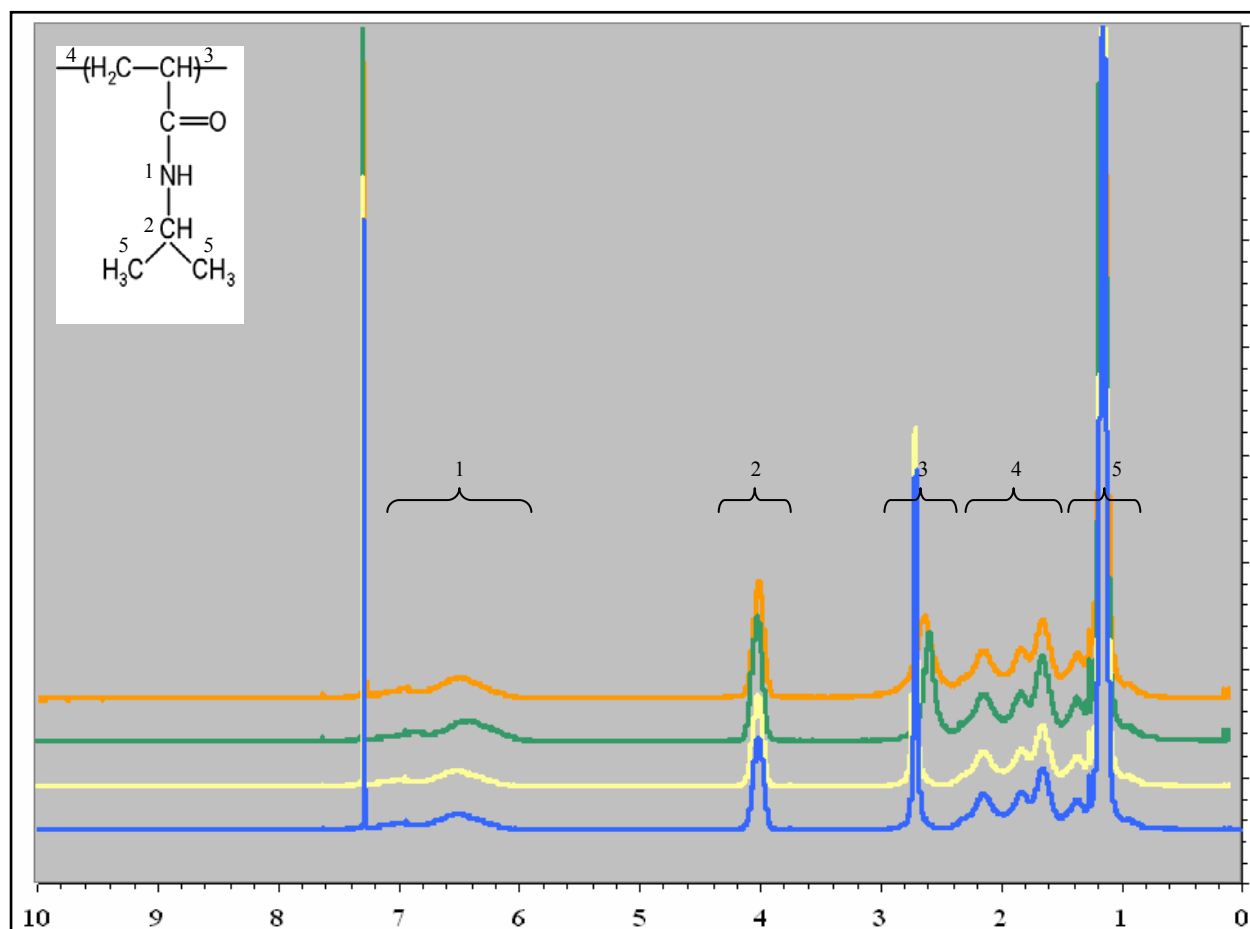
A-2 ^1H NMR spectra of pNIPAAm

A.3 ^1H NMR Spectrum of APPLD polymerized pNIPAAm



A-3 ^1H NMR spectra of APPLD polymerized pNIPAAm (ppNIPAAm) in triplicate

A.4 ^1H NMR Spectrum of APPLD deposited pNIPAAm



A-4 ^1H NMR spectra of APPLD deposited pNIPAAm. Blue line represents control pNIPAAm, yellow line represents pNIPAAm dissolved in IPA and film coated, green line represents APPLD sprayed pNIPAAm without HV, and orange line represents APPLD deposited pNIPAAm with HV.

BIBLIOGRAPHY

1. Langer R, Vacanti JP. Tissue Engineering. Science 1993;260(5110):920-926.
2. Specht EH, Neuman A, Neher HT, inventors. Preparation of acrylamides. United States Patent No. 2,773,063, 1956 4 December 1956.
3. Scarpa JS, Mueller DD, Klotz IM. Slow hydrogen-deuterium exchange in a non-alpha-helical polyamide. Journal of the American Chemical Society 1967;89(24):6024-6030.
4. Schild HG. Poly(N-isopropylacrylamide): experiment, theory and application. Progress in Polymer Science 1992;17:163-249.
5. Afrassiabi A, Hoffman AS, Cadwell LA. Effect of temperature on the release rate of biomolecules from thermally reversible hydrogels. Journal of Membrane Science 1987;33(2):191-200.
6. Okano T, Bae YH, Jacobs H, Kim SW. Thermally on-off switching polymers for drug permeation and release. Journal of Controlled Release 1990;11(1-3):255-265.
7. Huang X, Lowe TL. Biodegradable thermoresponsive hydrogels for aqueous encapsulation and controlled release of hydrophilic model drugs. Biomacromolecules 2005;6(4):2131-2139.
8. Idota N, Kikuchi A, Kobayashi J, Akiyama Y, Sakai K, Okano T. Thermal modulated interaction of aqueous steroids using polymer grafted capillaries. Langmuir 2006;22(1):425-430.
9. Recum HV, Okano T, Kim SW. Growth factor release from thermally reversible tissue culture substrates. Journal of Controlled Release 1998;55(2-3):121-130.
10. Guo H, Huang J, Wang X. The alternate temperature-change cleaning behaviors of PNIPAAm grafted porous polyethylene membranes fouled by proteins. Desalination 2008;234(1-3):42-50.
11. Ista LK, Perez-Luna VH, Lopez GP. Surface-grafted, environmentally sensitive polymers for biofilm release. Applied and Environmental Microbiology 1999;65(4):1603-1609.

12. Isenberg BC, Tsuda Y, Williams C, Shimizu T, Yamato M, Okano T, et al. A thermoresponsive, microtextured substrate for cell sheet engineering with defined structural organization. *Biomaterials* 2008;29(17):2565-2572.
13. Ito Y, Chen G, Guan Y, Imanishi Y. Patterned immobilization of thermoresponsive polymer. *Langmuir* 1997;13(10):2756-2759.
14. Takezawa T, Mori Y, Yoshizato K. Cell culture on a thermo-responsive polymer surface. *Nature Biotechnology* 1990;8:854-856.
15. Xu FJ, Zhong SP, Yung LYL, Tong YW, Kang ET, Neoh KG. Thermoresponsive comb-shaped copolymer-Si(1 0 0) hybrids for accelerated temperature-dependent cell detachment. *Biomaterials* 2006;27(8):1236-1245.
16. Yamada N, Okano T, Sakai H, Karikusa F, Sawasaki Y, Sakurai Y. Thermo-responsive polymeric surfaces; control of attachment and detachment of cultured cells. *Makromolekulare Chemie-Rapid Communications* 1990;11:571-576.
17. Ratner BD, Hoffman AS, Schoen FJ, Lemons JE. *Biomaterials Science. An Introduction to Materials in Medicine*. 1st Edition ed. San Diego: Academic Press, 1996.
18. Hubbard AT. *Encyclopedia of Surface and Colloid Science: Por-Z*: CRC Press, 2002.
19. Okano T, Yamada N, Okuhara M, Sakai H, Sakurai Y. Mechanism of cell detachment from temperature-modulated, hydrophilic-hydrophobic polymer surfaces. *Biomaterials* 1995;16:297-303.
20. Waymouth C. To disaggregate or not to disaggregate. Injury and cell disaggregation, transient or permanent? *In Vitro* 1974;10(1/2):97-111.
21. Akiyama Y, Kikuchi A, Yamato M, Okano T. Ultrathin poly(N-isopropylacrylamide) grafted layer on polystyrene surfaces for cell adhesion/detachment control. *Langmuir* 2004;20(13):5506-5511.
22. Canavan HE, Chen X, Graham DJ, Ratner BD, Castner DG. Surface characterization of the extracellular matrix remaining after cell detachment from a thermoresponsive polymer. *Langmuir* 2005;21(5):1949-1955.

23. Canavan HE, Cheng X, Graham DJ, Ratner BD, Castner DG. Cell sheet detachment affects the extracellular matrix: a surface science study comparing thermal liftoff, enzymatic and mechanical methods. *Journal of Biomedical Materials Research* 2005;75A:1-13.
24. Cheng X, Canavan HE, Stein MJ, Hull JR, Kweskin SJ, Wagner MS, et al. Surface chemical and mechanical properties of plasma-polymerized N-isopropylacrylamide. *Langmuir* 2005;21:7833-7841.
25. Hata H, Matsumiya G, Miyagawa S, Kondoh H, Kawaguchi N, Matsuura N, et al. Grafted skeletal myoblast sheets attenuate myocardial remodeling in pacing-induced canine heart failure model. *Journal of Thoracic Cardiovascular Surgery* 2006;132(4):918-924.
26. Ide T, Nishida K, Yamato M, Sumide T, Utsumi M, Nozaki T, et al. Structural characterization of bioengineered human corneal endothelial cell sheets fabricated on temperature-responsive culture dishes. *Biomaterials* 2006;27(4):607-614.
27. Ishida N, Kobayashi M. Interaction forces measured between poly(N-isopropylacrylamide) grafted surface and hydrophobic particle. *Journal of Colloid and Interface Science* 2006;297:513-519.
28. Kondoh H, Sawa Y, Miyagawa S, Sakakida-Kitagawa S, Memon IA, Kawaguchi N, et al. Longer preservation of cardiac performance by sheet-shaped myoblast implantation in dilated cardiomyopathic hamsters. *Cardiovascular Research* 2006;69(2):466-475.
29. Memon IA, Sawa Y, Fukushima N, Matsumiya G, Miyagawa S, Taketani S, et al. Repair of impaired myocardium by means of implantation of engineered autologous myoblast sheets. *Journal of Thoracic Cardiovascular Surgery* 2005;130(5):1333-1341.
30. Miyagawa S, Sawa Y, Sakakida S, Taketani S, Kondoh H, Memon IA, et al. Tissue cardiomyoplasty using bioengineered contractile cardiomyocyte sheets to repair damages myocardium: their integration with recipient myocardium. *Transplantation* 2005;80(1):1586-1595.
31. Miyahara Y, Nagaya N, Kataoka M, Yanagawa B, Tanaka K, Hao H, et al. Monolayered mesenchymal stem cells repair scarred myocardium after myocardial infarction. *Nature Medicine* 2006;12(4):459-465.
32. Ohashi K, Yokoyama T, Yamato M, Kuge H, Kanechiro H, Tsutsumi M, et al. Engineering functional two- and three-dimensional liver systems in vivo using hepatic tissue sheets. *Nature Medicine*;13(7):880-885.

33. Ohki T, Yamato M, Murakami D, Takagi R, Yang J, Namiki H, et al. Treatment of oesophageal ulcerations using endoscopic transplantation of tissue engineered autologous oral mucosal epithelial cell sheets in a canine model. *Gut* 2006;55(12):1704-1710.
34. Pan YV, Wesley RA, Luginbuhl R, Denton DD, Ratner BD. Plasma polymerized N-isopropylacrylamide: synthesis and characterization of a smart thermally responsive coating. *Biomacromolecules* 2001;2(1):32-36.
35. Sekine H, Shimizu T, Yang J, Kobayashi E, Okano T. Pulsatile myocardial tubes fabricated with cell sheet engineering. *Circulation* 2006;114(1 Suppl.):I87-I93.
36. Shimizu T, Sekine H, Isoi Y, Yamato M, Kikuchi A, Okano T. Long-term survival and growth of pulsatile myocardial tissue grafts engineered by layering of cardiomyocyte sheets. *Tissue Engineering* 2006;12(3):499-507.
37. Shimizu T, Sekine H, Yang J, Isoi Y, Yamato M, Kikuchi A, et al. Polysurgery of cell sheet grafts overcomes diffusion limits to produce thick, vascularized myocardial tissues. *FASEB Journal* 2006;20(6):708-710.
38. Shimizu T, Yamato M, Isoi Y, Akutsu T, Setomaru T, Abe K, et al. Fabrication of a pulsatile cardiac tissue grafts using a novel 3-dimensional cell sheet manipulation technique and temperature-responsive cell culture surfaces. *Circulation Research* 2002;90(3):e40.
39. Sumide T, Nishida K, Yamato M, Ide T, Hayashida Y, Watanabe K, et al. Functional human corneal endothelial cell sheets harvested from temperature-responsive culture surfaces. *FASEB Journal* 2006;20(2):392-394.
40. von Recum HA, Kim SW, Kikuchi A, Okuhara M, Sakurai Y, Okano T. Novel thermally reversible hydrogel as detachable cell culture substrate. *Journal of Biomedical Materials Research* 1998;40:631-639.
41. Yang J, Yamato M, Shimizu T, Sekine H, Ohashi K, Kanzaki M, et al. Reconstruction of functional tissues with cell sheet engineering. *Biomaterials* 2007;28:5033-5043.
42. Nishida K, Yamato M, Hayashida Y, Watanabe K, Yamamoto K, Adachi E. Corneal reconstruction with tissue-engineered cell sheets composed of autologous oral mucosal epithelium. *New England Journal of Medicine* 2004;351(12):1187-1196.

43. Nishida K, Yamato M, Hayashida Y, Watanabe K, Maeda N, Watanabe H. Functional bioengineered corneal epithelial cell sheet grafts from corneal stem cell expanded ex vivo on a temperature responsive cell culture surface. *Transplantation* 2004;77(3):379-385.
44. Han LM, Rajeshwar K, Timmons RB. Film chemistry control and electrochemical properties of pulsed plasma polymerized ferrocene and vinylferrocene. *Langmuir* 1997;13:5941-5950.
45. Goldston RJ, Rutherford PH. *Introduction to plasma physics*. London: Institute of Physics Publishing, 1995.
46. Bonizzoni G, Vassallo E. Plasma physics and technology; industrial applications. *Vacuum* 2002;64:327-336.
47. Goodwin AJ, Leadley S, Swallow F, Dobbyn P, inventors. An atmospheric pressure plasma assembly. Patent No. WO 03/086031 A1. 16 October 2003.
48. Pfender E. Thermal plasma technology: where do we stand and where are we going? *Plasma Chemistry and Plasma Processing* 1999;19(1):1-31.
49. McPherson R, Gane N, Bastow TJ. Structural characterization of plasma-sprayed hydroxylapatite coatings. *Journal of Materials Science: Materials in Medicine* 1995;6:327-334.
50. Heberlein J. New approaches in thermal plasma technology. *Pure and Applied Chemistry* 2002;74(3):327-335.
51. Swallow F, Dobbyn P, inventors. Plasma generating electrode assembly. Patent No. WO 2004/068916 A1. 12 August 2004.
52. Eliezer S, Eliezer Y. *The Fourth State of Matter*. 2nd Edition ed. Philadelphia: Institute of Physics Publishing, 2001.
53. Curtis ASG, Forrester JV, McInnes C, Lawrie F. Adhesion of cells to polystyrene surfaces. *Journal of Cell Biology* 1983;97(5):1500-1506.
54. Chu PK, Chen JY, Wang LP, Huang N. Plasma-surface modification of biomaterials. *Materials Science and Engineering R - Reports* 2002;36:143-206.

55. Yasuda H. Plasma Polymerization. Orlando: Academic Press, 1985.
56. Muguruma H, Hiratsuka A, Karube I. Thin-film glucose biosensor based on plasma-polymerized film: simple design for mass production. *Analytical chemistry* 2000;72(11):2671-2675.
57. Puleo DA, Kissling RA, Sheu MS. A technique to immobilize bioactive proteins, including bone morphogenetic protein-4 (BMP-4), on titanium alloy. *Biomaterials* 2002;23(9):2078-2087.
58. Gancarz I, Bryjak J, Bryjak M, Pozniak G, Tylus W. Plasma modified polymers as a support for enzyme immobilization 1.: allyl alcohol plasm. *European Polymer Journal* 2003;39(8):1615-1622.
59. Vargo TG, Bekos EJ, Kim YS, Ranieri JP, Bellamkonda R, Aebischer P, et al. Synthesis and characterization of fluoropolymeric substrata with immobilized minimal peptide sequences for cell adhesion studies. I. *Journal of Biomedical Materials Research* 1995;29(6):767-778.
60. Gupta B, Plummer C, Bisson I, Frey P, Hilborn J. Plasma-induced graft polymerization of acrylic acid onto poly(ethylene terephthalate) films: characterization and human smooth muscle cell growth on grafted films. *Biomaterials* 2002;23(3):863-871.
61. Ito Y, Kajihara M, Imanishi Y. Materials for enhancing cell adhesion by immobilization of cell-adhesive peptide. *Journal of Biomedical Materials Research* 1991;25(11):1325-1337.
62. Siow KS, Britcher L, Kumar S, Griesser HJ. Plasma methods for the generation of chemically reactive surfaces for biomolecule immobilization and cell colonization - a review. *Plasma Processes and Polymers* 2006;3:392-418.
63. Goodwin AJ, Leadley SR, O'Neill L, Duffield PJ, McKechnie MT, Pugh S, inventors. Coating compositions. Patent No. WO 2005/110626 A2. 24 November 2005.
64. Goodwin A, Merlin P, Badyal JP, inventors. Method and apparatus for forming a coating. Patent No. WO 02/28548 A2. 11 April 2002.
65. Friedrich J, Kuhn G, Mix R. Polymer surface modification with monofunctional groups of different type and density. In: D'Agostino R, Favia P, Oehr C, Wertheimer MR, editors. *Plasma Processes and Polymers: 16th International Symposium on Plasma Chemistry*; 2003; Taormina, Italy: Wiley-VCH; 2003. p. 3-22.

66. Han LM, Rajeshwar K, Timmons RB. Film chemistry control and electrochemical properties of pulsed plasma polymerized ferrocene and vinylferrocene. *Langmuir* 1997;13:5941-5950.
67. Han LM, Timmons RB. Ring retention via pulsed plasma polymerization of heterocyclic aromatic compounds. *Chemistry of Materials* 1998;10:1422-1429.
68. Chen X, Rajeshwar K, Timmons RB. Pulsed plasma polymerization and tetramethyltin: nanoscale compositional control of film chemistry. *Chemistry of Materials* 1996;8:1067-1077.
69. Bell KL, Dalgarno A, Kingston AE. Penning ionization by metastable helium atoms. *Journal of Physics B* 1968;1(2):18-22.
70. Fridman AA, Kennedy LA. *Plasma Physics and Engineering*: Taylor & Francis, 2004.
71. Kanazawa S, Kogoma M, Moriwaki T, Okazaki S. Stable glow plasma at atmospheric pressure. *Journal of Physics D-Applied Physics* 1988;21:838-840.
72. Nozaki T, Kimura Y, Okazaki K, Kado S. Controlled growth of carbon nanotubes using pulsed plasma glow-barrier discharge. In: D'Agostino R, Favia P, Oehr C, Wertheimer MR, editors. *Plasma Processes and Polymers: 16th International Symposium on Plasma Chemistry*; 2003; Taormina, Italy: Wiley-VCH; 2003. p. 477-489.
73. O'Hare L-A, O'Neill L. Problems with nebulization. In: Wargo S, editor. *Pittsburgh*, 2007.
74. Chinn JA, Horbett TA, Ratner BD. Laboratory preparation of plasticware to support cell culture. *Methods in Cell Science* 1994;16(3-4):1381-5741.
75. Pieper JS, Hafmans T, Veerkamp JH, Kuppevelt THV. Development of tailor-made collagen-glycosaminoglycan matrices: EDC/NHS crosslinking, and ultrastructural aspects. *Biomaterials* 2000;21(6):581-593.
76. Tang C, Kligman F, Larsen CC, Kottke-Marchant K, Marchant RE. Platelet and endothelial adhesion on fluorosurfactant polymers designed for vascular graft modification. *Journal of biomedical Materials Research - Part A* 2009;88(2):348-358.

77. Yasuda H, Gazicki M. Biomedical applications of plasma treatment polymerization and plasma treatment of polymer surfaces. *Biomaterials* 1982;3:68-77.
78. Bullett NA, Talib RA, Short RD, McArthur SL, Shard AG. Chemical and thermo-responsive characterization of surfaces formed by plasma polymerisation of N-isopropyl acrylamide. *Surface and Interface Analysis* 2006;38:1109-1116.
79. Schild HG, Tirrell DA. Microcalorimetric detection of lower critical solution temperatures in aqueous polymer solutions. *Journal of Physical Chemistry* 1990;94:4352-4356.
80. Gristina AG. Biomaterial-centered infection: microbial adhesion versus tissue integration. *Science* 1987;237(4822):1588-1595.
81. Stickler DJ, McLean RJC. Biomaterials associated infections: the scale of the problem. *Cells and Materials* 1995;5(2):167-182.
82. Gristina AG, Costerton JW. Bacterial adherence to biomaterials and tissue. *Journal of Bone and Joint Surgery* 1985;67:264-273.
83. Kuijter R, Jansen EJP, Emans PJ, Bulstra SK, Riesle J, Pieper J, et al. Assessing infection risk in implanted tissue-engineered devices. *Biomaterials* 2007;28:5148-5154.
84. Park JH, Cho YW, Kwon IC, Jeong SY, Bae YH. Assessment of PEO/PTMO multiblock copolymers/segmented polyurethane blends as coating materials for urinary catheters: in vitro bacterial adhesion and encrustation behavior. *Biomaterials* 2002;23:3991-4000.
85. Park KD, Kim YS, Han DK, Kim YH, Lee EH, Suh H, et al. Bacterial adhesion on PEG modified polyurethane surfaces. *Biomaterials* 1998;19:851-859.
86. Yoo HJ, Kim HD. Properties of crosslinked blends of pellethene adn multiblock polyurethane containing poly(ethylene oxide) for biomaterials. *Journal of Applied Polymer Science* 2004;91:2348-2357.
87. Harris LG, Tosatti S, Wieland M, Textor M, Richards RG. Staphylococcus aureus adhesion to titanium oxide surfaces coated with non-functionalized and peptide-functionalized poly(L-lysine)-grafted-poly(ethylene glycol) copolymers. *Biomaterials* 2004;25:4135-4148.

88. Schierholz JM, Lucas LJ, Rump A, Pulverer G. Efficacy of silver-coated medical devices. *Journal of Hospital Infection* 1998;40:257-262.
89. Silver S. Bacterial silver resistance: molecular biology and uses and misuses of silver compounds. *FEMS Microbiology Reviews* 2003;27:341-353.
90. Kamal GD, Pfaller MA, Rempe LE, Jebson PJ. Reduced intravascular catheter infection by antibiotic bonding. A prospective, randomized, controlled trial. *Journal of the American Medical Association* 1991;265:2364-2368.
91. Schierholz JM, Steinhauser H, Rump AF, Berkels R, Pulverer G. Controlled release of antibiotics from biomedical polyurethanes: morphological and structural features. *Biomaterials* 1997;18:839-844.
92. Gamelli RL, Paxton TP, O'Reilly M. Bone marrow toxicity by silver sulfadiazine. *Surgery Gynecology and Obstetrics* 1993;177:115-120.
93. Lee AR, Moon HK. Effect of topically applied silver sulfadiazine on fibroblast cell proliferation and biomechanical properties of the wound. *Archives of Pharmacal Research* 2003;26:855-860.
94. Arciola CR, Alvi FI, An YH, Campoccia D, Montanaro L. Implant infection and infection resistant materials: a mini review. *International Journal of Artificial Organs* 2005;28(11):1119-1125.
95. Murata H, Koepsel RR, Matyjaszewski K, Russell AJ. Permanent, non-leaching antibacterial surfaces - 2: How high density cationic surfaces kill bacterial cells. *Biomaterials* 2007;28:4870-4879.
96. Huang J, Murata H, Koepsel RR, Russell AJ, Matyjaszewski K. Antibacterial polypropylene via surface-initiated atom transfer radical polymerization. *Biomacromolecules* 2007;8(5):1396-1399.
97. Lee SB, Koepsel RR, Morley SW, Matyjaszewski K, Sun Y, Russell AJ. Permanent, nonleaching antibacterial surfaces. 2. Synthesis by atom transfer radical polymerization. *Biomacromolecules* 2004;5:877-882.

98. Lin J, Qiu S, Lewis K, Klibanov AM. Mechanism of bactericidal and fungicidal activities of textiles covalently modified with alkylated polyethyleneimine. *Biotechnology and Bioengineering* 2003;83(2):168-172.
99. Tiller JC, Lee SB, Lewis K, Klibanov AM. Polymer surfaces derivatized with poly(vinyl-N-hexylpyridinium) kill airborne and waterborne bacteria. *Biotechnology and Bioengineering* 2002;79(4):465-471.
100. Cen L, Neoh KG, Kang ET. Surface functionalization technique for conferring antibacterial properties to polymeric and cellulosic surfaces. *Langmuir* 2003;19(24):10295-10303.
101. Hsiue G-H, Hsu S-H, Yang C-C, Lee S-H, Yang I-K. Preparation of controlled release ophthalmic drops, for glaucoma therapy using thermoresponsive poly-N-isopropylacrylamide. *Biomaterials* 2002;23:457-462.